Fetkovich Method for Production Analysis

Orientation

Production Analysis:

- Arps:
  - Exponential, Hyperbolic and Harmonic time-rate relations,
  - Early correlation of EUR and initial production (from exponential relation), and
  - Arps "hyperbolic" type curve solution.
- Fetkovich Type Curve (Radial Flow — Liquid Case).
- Carter Type Curve (Radial Flow — Gas Case).

SPE 004629: Fetkovich

- Introduced "decline type curve" analysis.
- Mostly focused on liquid cases.
- Had a few rate models that did not pass the test of time.
- Showed that you could estimate reservoir properties from production data.

SPE 013169: Fetkovich

- "Case Histories" paper.
- West Virginia Well A will be a focus for us.
- Monterey well overlay concept may be useful for any play.

Production Analysis (PA) — Arps

Q. Theory for Arps' relations?

A. Arps derived the exponential and hyperbolic relations from loss ratio.

Case	Rate Relation	Cumulative Relation
***Exponential*: (*b*=0)**	$q = q_i \exp(-D_i t)$	$N_p = \frac{q_i}{D_i}[1-\exp(-D_i t)]$
***Hyperbolic*: (0<*b*<1)**	$q = \frac{q_i}{(1+bD_i t)^{(1/b)}}$	$N_p = \frac{q_i}{(1-b)D_i}\left[1-(1+bD_i t)^{1-(1/b)}\right]$
***Harmonic*: (*b*=1)**	$q = \frac{q_i}{(1+D_i t)}$	$N_p = \frac{q_i}{D_i}\ln(1+D_i t)$

— From: Arps, J.J: "Analysis of Decline Curves," *Trans.*, AIME (1945) 160, 228-247.

Arps' observations:

- *b*=0 — Reservoir is highly undersaturated ($p>p_b$).
- *b*=0 — Gravity drainage and no free surface.
- *b*=0.5 — Gravity drainage with free surface.
- *b*=0.667 — Soln. gas-drive reservoir ($\bar{p}$ vs. N_p → linear).
- *b*=0.333 — Soln. gas-drive reservoir ($\bar{p}^2$ vs. N_p → linear).

Theory???

Loss Ratio:

$$a \equiv \frac{1}{D} \equiv -\frac{q}{dq/dt}$$

Theory???

Loss Ratio Derivative:

$$b \equiv \frac{d}{dt}[a] \equiv \frac{d}{dt}\left[\frac{1}{D}\right] \equiv -\frac{d}{dt}\left[\frac{q}{dq/dt}\right]$$

- **Discussion**: History — *Production Analysis (PA) — Arps*
  - *"Theory" for the Arps' relations?* (loss ratio (*exp*) and its derivative (*hyp*))
  - *Validity of the Arps' observations?* (only qualitative (except for $p>p_b$ case))
  - *Graphical analysis using the hyperbolic relation?* (only using Fetkovich TC)

Production Analysis (PA) — EUR vs. $q_{o,1yr}$

Q. Origin and purpose of the EUR versus $q_{o,1yr}$ correlation?

A. Potential value as a correlation, but must quantify theory (N, k, s, etc).

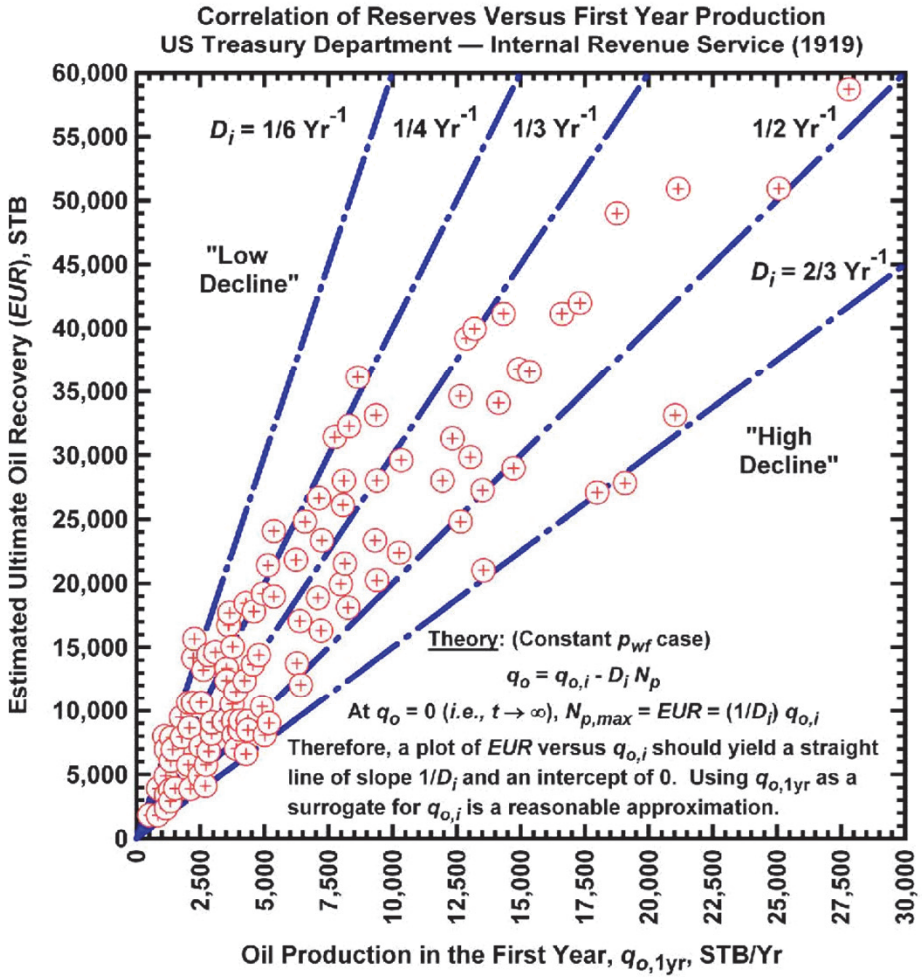

— From: *Manual for The Oil and Gas Industry Under The Revenue Act of* 1918, Treasury Department — United States Internal Revenue Service (1919).

"Ancient" Technique:

The proposed correlation of EUR vs. $q_{o,1yr}$ was used to estimate oil reserves from initial production performance data.

Modern Application:

Approach is based in theory — EUR = f[k, s, x_f, ... and contacted fluids in-place (i.e., N or G)].

Could be used as a "reservoir characterization" tool to classify well performance.

- **Discussion**: History — *Production Analysis* (*PA*) — *EUR* vs. $q_{o,1yr}$
  - *Origin?* (1919 — production data correlation (>85 years old)!)
  - *Theory?* (*Constant p_{wf}* (liquid) boundary-dominated flow conditions)
  - *Rationale?* (Correlate reserves versus production (or reservoir properties))

Hyperbolic EUR Methods (Type Curves)

Q. Straight-line or characteristic behavior for Arps hyperbolic relation?

A. Rate-cumulative ratios used to define "type curve" behavior.

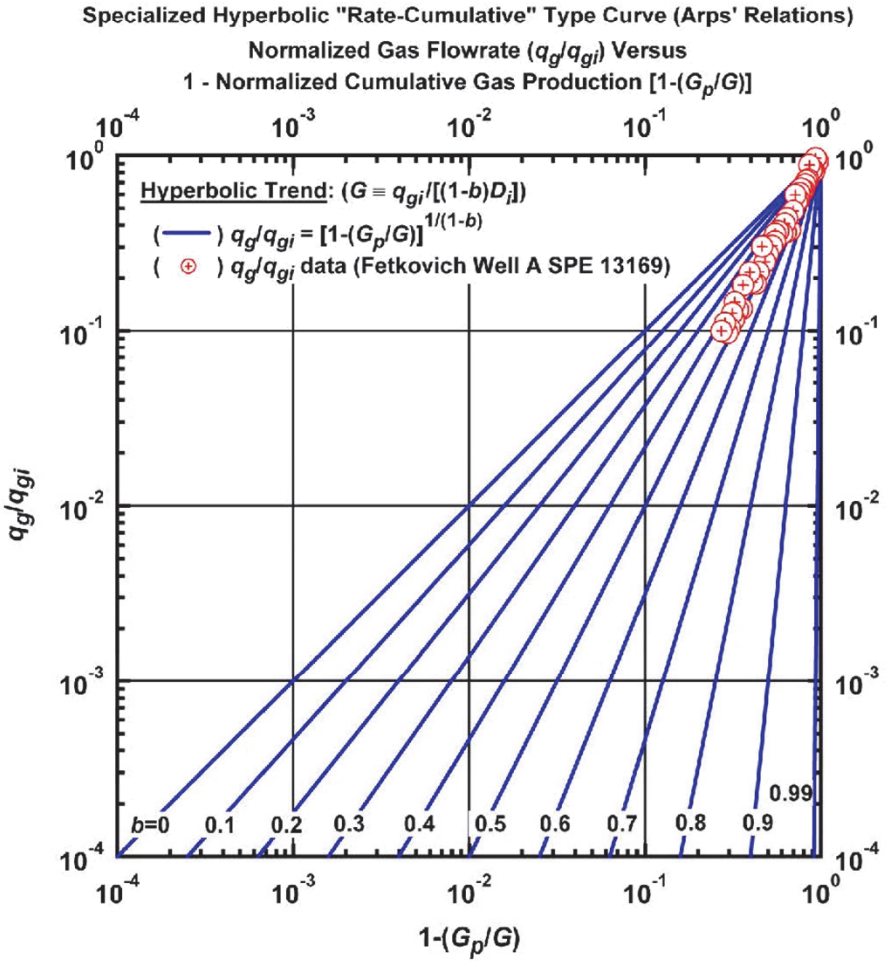

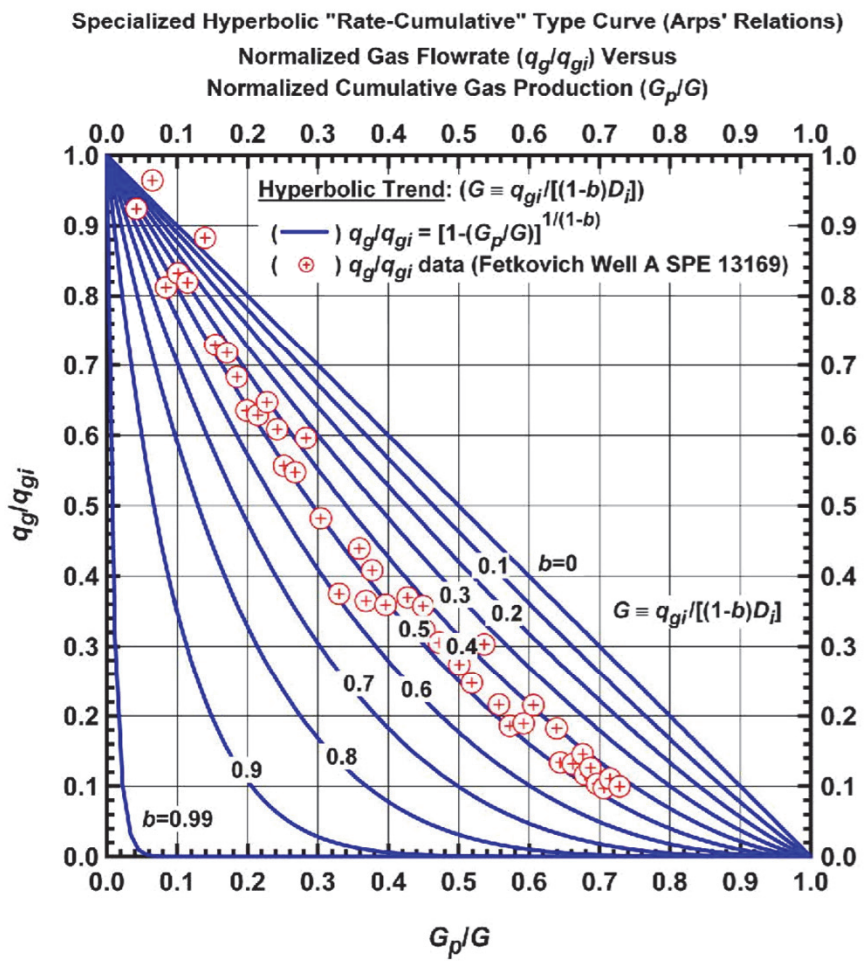

- **Discussion**: Modern *PA* — *Hyperbolic EUR Methods (Type Curves)*
  - *Example gas case from Fetkovich (SPE 13169)?* ("typical" gas case)
  - log[(q_g/q_{gi})] *versus* log[1-(G_p/G)]? (straight-line characteristic behavior)
  - *Cartesian* (q_g/q_{gi}) *versus* (G_p/G)? (note that 0.4<*b*<0.5)

Production Analysis (PA) — Fetkovich

Q. What is the "Fetkovich" Decline Type Curve, and how is it used?

A. A composite of analytical (p_{wf}=con) and empirical (Arps) solutions — used as a "type curve" (data overlay) to estimate reservoir properties.

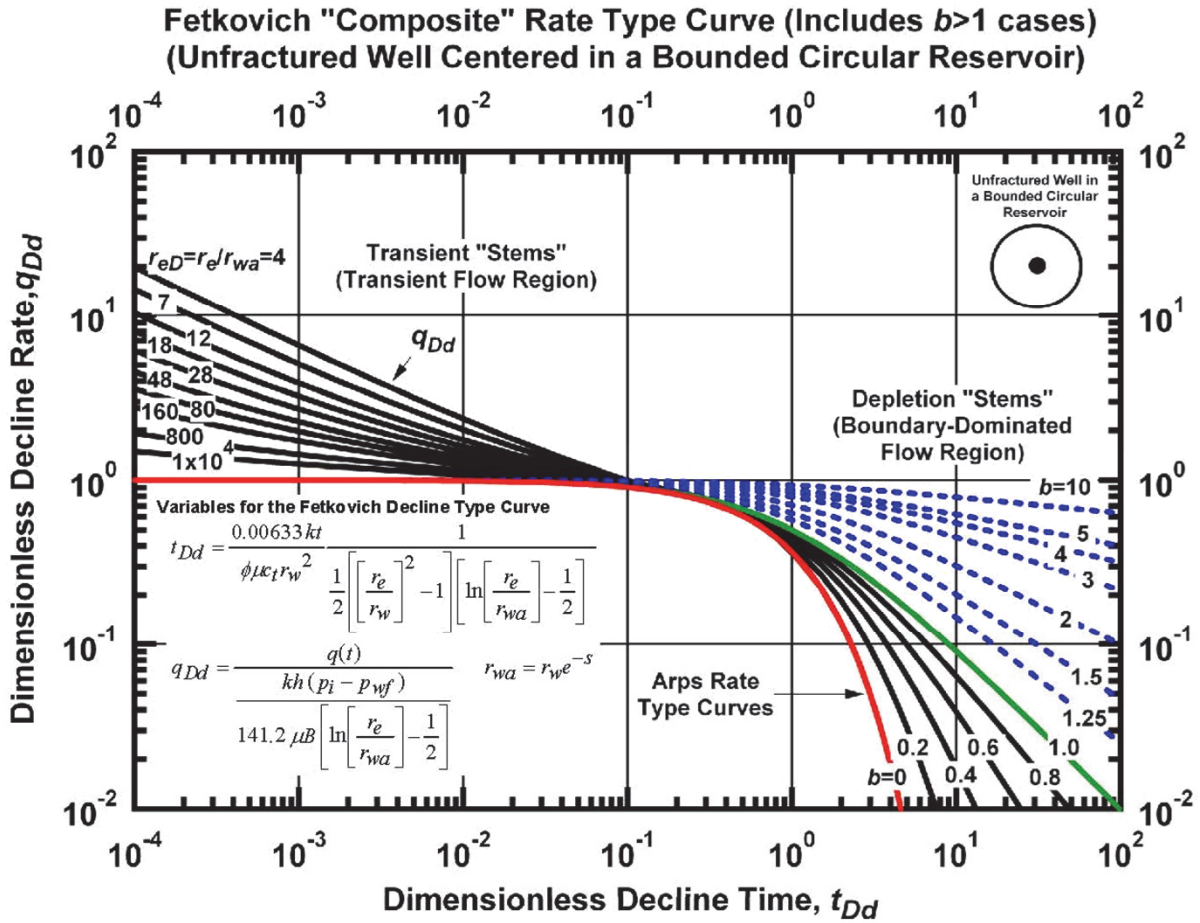

— From: Fetkovich, M.J.: "Decline Curve Analysis Using Type Curves," *JPT* (June 1980) 1065-1077.

Transient Stems: (left)

- *Infinite-acting radial flow model (p_{wf} = con).*
- *q(t) is concave up.*

Depletion Stems: (right)

- *Bounded circular reservoir (p_{wf} = con).*
- *q(t) is concave down.*
- *b=0: p_{wf} = con.*
- *b=1: q_o = con. ($q_o/\Delta p$).*
- *b>1: transient flow or external drive energy.*

Reservoir Properties:

- *k — y-axis match.*
- *N — x&y-axis matches.*
- *s — r_{eD} match.*

- **Discussion: History — *Production Analysis (PA) — Fetkovich***
  - *An original purpose of the Fetkovich TC?* (graphical solution of Arps Eqs.)
  - *Use of "transient" stems?* (estimate reservoir properties — *k* and *s*)
  - *Use of "depletion" stems?* (estimate reservoir volume, predict rate)

Production Analysis (PA) — Carter

Q. What is the "Carter" Decline Type Curve, and how is it used?

A. A numerically-generated gas rate solution (p_{wf}=con) — used as a "type curve" (data overlay) to estimate reservoir properties.

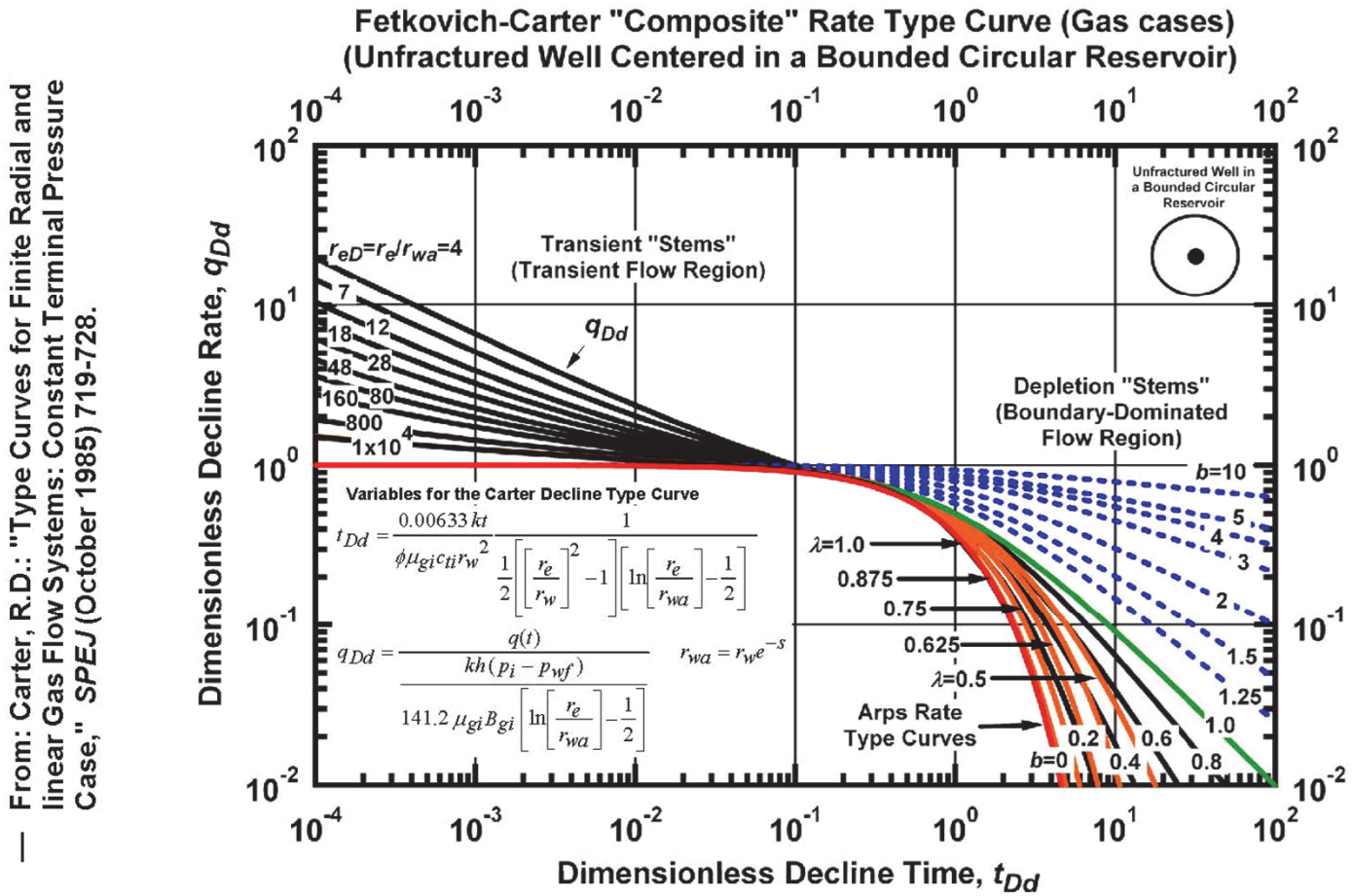

— From: Carter, R.D.: "Type Curves for Finite Radial and linear Gas Flow Systems: Constant Terminal Pressure Case," *SPEJ* (October 1985) 719-728.

Transient Stems: (left)

- *Numerical flow model (p_{wf} = con).*
- *q(t) is concave up.*

Depletion Stems: (right)

- *q(t) is concave down.*
- *b=0: p_{wf} = con.*
- *b=1: q_o = con. ($q_o/\Delta p$).*
- *b>1: transient flow or external drive energy.*
- *λ: numerical gas flow cases ($\lambda = f(p_{wf}/p_i)$).*

Reservoir Properties:

- *k — y-axis match.*
- *G — x&y-axis matches.*
- *s — r_{eD} match.*

- **Discussion: History — *Production Analysis (PA) — Carter***
  - *Genisis of the Carter TC?* ("correction" of Fetkovich gas flow solutions)
  - *Use of "transient" stems?* (estimate reservoir properties — *k* and *s*)
  - *Use of "depletion" stems?* (estimate reservoir volume, predict rate)

Fetkovich Papers

SPE 4629

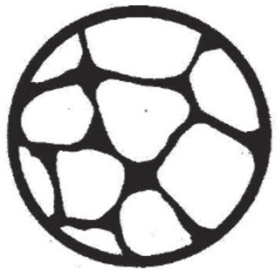

Decline Curve Analysis Using Type Curves

M.J. Fetkovich, SPE, Phillips Petroleum Co.

This paper demonstrates that decline curve analysis not only has a solid fundamental base but also provides a tool with more diagnostic power than has been suspected previously. The type curve approach provides unique solutions on which engineers can agree or shows when a unique solution is not possible with a type curve only.

JUNE 1980

Fetkovich Decline Type Curve

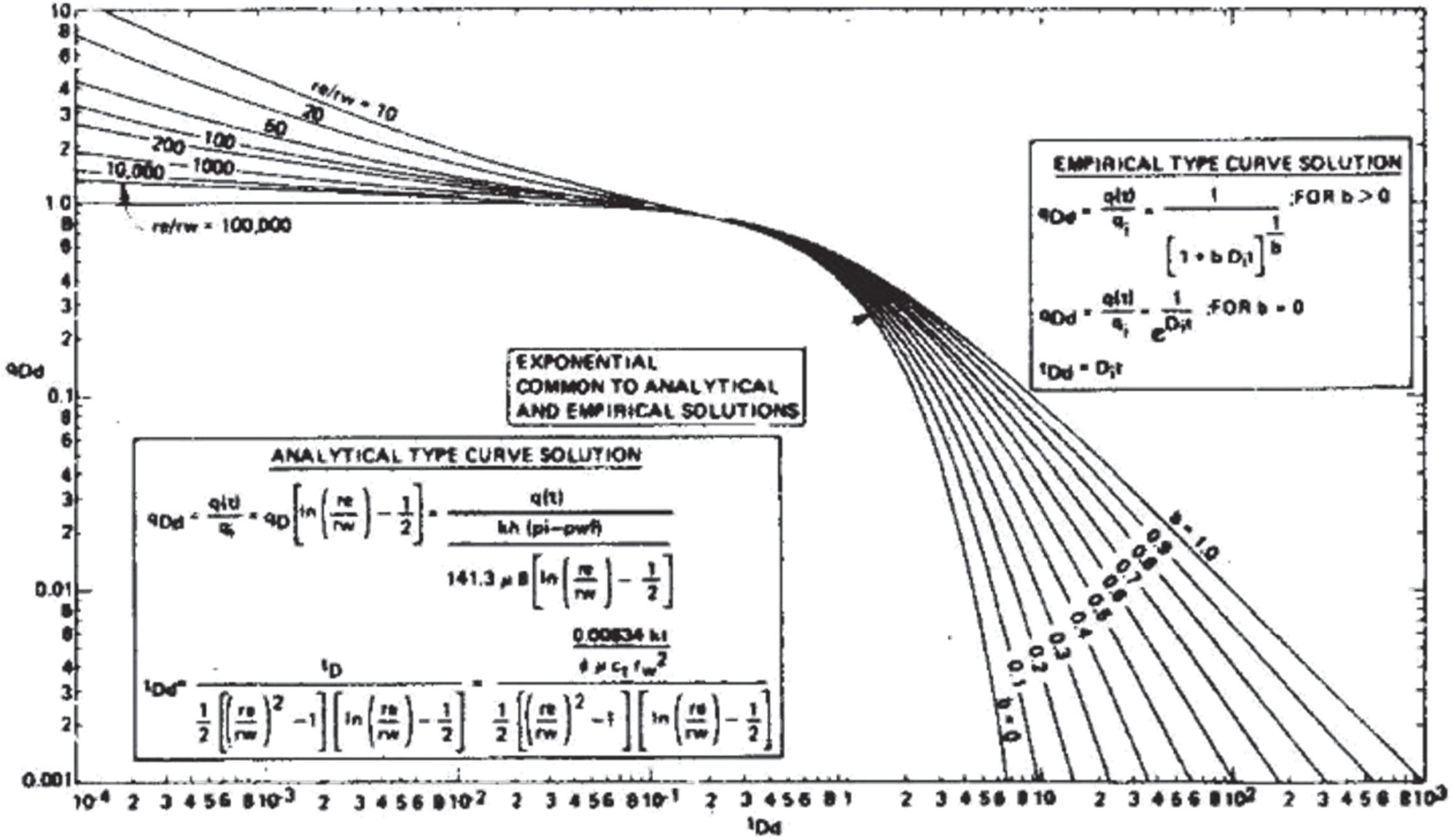

Fetkovich, M.J.: "Decline Curve Analysis Using Type Curves," JPT (March 1980) 1065-1077.

Fetkovich Example Cases (SPE 004629)

TABLE 3 – COMPARISONS OF *kh* DETERMINED FROM BUILDUP AND DECLINE CURVE ANALYSIS, FIELD A (SANDSTONE RESERVOIR); 160-ACRE SPACING, r_e = 1,490 ft, r_w = 0.25 ft

				Pressure Buildup Results			Decline Curve Analysis Results				
Well No.	h (ft)	ϕ (%)	S_{wc} (%)	Skin s	r_w' (ft)	kh (md-ft)	r_e/r_w' Matched	q_{Dd} (10,000 BOPM)	$\frac{p_i - p_{wf}}{(\mu_o B_o)}$	kh (md-ft)	k (md)
1	34	9.4	32.9	– 0.23	0.3	120.5	*	0.52	6658	108	3.18
2	126	10.5	18.3	– 2.65	3.5	56.7	*	0.68	7979	48	0.38
3	32	9.9	20.4	– 3.71	10.3	63.0	*	0.43	8048	60	1.88
4	63	9.5	18.6	– 3.41	7.6	28.5	40	0.58	8273	31	0.49
5	67	10.2	15.1	– 4.29	18.3	44.4	20	0.57	6296	32	0.48
6	28	10.3	12.6	– 2.07	2.0	57.9	*	0.60	7624	62	2.21
7	17	10.0	17.5	– 3.41	7.6	16.8	10	1.30	7781	8.3	0.49
8	47	9.1	24.2	– 3.74	10.6	16.6	10	1.14	7375	10	0.21
9	87	10.2	18.0	– 4.19	16.5	104.7	*	0.435	5642	76	0.87
10	40	10.4	21.7	– 5.80	82.9	363.2	*	0.36	1211	255	6.38
11	29	11.5	19.2	– 1.00	2.0	59.9	*	0.56	7669	66	2.28
12	19	11.1	17.0	– 3.97	13.3	8.9	50	3.30	5045	9.5	0.50
13	121	10.1	18.8	– 3.85	11.8	47.5	50	0.54	7259	40.5	0.33
16	74	9.4	20.4	– 4.10	15.0	224.8	*	0.32	5737	104	1.41
15	49	10.9	28.6	– 3.59	9.1	101.9	*	0.43	4312	115	2.35
16	35	10.0	25.6	– 4.57	24.2	14.3	20	0.96	5110	24	0.69
17	62	8.8	22.4	– 3.12	5.7	27.2	*	0.82	8198	35	0.56
18	75	9.4	18.1	– 1.50	1.2	65.1	*	0.52	6344	93	1.24
19	38	8.9	19.2	– 2.11	2.1	40.5	20	0.54	6728	32	0.84
20	60	9.6	24.6	– 5.48	60.1	88.1	*	0.345	5690	64	1.07
21	56	11.1	16.5	– 2.19	2.2	39.1	20	0.72	5428	30	0.54
22	40	8.9	22.5	– 3.79	11.1	116.0	100	0.46	8114	51	1.28

*r_w' used from buildup analysis with r_e of 1,490 ft.

Fetkovich, M.J.: "Decline Curve Analysis Using Type Curves," JPT (March 1980) 1065-1077.

Fetkovich Well 13 (SPE 004629)

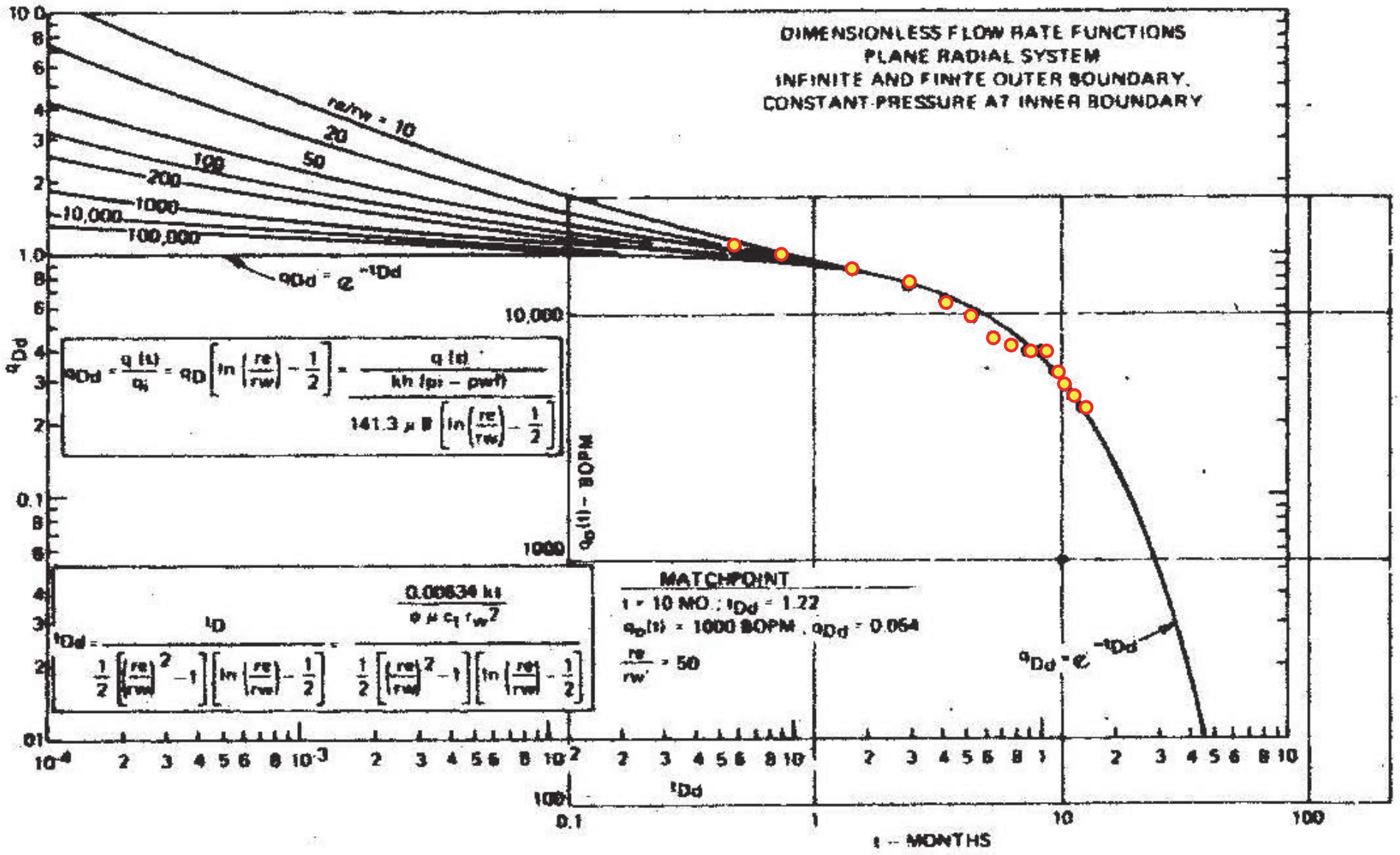

Fetkovich, M.J.: "Decline Curve Analysis Using Type Curves," JPT (March 1980) 1065-1077.

Fetkovich Decline Time and Rate Functions (SPE 004629)

$$t_{Dd} = \frac{0.00634\,kt}{\phi\mu c_t r_w^2} \cdot \frac{1}{\frac{1}{2}\left[\left(\frac{r_e}{r_w}\right)^2 - 1\right]\left[\ln\left(\frac{r_e}{r_w}\right) - \frac{1}{2}\right]}$$

$$q_{Dd} = \frac{\frac{q(t)}{kh(p_i - p_{wf})}}{141.3\,\mu B\left[\ln\left(\frac{r_e}{r_w}\right) - \frac{1}{2}\right]}$$

Fetkovich, M.J.: "Decline Curve Analysis Using Type Curves," JPT (March 1980) 1065-1077.

Decline-Curve Analysis Using Type Curves—Case Histories

M.J. Fetkovich, SPE, Phillips Petroleum Co.
M.E. Vienot, SPE, Phillips Petroleum Co.
M.D. Bradley, SPE, Phillips Petroleum Co.
U.G. Kiesow, SPE, Phillips Petroleum Co.

SPE Formation Evaluation, December 1987

Fetkovich West Virginia Well A (SPE 013169)

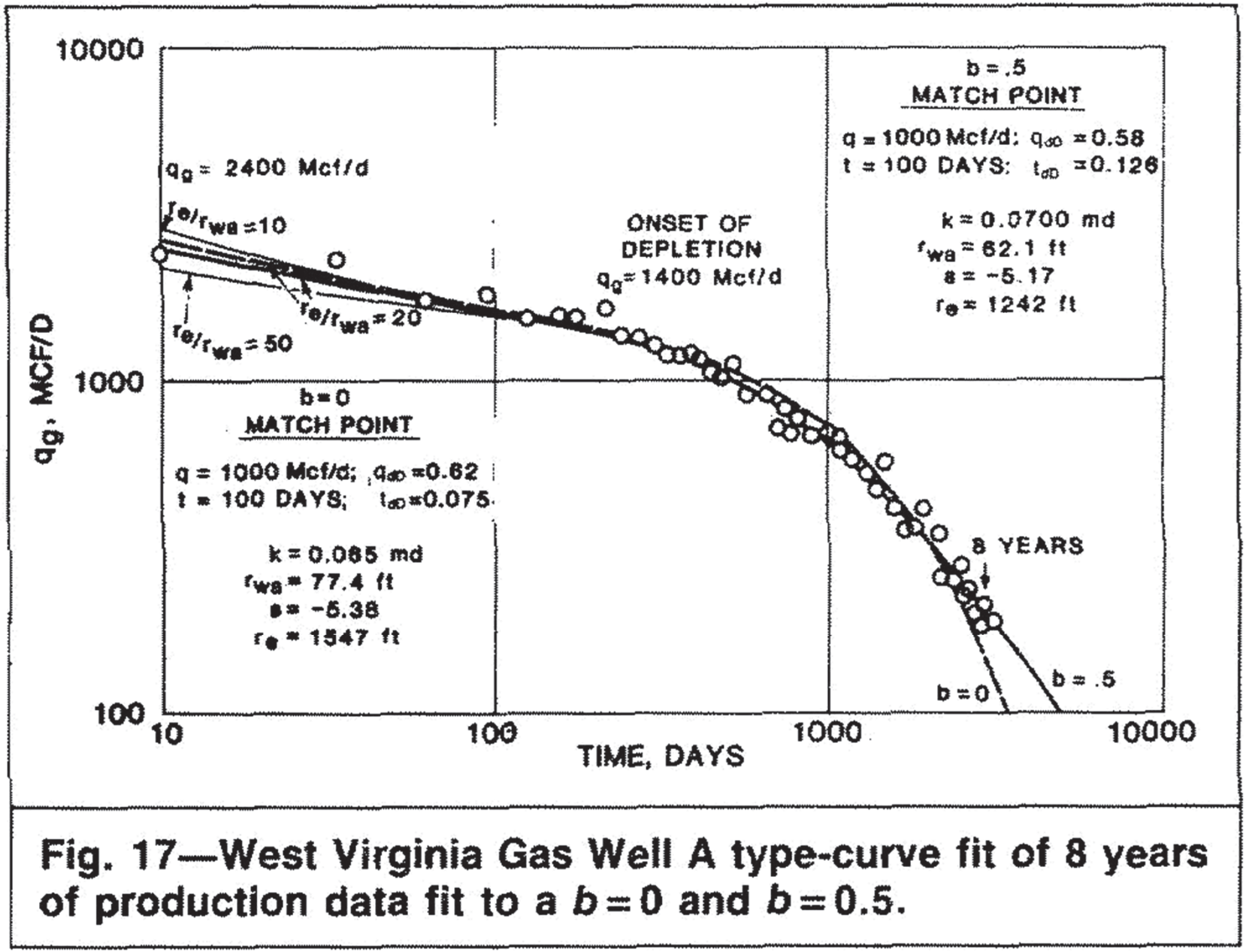

Fig. 17—West Virginia Gas Well A type-curve fit of 8 years of production data fit to a $b = 0$ and $b = 0.5$.

Fetkovich, M.J., Vienot, M.E., Bradley and M.D., Kiesow, U.G.: "Decline Curve Analysis Using Type Curves – Case Histories," SPEFE (Dec. 1987) 637-656.

Fetkovich West Virginia Well A (SPE 013169)

TABLE 3—WEST VIRGINIA GAS WELL A

Reservoir and Fluid Properties	
Gas specific gravity	0.57 (air = 1.00)
Porosity	0.06
Water saturation	0.35
Original pressure, psia	4,175
Pressure at start of decline, psia	3,268
Viscosity at 3,268 psia, cp	0.0171
System compressibility at 3,268 psia, psi^{-1}	177×10^{-6}
Thickness, ft	70
Temperature, °F	160
Wellbore radius, ft	0.354
Rate before 106-day pressure buildup, Mscf/D	2,181
Δp_p, psi^2/cp	774×10^6
B_g at 3,268 psia, scf/ft^3	208.8
B_g at 4,175 psia, scf/ft^3	253.9

TABLE 5—WEST VIRGINIA GAS WELL A: SUMMARY OF RATE-TIME ANALYSIS RESULTS

Match Points					
Composite Type Curve $b = 0$		Composite Type Curve $b = 0.5$		Carter Type Curve $\lambda = 0.55$ ($b = 0.5$)	
q_{dD}	0.62	q_{dD}	0.58	q_{DR}	0.24
t_{dD}	0.075	t_{dD}	0.126	t_{DR}	60
$q(t)$, Mscf/D	1,000	$q(t)$, Mscf/D	1,000	$q(t)$, Mscf/D	1,000
t, days	100	t, days	100	t, days	100

	$r_e/r_{wa} = 10$	$r_e/r_{wa} = 20$	$r_e/r_{wa} = 50$	Horner Analysis
	$b = 0$ Evaluation			
kh, md-ft	3.292	4.558	6.231	
k, md	0.047	0.065	0.089	0.0805
r_{wa}, ft	154.7	77.4	30.9	
s	−6.08	−5.38	−4.47	−5.52
r_e, ft	1,547	1,547	1,547	
	$b = 0.5$ Evaluation			
kh, md-ft	3.542	4.902	6.705	
k, md	0.0506	0.0700	0.0958	
r_{wa}, ft	124.2	62.1	24.8	
s	−5.86	−5.17	−4.25	
r_e, ft	1,242	1,242	1,242	
	Carter's $\lambda = 0.55$ Evaluation			
kh, md-ft	3.451	4.746	6.699	
k, md	0.0493	0.0678	0.0957	
r_{wa}, ft	126.4	62.6	24.8	
s	−5.88	−5.17	−4.25	
r_e, ft	1,264	1,252	1,240	

Fetkovich, M.J., Vienot, M.E., Bradley and M.D., Kiesow, U.G.: "Decline Curve Analysis Using Type Curves – Case Histories," SPEFE (Dec. 1987) 637-656.

Fetkovich Monterey Wells (SPE 013169)

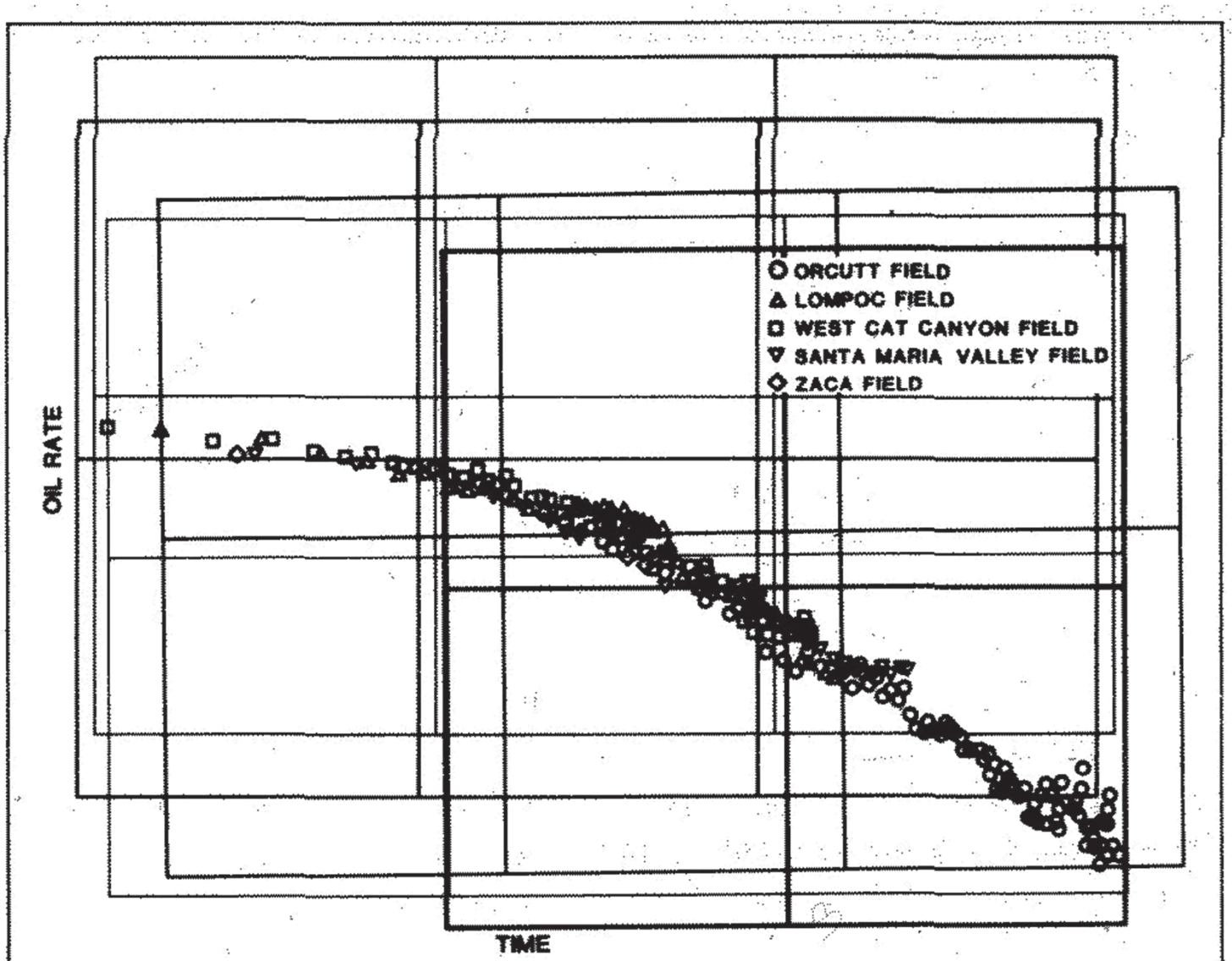

Fig. 42—Overlay of log-rate-vs.-log-time production data of five California Monterey producing fields.

Fetkovich, M.J., Vienot, M.E., Bradley and M.D., Kiesow, U.G.: "Decline Curve Analysis Using Type Curves – Case Histories," SPEFE (Dec. 1987) 637-656.

Plots for Well 13
SPE 004629 (*Fetkovich*)

Fetkovich West Virginia Well A (SPE 013169)

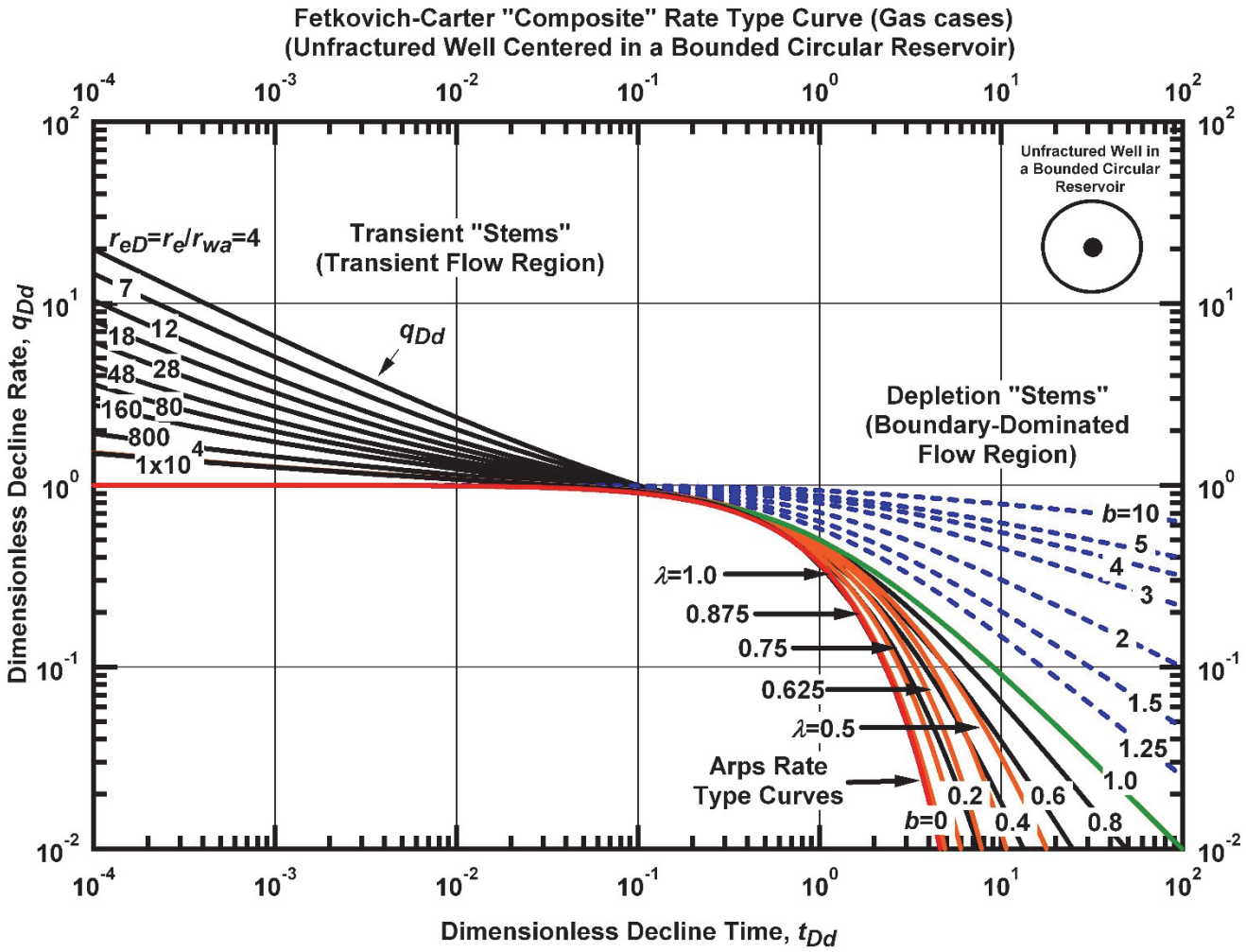

Decline Type Curve
Dimensionless Decline Rate versus Dimensionless Decline Time

Fetkovich, M.J.: "Decline Curve Analysis Using Type Curves," JPT (March 1980) 1065-1077.

Fetkovich West Virginia Well A (SPE 013169)

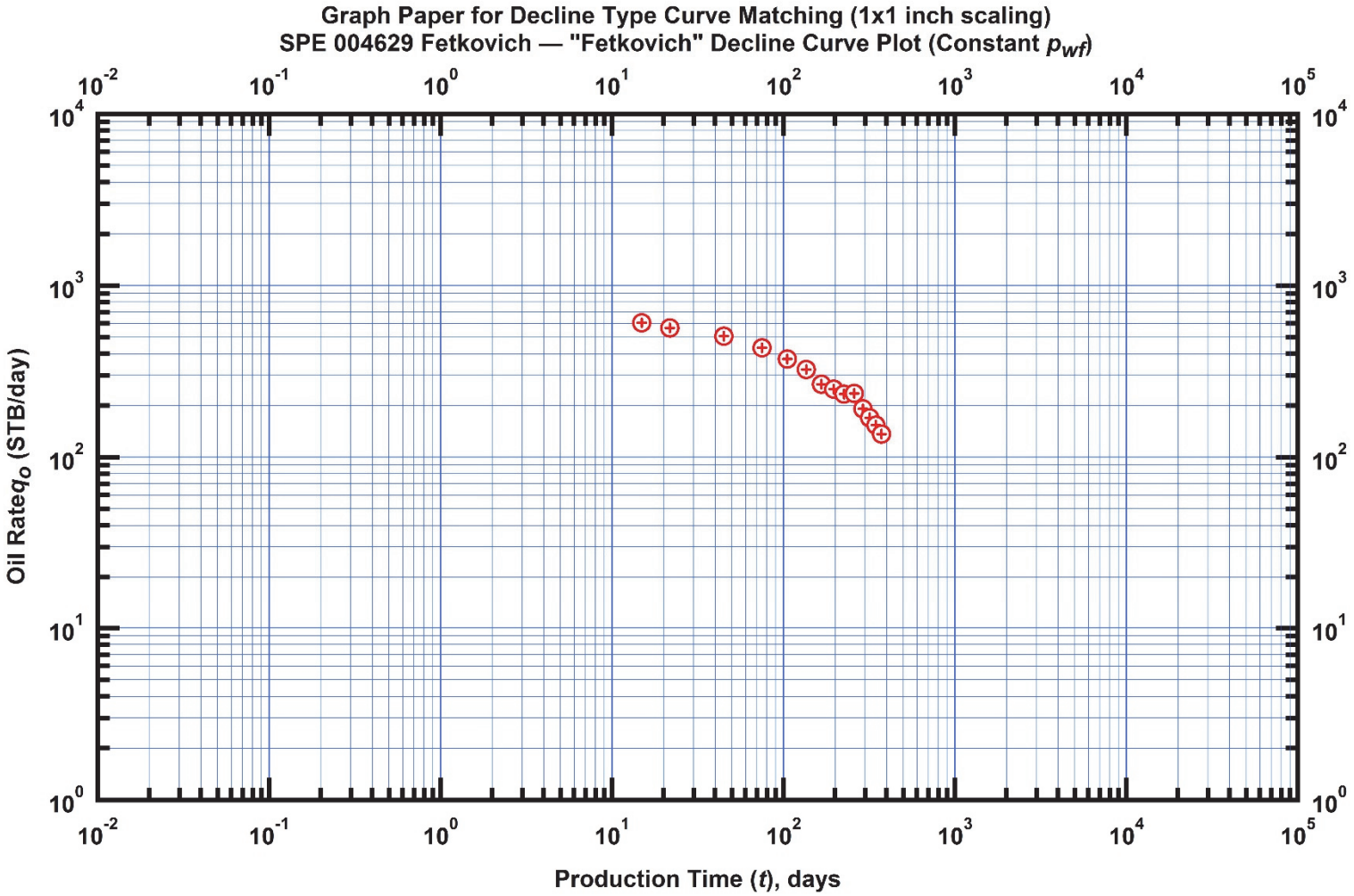

Oil Rate versus Time
Fetkovich Well 13 (SPE 004629)

Fetkovich, M.J.: "Decline Curve Analysis Using Type Curves," JPT (March 1980) 1065-1077.

Fetkovich West Virginia Well A (SPE 013169)

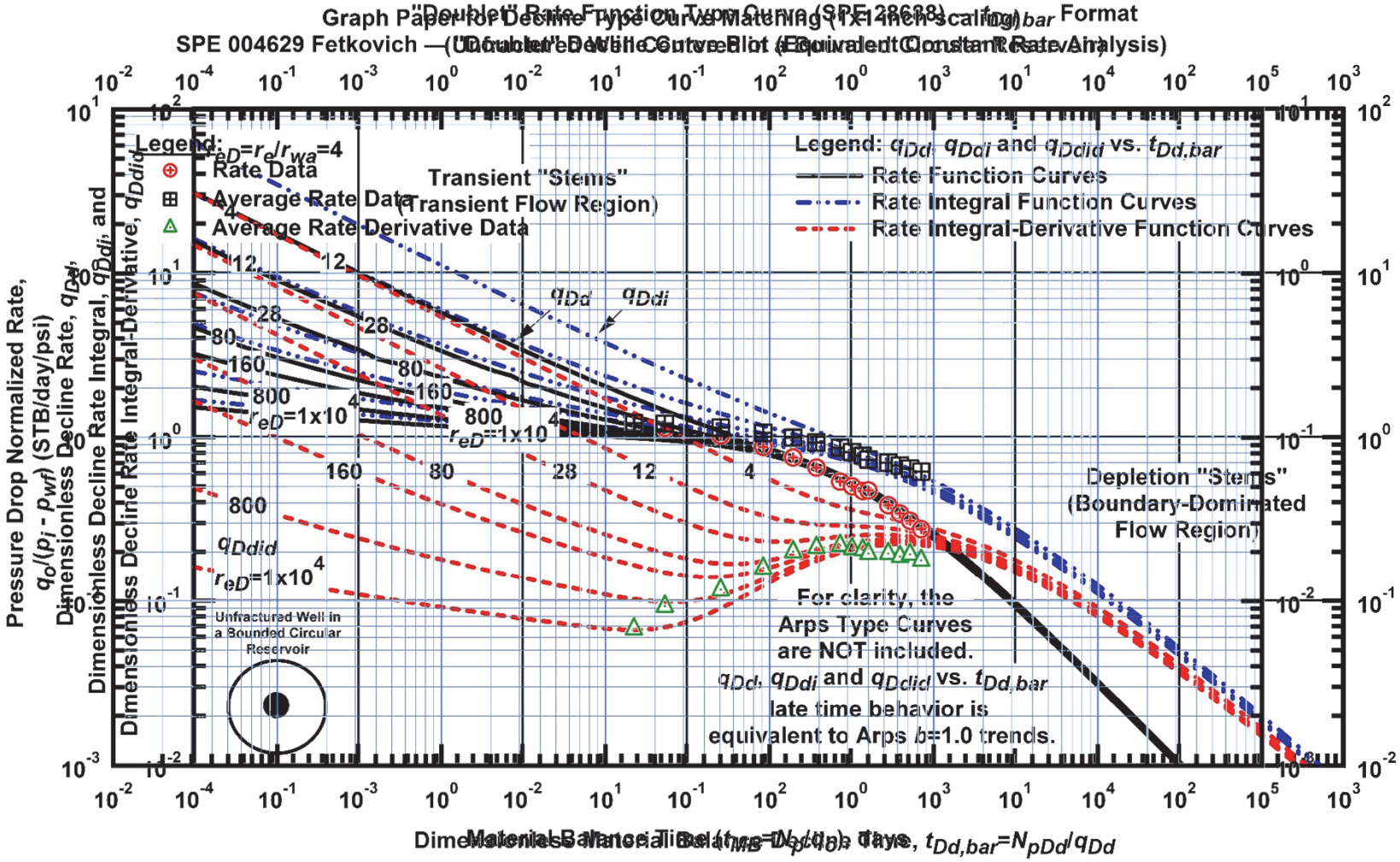

Material Balance Decline Type Curve:
Dimensionless Productivity Index and Auxiliary Functions versus Dimensionless Material Balance Time

Fetkovich, M.J.: "Decline Curve Analysis Using Type Curves," JPT (March 1980) 1065-1077.

Fetkovich West Virginia Well A (SPE 013169)

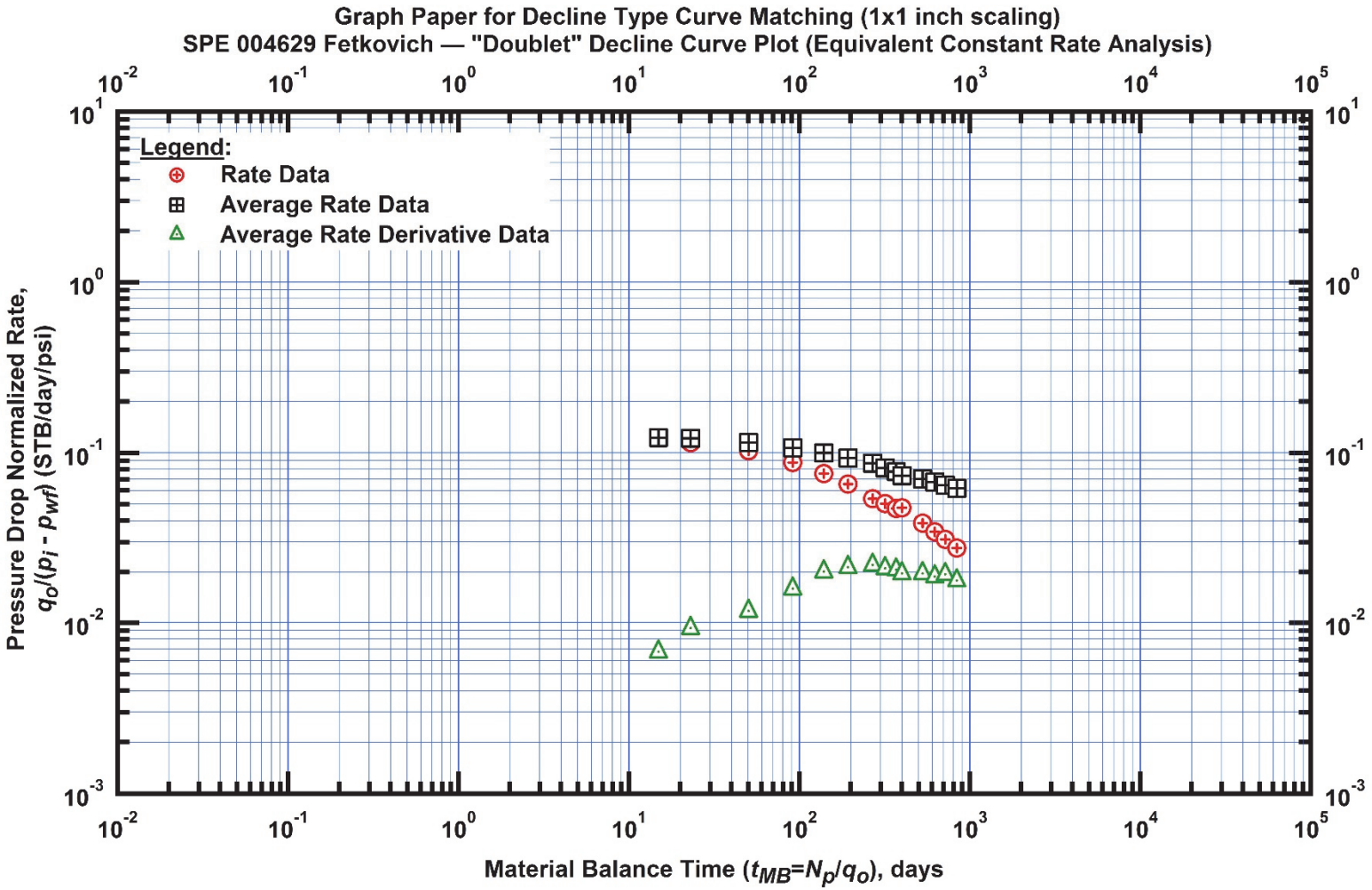

Fetkovich, M.J.: "Decline Curve Analysis Using Type Curves," JPT (March 1980) 1065-1077.

Oil Productivity Index versus Oil Material Balance Time
Fetkovich Well 13 (SPE 004629)

Plots for West Virginia Well A
SPE 013160 (*Fetkovich, et al*)

Fetkovich West Virginia Well A (SPE 013169)

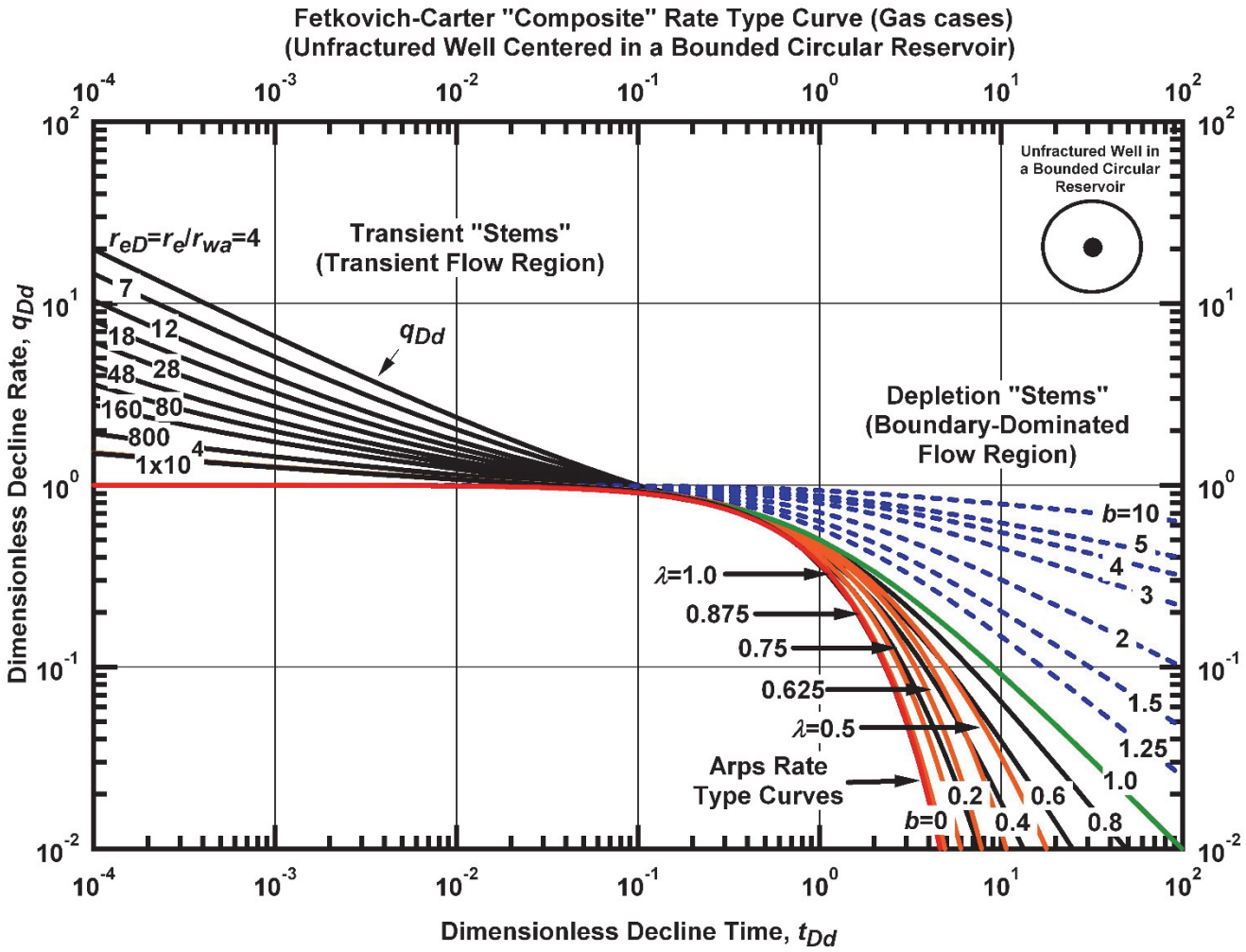

Decline Type Curve
Dimensionless Decline Rate versus Dimensionless Decline Time

Fetkovich, M.J., Vienot, M.E., Bradley and M.D., Kiesow, U.G.: "Decline Curve Analysis Using Type Curves – Case Histories," SPEFE (Dec. 1987) 637-656.

Fetkovich West Virginia Well A (SPE 013169)

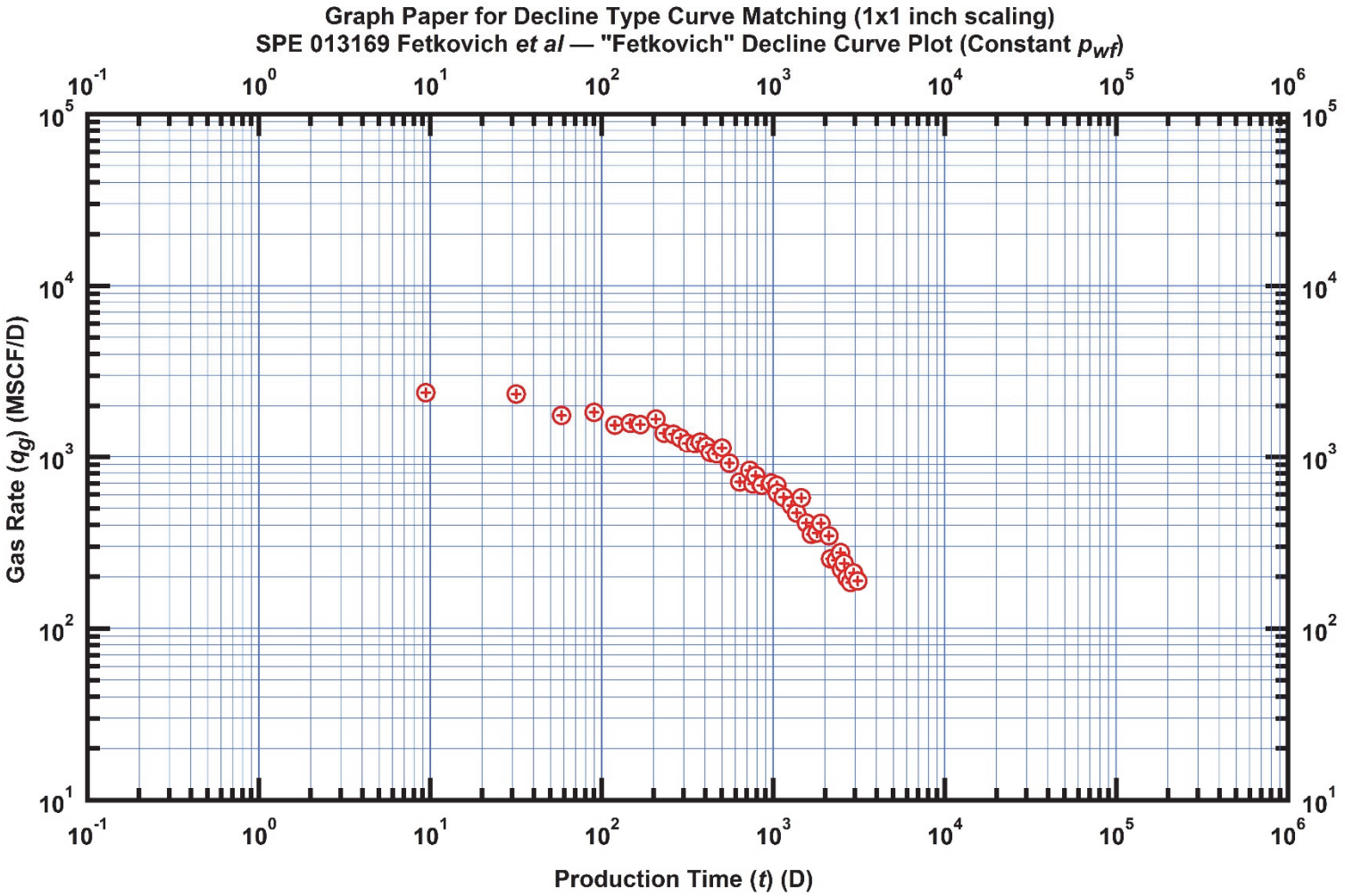

Gas Rate versus Time
Fetkovich West Virginia Well A (SPE 013169)

Fetkovich, M.J., Vienot, M.E., Bradley and M.D., Kiesow, U.G.: "Decline Curve Analysis Using Type Curves – Case Histories," SPEFE (Dec. 1987) 637-656.

Fetkovich West Virginia Well A (SPE 013169)

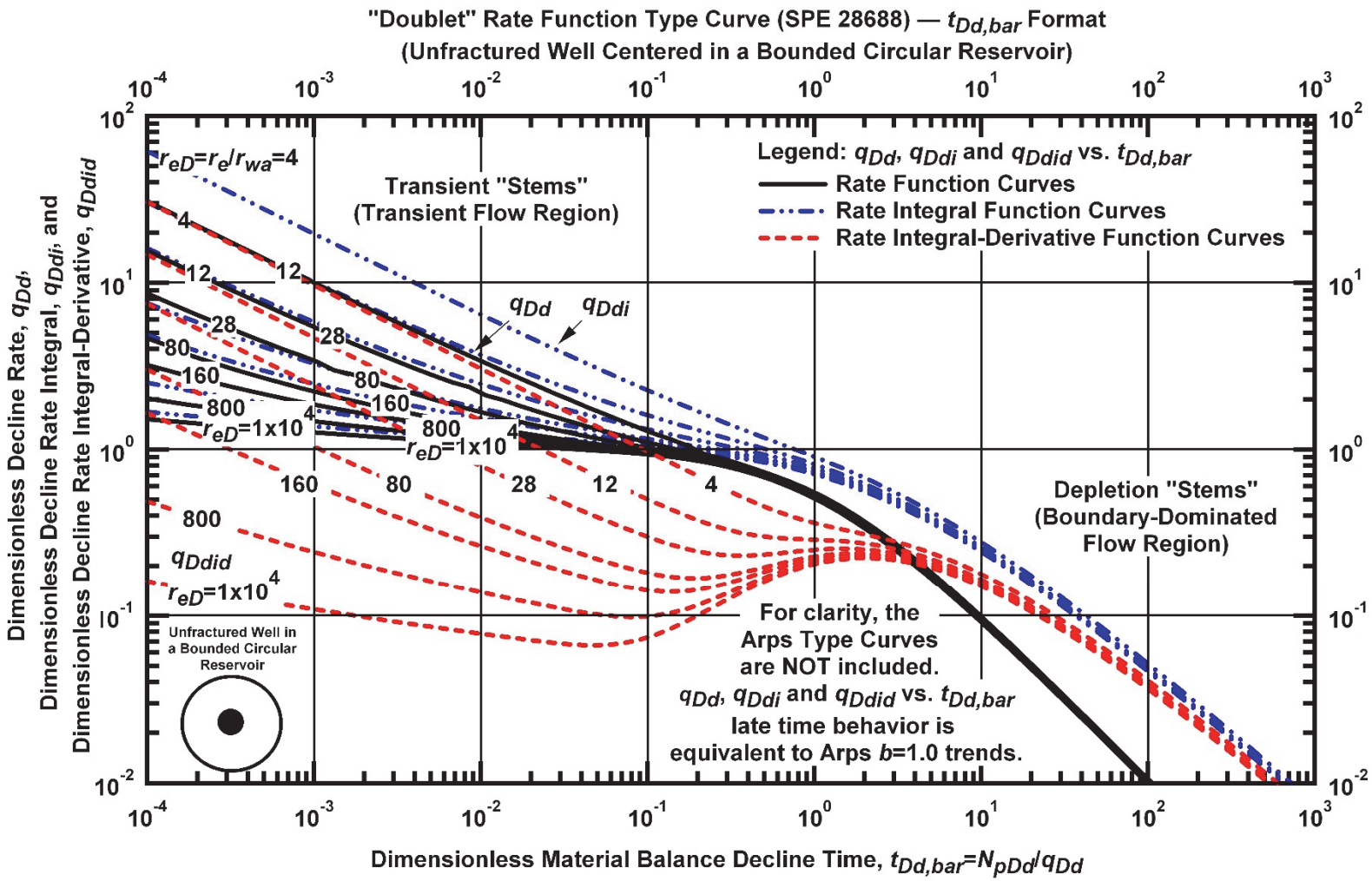

Material Balance Decline Type Curve:
Dimensionless Productivity Index and Auxiliary Functions versus Dimensionless Material Balance Time

Fetkovich, M.J., Vienot, M.E., Bradley and M.D., Kiesow, U.G.: "Decline Curve Analysis Using Type Curves – Case Histories," SPEFE (Dec. 1987) 637-656.

Fetkovich West Virginia Well A (SPE 013169)

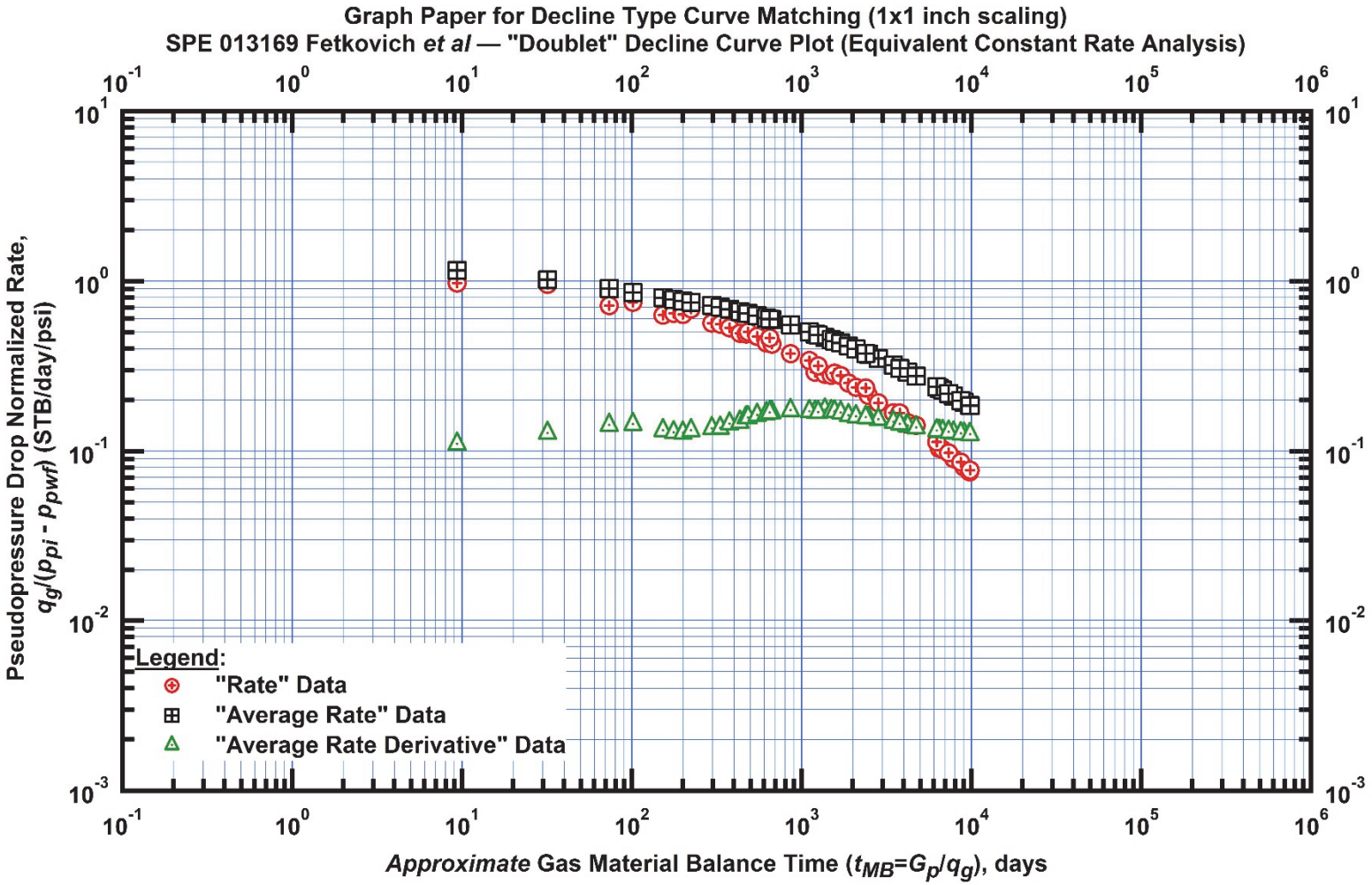

Gas Productivity Index versus Gas Material Balance Time
Fetkovich West Virginia Well A (SPE 013169)

Fetkovich, M.J., Vienot, M.E., Bradley and M.D., Kiesow, U.G.: "Decline Curve Analysis Using Type Curves – Case Histories," SPEFE (Dec. 1987) 637-656.

Reference Articles

Fetkovich, M.J.: "Decline Curve Analysis Using Type Curves," Paper SPE 4629 presented at the 1973 SPE Annual Technical Conference and Exhibition held in Las Vegas, NV 30 Sep-03 Oct 1973.

SOCIETY OF PETROLEUM ENGINEERS OF AIME
6200 North Central Expressway
Dallas, Texas 75206

PAPER NUMBER SPE 4629

THIS IS A PREPRINT --- SUBJECT TO CORRECTION

Decline Curve Analysis Using Type Curves

By

M. J. Fetkovich, Member AIME, Phillips Petroleum Co.

SOCIETY OF PETROLEUM ENGINEERS OF AIME
6200 North Central Expressway
Dallas, Texas 75206

PAPER NUMBER SPE 4629

THIS IS A PREPRINT --- SUBJECT TO CORRECTION

Decline Curve Analysis Using Type Curves

By

M. J. Fetkovich, Member AIME, Phillips Petroleum Co.

ABSTRACT

This paper shows that the decline-curve analysis approach does have a solid fundamental basis. The exponential decline is shown to be a longtime solution of the constant-pressure case. The constant-pressure infinite and finite reservoir solutions are placed on a common dimensionless curve with all the standard "empirical" exponential, hyperbolic, and harmonic decline-curve equations. Simple combinations of material balance equations and new forms of oil well rate equations for solution-gas drive reservoirs illustrate under what circumstances specific values of the hyperbolic decline exponent (1/b) or "b" should result.

Log-log type curve analysis can be performed on declining rate data (constant-terminal pressure case) completely analogous to the log-log type curve matching procedure presently being employed with constant-rate case pressure transient data. Production forecasting is done by extending a line drawn through the rate-time data overlain along the uniquely matched or best theoretical type curve. Future rates are then simply read from the real time scale on which the rate-time data is plotted. The ability to calculate kh from decline-curve data by type curve matching is demonstrated.

This paper demonstrates that decline-curve analysis not only has a solid fundamental base, but provides a tool with more diagnostic power than has previously been suspected. The type curve approach provides unique solutions upon which engineers can agree, or shows when a unique solution is not possible with a type curve only.

References and illustrations at end of paper.

INTRODUCTION

Rate-time decline-curve extrapolation is one of the oldest and most often used tools of the petroleum engineer. The various methods used have always been regarded as strictly empirical and not very scientific. Results obtained for a well or lease are subject to a wide range of alternate interpretations, mostly as a function of the experience and objectives of the evaluator. Recent efforts in the area of decline-curve analysis have been directed towards a purely computerized statistical approach. Its basic objective being to arrive at a unique "unbiased" interpretation. As pointed out in a comprehensive review of the literature by Ramsay[1], "in the period from 1964 to date, (1968), several additional papers were published which contribute to the understanding of decline-curves but add little new technology".

A new direction for decline-curve analysis was given by Slider[2] with his development of an overlay method to analyze rate-time data. Because his method was rapid and easily applied, it was used extensively by Ramsay in his evaluation of some 200 wells to determine the distribution of the decline-curve exponent term "b". Gentry's[3] Fig. 1 displaying the Arps'[4] exponential, hyperbolic, and harmonic solutions all on one curve could also be used as an overlay to match all of a wells' decline data. He did not, however, illustrate this in his example application of the curve.

The overlay method of Slider is similar in principal to the log-log type curve matching procedure presently being employed to analyze constant-rate pressure build-up and drawdown data [5-9]. The exponential decline, often used in decline-curve analysis, can be readily shown to be a long-time solution of the constant-pressure case[10-13]. It followed then that a log-log type curve matching procedure could be developed to analyze decline-curve data.

This paper demonstrates that both the analytical constant-pressure infinite (early transient period for finite systems) and finite reservoir solutions can be placed on a common dimensionless log-log type curve with all the standard "empirical" exponential, hyperbolic, and harmonic decline curve equations developed by Arps. Simple combinations of material balance equations and new forms of oil well rate equations from the recent work of Fetkovich[14] illustrate under what circumstances specific values of the hyperbolic decline exponent "b" should result in dissolved-gas drive reservoirs. Log-log type curve analysis is then performed using these curves with declining rate data completely analogous to the log-log type curve matching procedure presently being employed with constant-rate case pressure transient data.

BASIC EQUATIONS

ARPS' RATE-TIME EQUATIONS

Nearly all conventional decline-curve analysis is based on the empirical rate-time equations given by Arps[4] as

$$\frac{q(t)}{q_i} = \frac{1}{[1+bD_it]^{\frac{1}{b}}} \quad \ldots\ldots (1)$$

For b = 0, we can obtain the exponential decline equation from Eq. 1

$$\frac{q(t)}{q_i} = \frac{1}{D_it} \quad \ldots\ldots (2)$$

and for b = 1, referred to as harmonic decline, we have

$$\frac{q(t)}{q_i} = \frac{1}{[1+D_it]} \quad \ldots\ldots (3)$$

A unit solution ($D_i = 1$) of Eq. 1 was developed for values of "b" between 0 and 1 in 0.1 increments. The results are plotted as a set of log-log type curves (Fig. 1) in terms of a decline-curve dimensionless rate

$$q_{Dd} = \frac{q(t)}{q_i} \quad \ldots\ldots (4)$$

and a decline-curve dimensionless time

$$t_{Dd} = D_it \quad \ldots\ldots (5)$$

From Fig. 1 we see that when all the basic decline-curves and normal ranges of "b" are displayed on a single graph, all curves coincide and become indistinguishable at $t_{Dd} \cong 0.3$. Any data existing prior to a t_{Dd} of 0.3 will appear to be an exponential decline regardless of the true value of b and thus plot as a straight line on semi-log paper. A statistical or least-squares approach could calculate any value of b between 0 and 1.

ANALYTICAL SOLUTIONS (CONSTANT-PRESSURE AT INNER BOUNDARY)

Constant well pressure solutions to predict declining production rates with time were first published in 1933 by Moore, Schilthuis and Hurst[10], and Hurst[11]. Results were presented for infinite and finite, slightly compressible, single-phase plane radial flow systems. The results were presented in graphical form in terms of a dimensionless flow rate and a dimensionless time. The dimensionless flow rate q_D can be expressed as

$$q_D = \frac{141.3\, q(t)\, \mu B}{kh(p_i - p_{wf})} \quad \ldots\ldots (6)$$

and the dimensionless time t_D as

$$t_D = \frac{0.00634\, kt}{\phi \mu c_t r_w^2} \quad \ldots\ldots (7)$$

The original publications did not include tabular values of q_D and t_D. For use in this paper infinite solution values were obtained from Ref. 15, while the finite values were obtained from Ref. 16. The infinite solution, and finite solutions for r_e/r_w from 10 to 100,000, are plotted on Figs. 2-a and 2-b.

Most engineers utilize the constant-pressure solution not in a single constant-pressure problem but as a series of constant-pressure step functions to solve water influx problems using the dimensionless cumulative production Q_D (13). The relationship between Q_D and q_D is

$$\frac{d(Q_D)}{dt_D} = q_D \quad . \quad . \quad . \quad . \quad . \quad . \quad . \quad . \quad (8)$$

Fetkovich[17] presented a simplified approach to water influx calculations for finite systems that gave results which compared favorably with the more rigorous analytical constant-pressure solutions. Equation 3 of his paper, for a constant-pressure p_{wf}, can be written as

$$q(t) = \frac{J_o (p_i - p_{wf})}{e^{\left[\frac{(q_i)_{max}}{N_{pi}}\right] t}} \quad . \quad . \quad . \quad (9)$$

but

$$q_i = J_o (p_i - p_{wf}) \quad . \quad . \quad . \quad . \quad . \quad (10)$$

and

$$J_o = \frac{(q_i)_{max}}{p_i} \quad . \quad . \quad . \quad . \quad . \quad (11)$$

Substituting Eq. 11 into 10 we can write

$$(q_i)_{max} = \frac{q_i}{\left[1 - \frac{p_{wf}}{p_i}\right]} \quad . \quad . \quad . \quad . \quad (12)$$

Now substituting Eq. 10 and 12 into 9 we obtain

$$\frac{q(t)}{q_i} = e^{-\left[\frac{q_i t}{\left(1 - \frac{p_{wf}}{p_i}\right) N p_i}\right]} \quad . \quad . \quad (13)$$

Equation 13 can be considered as a derivation of the exponential decline equation in terms of reservoir variables and the constant-pressure imposed on the well. For the same well, different values of a single constant back-pressure p_{wf} will always result in an exponential decline i.e., the level of back-pressure does not change the type of decline. For $p_{wf} = 0$, a more realistic assumption for a well on true wide-open decline, we have

$$\frac{q(t)}{q_i} = e^{-\left[\frac{(q_i)_{max}}{N_{pi}}\right] t} \quad . \quad . \quad . \quad (14)$$

In terms of the empirical exponential decline-curve, Eq. 2, D_i is then defined as

$$D_i = \frac{(q_i)_{max}}{N_{pi}} \quad . \quad . \quad . \quad . \quad . \quad (15)$$

In terms of a dimensionless time for decline-curve analysis we have from Eqs. 5 and 15

$$t_{Dd} = \left[\frac{(q_i)_{max}}{N_{pi}}\right] t \quad . \quad . \quad . \quad . \quad (16)$$

Defining N_{pi} and $(q_i)_{max}$ in terms of reservoir variables,

$$N_{pi} = \frac{\pi (r_e^2 - r_w^2) \phi c_t h p_i}{5.615 B} \quad . \quad . \quad (17)$$

and

$$(q_i)_{max} = \frac{khp_i}{141.3 \mu B \left[\ln\left(\frac{r_e}{r_w}\right) - \frac{1}{2}\right]} \quad . \quad . \quad (18)$$

The decline-curve dimensionless time, in terms of reservoir variables, becomes

$$t_{Dd} = \frac{0.00634 kt}{\phi \mu c_t r_w^2} \cdot \frac{1}{\frac{1}{2}\left[\left(\frac{r_e}{r_w}\right)^2 - 1\right]\left[\ln\left(\frac{r_e}{r_w}\right) - \frac{1}{2}\right]} \quad . \quad . \quad (19)$$

or

$$t_{Dd} = \frac{t_D}{\frac{1}{2}\left[\left(\frac{r_e}{r_w}\right)^2 - 1\right]\left[\ln\left(\frac{r_e}{r_w}\right) - \frac{1}{2}\right]} \quad . \quad . \quad . \quad . \quad (20)$$

To obtain a decline-curve dimensionless rate q_{Dd} in terms of q_D

$$q_{Dd} = \frac{q(t)}{q_i} = q_D \left[\ln\left(\frac{r_e}{r_w}\right) - \frac{1}{2}\right] \quad . \quad . \quad (21)$$

or

$$q_{Dd} = \frac{q(t)}{\frac{kh (p_i - p_{wf})}{141.3 \mu B \left[\ln\left(\frac{r_e}{r_w}\right) - \frac{1}{2}\right]}} \quad . \quad (22)$$

The published values of q_D and t_D for the infinite and finite constant-pressure solutions were thus transformed into a decline-curve dimensionless rate and time, q_{Dd} and t_{Dd}, using Eqs. 20 and 21. Fig. 3 is a plot of the newly defined dimensionless rate and time, q_{Dd} and t_{Dd}, for various values of r_e/r_w.

At the onset of depletion, (a type of pseudo-steady state) all solutions for various values of r_e/r_w develop exponential decline and converge to a single curve. Figure 4 is a combination of the constant-pressure analytical solutions and the standard "empirical" exponential, hyperbolic, and harmonic decline-curve solutions on a single dimensionless curve. The exponential decline is common to both the analytical and empirical solutions. Note from the composite curve that rate data existing only in the transient period of the constant terminal pressure solution, if analyzed by the empirical Arps approach, would require values of "b" much greater than 1 to fit the data.

SOLUTIONS FROM RATE AND MATERIAL BALANCE EQUATIONS

The method of combining a rate equation and material balance equation for finite systems to obtain a rate-time equation was outlined in Ref. 17. The rate-time equation obtained using this simple approach, which neglects early transient effects, yielded surprisingly good results when compared to those obtained using more rigorous analytical solutions for finite aquifer systems. This rate-equation material-balance approach was used to derive some useful and instructive decline-curve equations for solution-gas drive reservoirs and gas reservoirs.

RATE EQUATIONS

Until recently, no simple form of a rate equation existed for solution-gas drive reservoir shut-in pressure. Fetkovich[14] has proposed a simple empirical rate equation for solution-gas drive reservoirs that yields results which compare favorably with computer results obtained using two-phase flow theory. The proposed rate equation was given as

$$q_o = J'_{oi} \left(\frac{\bar{p}_R}{\bar{p}_{Ri}}\right) (\bar{p}_R^2 - p_{wf}^2)^n \quad . \quad . \quad . \quad (23)$$

where n will be assumed to lie between 0.5 and 1.0.

Although the above equation has not been verified by field results, it offers the opportunity to define the decline exponent (1/b) in terms of the back pressure curve slope (n) and to study its range of expected values. Also, the initial decline rate D_i can be expressed in terms of reservoir variables. One further simplification used in the derivations is that $p_{wf} = 0$. For a well on decline, p_{wf} will usually be maintained at or near zero to maintain maximum flow rates. Equation 23 then becomes

$$q_o = J'_{oi} \left(\frac{\bar{p}_R}{\bar{p}_{Ri}}\right) (\bar{p}_R^{2n}) \quad . \quad . \quad . \quad . \quad (23A)$$

The form of Eqs. 23 and 23A could also be used to represent gas well behavior with a pressure dependent interwell permeability effect defined by the ratio $(\bar{p}_R/\bar{p}_{Ri})$. The standard form of the gas well rate equation is usually given as

$$q_g = C_g (\bar{p}_R^2 - p_{wf}^2)^n \quad . \quad . \quad . \quad . \quad (24)$$

MATERIAL BALANCE EQUATIONS

Two basic forms of a material balance equation are investigated in this study, p_R is linear with N_p or G_p, and $\bar{p}_R^2$ is linear with N_p or G_p (See Figs. 5a and 5b). The linear $\bar{p}_R$ relationship for oil is

$$\bar{p}_R = -\left(\frac{\bar{p}_{Ri}}{N_{pi}}\right) N_p + \bar{p}_{Ri} \quad . \quad . \quad . \quad . \quad (25)$$

and for gas

$$\bar{p}_R = -\left(\frac{\bar{p}_{Ri}}{G}\right) G_p + \bar{p}_{Ri} \quad . \quad . \quad . \quad . \quad (26)$$

Equation 25 is a good approximation for totally undersaturated oil reservoirs, or is simply assuming that during the decline period $\bar{p}_R$ vs. N_p can be approximated by a straight line. For gas reservoirs, Eq. 26 is correct for the assumption of gas compressibility (Z) = 1.

In terms of $\bar{p}_R^2$ being linear with cumulative production, we would have

$$\bar{p}_R^2 = -\left(\frac{\bar{p}_{Ri}^2}{N_{pi}}\right) N_p + \bar{p}_{Ri}^2 \quad . \quad . \quad (27)$$

This form of equation results in the typical shape of the pressure ($\bar{p}_R$) vs. cumulative production (N_p) relationship of a solution-gas

Fetkovich, M.J.: "Decline Curve Analysis Using Type Curves," Paper SPE 4629 presented at the 1973 SPE Annual Technical Conference and Exhibition held in Las Vegas, NV 30 Sep-03 Oct 1973.

drive reservoir as depicted in Fig. 5-b. Applications would be more appropriate in non-prorated fields, i.e., wells are produced wide-open and go on decline from initial production. This would more likely be the case for much of the decline-curve data analyzed by Cutler[18] obtained in the early years of the oil industry before proration.

RATE-TIME EQUATIONS, OIL WELLS

Rate-time equations using various combinations of material balance and rate equations were derived as outlined in Appendix B of Ref. 17. Using Eq. 23A and Eq. 25 the resulting rate-time equation is

$$\frac{q_o(t)}{q_{oi}} = \frac{1}{\left[2n\left(\frac{q_{oi}}{N_{pi}}\right)t + 1\right]^{\frac{2n+1}{2n}}} \quad . . (28)$$

A unit solution, $(q_{oi}/N_{pi}) = 1$, of Eq. 28 is plotted as a log-log type curve for various values of n, Fig. 6, in terms of the decline-curve dimensionless ltime t_{Dd}. (For these derivations with $p_{wf} = 0$, $q_{oi} \equiv (q_{oi})_{max}$. For the limiting range of back-pressure curve slopes (n) of 0.5 and 1.0, the Arps empirical decline-curve exponent (1/b) is 2.0 and 1.5 respectively or "b" = 0.500 and 0.667 respectively ___ a surprisingly narrow range. To achieve an exponential decline, n must be equal to zero, and a harmonic decline requires $n \to \infty$. In practical applications, if we assume an n of 1.0 dominates in solution-gas (dissolved-gas) drive reservoirs and $\bar{p}_R$ vs. N_p is linear for non-uniquely defined rate-time data, we would simply fit the rate-time data to the n = 1.0 curve. On the Arps' solution type curves, Fig. 1, we would use (1/b) = 2 or b = 0.667.

The rate-time equatior obtained using Eq. 23A and Eq. 27 is

$$\frac{q_o(t)}{q_{oi}} = \frac{1}{\left[0.5\left(\frac{q_{oi}}{N_{pi}}\right)t + 1\right]^{2n+1}} \quad . . (29)$$

The unit solution of Eq. 29 is plotted as a log-log type curve for various values of n, Fig. 7. This solution results in a complete reversal from that of the previous one, n = 0 yields the harmonic decline and $n \to \infty$ gives the exponential decline. For the limiting range of back-pressure curve slopes (n) of 0.5 and 1.0, the decline-curve exponent (1/b) is 2.0 and 3.0 or b = 0.500 and 0.333 respectively. This range of "b" values fits Arps' findings using Cutler's decline-curve data. He found that over 90 percent of the values of "b" lie in the range $0 \leq b \leq 0.5$. Ramsay[1] found a different distribution of the value of "b" analyzing modern rate decline data from some 202 leases. His distribution may be more a function of analyzing wells that have been subject to proration and are better represented by the assumptions underlying the rate-time solution given by Eq. 28, i.e., $\bar{p}_R$ vs. N_p was linear over the decline period.

DECLINE-CURVE ANALYSIS OF GAS WELLS

Decline-curve analysis of rate-time data obtained from gas wells has been reported in only a few instances [19, 20]. Using Eq. 24 with $p_{wf} = 0$, and Eq. 26, the rate-time equation for a gas well is

$$\frac{q_g(t)}{q_{gi}} = \frac{1}{\left[(2n-1)\left(\frac{q_{gi}}{G}\right)t + 1\right]^{\frac{2n}{2n+1}}} \quad . . . (30)$$

for all back-pressure curve slopes where $n > 0.5$.

For n = 0.5, the exponential decline is obtained

$$\frac{q_g(t)}{q_{gi}} = e^{-\left(\frac{q_{gi}}{G}\right)t} \quad . . . . . (31)$$

The unit solutions of Eqs. 30 and 31 are plotted as a log-log type curve on Fig. 8. For the limiting range of back-pressure curve slopes (n) of 0.5 and 1.0, the Arps decline-curve exponent (1/b) is ∞ and 2, or b = 0 (exponential) and 0.500 respectively.

The effect of back-pressure on a gas well is demonstrated for a back-pressure curve slope n = 1.0 on Fig. 9. The back-pressure is expressed as a ratio of p_{wf}/p_i. Note that as $p_{wf} \to p_i$ $(\Delta p \to 0)$ the type curve approaches exponential decline, the liquid case solution. Whereas back-pressure does not change the type of decline for the liquid-case solution it does change the type of decline in this case.

Using the more familiar rate and material balance equations for gas wells, we can obtain the cumulative-time relationship by integrating the rate-time equations 30 and 31 with

$$G_p = \int_o^t q_g(t)dt \quad . . . . . (32)$$

For $n > 0.5$ we obtain

$$\frac{G_p}{G} = 1 - \left[1 + (2n-1)\left(\frac{q_{gi}}{G}\right)t\right]^{\frac{1}{(1-2n)}} \quad . . (33)$$

and n = 0.5

$$\frac{G_p}{G} = 1 - e^{-\left(\frac{q_{gi}}{G}\right)t} \quad . . . . (34)$$

Log-log type curves of Eqs. 33 and 34 could be prepared for convenience in obtaining cumulative production.

TYPE CURVE ANALYSIS

Recent papers by Agarwal, et.al.[5], Ramey[6], Raghavan, et.al.[7] and Gringarten, et.al.[8], have demonstrated or discussed the application and usefulness of a type-curve matching procedure to interpret constant-rate pressure build-up and drawdown data. van Poolen[21] demonstrated the application of the type-curve procedure in analyzing flow-rate data obtained from an oil well producing with a constant pressure at the well bore. All of his data, however, were in the early transient period. No depletion was evident in his examples. This same type-curve matching procedure can be used for decline-curve analysis.

The basic steps used in type-curve matching declining rate-time data is as follows:

1. Plot the actual rate versus time data in any convenient units on log-log tracing paper of the same size cycle as the type curve to be used. (For convenience all type curves should be plotted on the same log-log scale so that various solutions can be tried.)

2. The tracing paper data curve is placed over a type curve, the coordinate axes of the two curves being kept parallel and shifted to a position which represents the best fit of the data to a type curve. More than one of the type curves presented in this paper may have to be tried to obtain a best fit of all the data.

3. Draw a line through and extending beyond the rate-time data overlain along the uniquely matched type curve. Future rates are then simply read from the real-time scale on which the rate data is plotted.

4. To evaluate decline-curve constants or reservoir variables, a match point is selected anywhere on the overlapping portion of the curves and the coordinates of this common point on both sheets are recorded.

5. If none of the type curves will reasonably fit all the data, the departure curve method [15, 22] should be attempted. This method assumes that the data is a composite of two or more different decline-curves. After a match of the late time data has been made, the matched curve is extrapolated backwards in time and the departure, or difference, between the actual rates and rates determined from the extrapolated curve at corresponding times is replotted on the same log-log scale. An attempt is then made to match the departure curve with one of the type curves. (At all times some consideration of the type of reservoir producing mechanism should be considered.) Future predictions should then be made as the sum of the rates determined from the two (or more if needed) extrapolated curves.

TYPE CURVE MATCHING EXAMPLES

Several examples will be presented to illustrate the method of using type curve matching to analyze typical declining rate-time data. The type curve approach provides unique solutions upon which engineers can agree, or shows when a unique solution is not possible with a type curve only. In the event of a non-unique solution, a most probable solution can be obtained if the producing mechanism is known or indicated.

ARPS' HYPERBOLIC DECLINE EXAMPLE

Fig. 10 illustrates a type curve match of Arps' example of hyperbolic decline[4]. Every single data point falls on the b = 0.5 type curve. This match was found to be unique in that the data would not fit any other value of "b". Future producing rates can be read directly from the real-time scale on which the data is plotted. If we wish to determine q_i and D_i, use the match points indicated on Fig. 10 as follows

$$q_{Dd} = 0.33 = \frac{q(t)}{q_i} = \frac{1000 \text{ BOPM}}{q_i}$$

$$q_i = \frac{1000 \text{ BOPM}}{0.033} = 30{,}303 \text{ BOPM}$$

$$t_{Dd} = 12.0 = D_i t = D_i \ 100 \text{ MO.}$$

$$D_i = \frac{12.0}{100 \text{ MO}} = 0.12 \text{ MO.}^{-1}$$

The data could have also been matched using the type curves on Figs. 6 and 7. In both cases the match would have been obtained with a back-pressure curve slope n = 0.5 which

Fetkovich, M.J.: "Decline Curve Analysis Using Type Curves," Paper SPE 4629 presented at the 1973 SPE Annual Technical Conference and Exhibition held in Las Vegas, NV 30 Sep-03 Oct 1973.

is equivalent to b = 0.5. Match points determined from these curves could have been used to calculate q_i and q_i/N_{pi} and finally N_{pi}.

The fact that this example was for a lease, a group of wells, and not an individual well raises an important question. Should there be a difference in results between analyzing each well individually and summing the results, or simply adding all wells production and analyzing the total lease production rate? Consider a lease or field with fairly uniform reservoir properties, "b" or n is similar for each well, and all wells have been on decline at a similar terminal wellbore pressure, p_{wf}, for a sufficient period of time to reach pseudo-steady state. According to Matthews et.al.[23] "at (pseudo) steady state the drainage volumes in a bounded reservoir are proportional to the rates of withdrawal from each drainage volume." It follows then that the ratio q_i/N_{pi} will be identical for each well and thus the sum of the results from each well will give the same results as analyzing the total lease or field production rate. Some rather dramatic illustrations of how rapidly a readjustment in drainage volumes can take place by changing the production rate of an offset well or drilling an offset well is illustrated in a paper by Marsh[24]. Similar drainage volume readjustments in gas reservoirs have also been demonstrated by Stewart[25].

For the case where some wells are in different portions of a field separated by a fault or a drastic permeability change, readjustment of drainage volumes proportional to rate cannot take place among all wells. The ratio q_i/N_{pi} may then be different for different group of wells. A total lease or field production analysis would then give different results than summing the results from individual well analysis. A similar situation can also exist for production from stratified reservoirs 26, 27, (no-crossflow).

ARPS' EXPONENTIAL DECLINE EXAMPLE

Fig. 11 shows the results of a type curve analysis of Arps' example of a well with an apparent exponential decline. In this case, there is not sufficient data to uniquely establish a value of "b". The data essentially fall in the region of the type curves where all curves coincide with the exponential solution. As shown on Fig. 11 a value of b = 0, (exponential) or b = 1.0 (harmonic) appear to fit the data equally well. (Of course all values in between would also fit the data.) The difference in forecasted results from the two extreme interpretations would be great in later years. For an economic limit of 20 BOPM, the exponential interpretation gives a total life of 285 MONTHS, the harmonic 1480 MONTHS. This points out yet a further advantage of the type curve approach, all possible alternate interpretations can be conveniently placed on one curve and forecasts made from them. A statistical analysis would of course yield a single answer, but it would not necessarily be the correct or most probable solution. Considering the various producing mechanisms we could select.

a) b = 0, (exponential), if the reservoir is highly undersaturated.

b) b = 0, (exponential), gravity drainage with no free surface[28].

c) b = 0.5, gravity drainage with a free surface[28].

d) b = 0.667, solution-gas drive reservoir, (n = 1.0) if $\bar{p}_R$ vs. N_p is linear.

e) b = 0.333, solution-gas drive reservoir, (n = 1.0) if $\bar{p}_R^2$ vs. N_p is approximately linear.

FRACTURED WELL EXAMPLE

Fig. 12 is an example of type curve matching for a well with declining rate data available both before and after stimulation. (The data was obtained from Ref. 1.) This type problem usually presents some difficulties in analysis. Both before and after frac. log-log plots are shown on Fig. 12 with the after frac. data reinitialized in time. These before and after log-log plots will exactly overlay each other indicating that the value of "b" did not change for the well after the fracture treatment. (The before frac. plot can be considered as a type curve itself and the after frac. data overlayed and matched on it.) Thus all the data were used in an attempt to define "b". When a match is attempted on the Arps unit solution type curves, it was found that a "b" of between 0.6 and 1.0 could fit the data. Assuming a solution-gas drive, a match of the data was made on the Fig. 6 type curve with n = 1.0, b = 0.667.

Using the match points for the before frac. data we have from the rate match point,

$$q_{Dd} = 0.243 = \frac{q\,(t)}{q_{oi}} = \frac{1000\ \text{BOPM}}{q_{oi}}$$

$$q_{oi} = \frac{1000\ \text{BOPM}}{.243} = 4115\ \text{BOPM}$$

From the time match point,

$$t_{Dd} = 0.60 = \left(\frac{q_{oi}}{N_{pi}}\right) t = \frac{(4115\ \text{BOPM})(100\ \text{MO})}{N_{pi}}$$

$$N_{pi} = \frac{(4115\ \text{BOPM})\ (100\ \text{MO.})}{0.60} = 685{,}833\ \text{BBL}$$

then

$$\frac{q_{oi}}{N_{pi}} = \frac{4115\ \text{BOPM}}{685{,}833} = .006000\ \text{MO.}^{-1}$$

Now using the match points for the after frac. data we have from the rate match point,

$$q_{Dd} = 0.134 = \frac{q\,(t)}{q_{oi}} = \frac{1000\ \text{BOPM}}{q_{oi}}$$

$$q_{oi} = \frac{1000\ \text{BOPM}}{0.134} = 7463\ \text{BOPM}$$

From the time match point

$$t_{Dd} = 1.13 = \left(\frac{q_{oi}}{N_{pi}}\right) t = \frac{(7463\ \text{BOPM})(100\ \text{MO.})}{N_{pi}}$$

$$N_{pi} = \frac{(7463\ \text{BOPM})\ (100\ \text{MO.})}{1.13} = 660{,}442\ \text{BBL}$$

then

$$\frac{q_{oi}}{N_{pi}} = \frac{7463\ \text{BOPM}}{660{,}442\ \text{BBL}} = .011300\ \text{MO.}^{-1}$$

We can now check the two limiting conditions to be considered following an increase in rate after a well stimulation. They are:

1. Did we simply obtain an acceleration of production, the wells reserves remaining the same?

2. Did the reserves increase in direct proportion to the increase in producing rate as a result of a radius of drainage readjustment[23]? Before treatment, N_{pi} was found to be 685,833 BBL. Cumulative production determined from the rate data prior to stimulation was 223,500 BBL. N_{pi} then at the time of the fracture treatment is

$$N_{pi} = 685{,}833\ \text{BBL} - 223{,}500\ \text{BBL} = 462{,}333\ \text{BBL}.$$

If only accelerated prodution was obtained and the reserves remained the same, $\frac{q_i}{N_{pi}}$ after the fracture treatment should have been

$$\frac{7463\ \text{BOPM}}{462{,}333\ \text{BBL}} = 0.016142\ \text{MO.}^{-1}$$

Actual (q_{oi}/N_{pi}) after treatment was 0.011300 MO.^{-1}. If the reserves increased in direct proportion to the flow-rate, the ratio q_{oi}/N_{pi} should have remained the same as that obtained prior to treatment or 0.006000 MO.^{-1}. This then would have indicated an N_{pi} of

$$N_{pi} = \frac{7463\ \text{BOPM}}{.006000\ \text{MO.}^{-1}} = 1{,}243{,}833\ \text{BBL}$$

Actual increase in reserves as a result of the fracture treatment appears to lie between the two extremes. Based on the method of analysis used, the actual increase in reserves attributable to the fracture treatment is 198,109 BBL, (660,442 BBL - 462,333 BBL).

STRATIFIED RESERVOIR EXAMPLE

This example illustrates a method of analyzing decline-curve data for a layered (no-crossflow) or stratified reservoir using type curves. The data is taken from Ref. 18 and is for the East Side Colinga Field. Ambrose[29] presented a cross section of the field showing an upper and lower oil sand separated by a continuous black shale. This layered description for the field along with the predictive equation for stratified reservoir presented in Ref. 29 led to the idea of using the departure curve method (differencing) to analyzed decline-curve data.

After Russell and Prats[27], the production rate of a well (or field) at pseudo-steady state producing a single phase liquid at the same constant wellbore pressure, ($p_{wf} = 0$ for simplicity), from two stratified layers is

$$q_T(t) = q_{il}\ e^{-\left(\frac{q_i}{N_{pi}}\right)_1 t} + q_{i2} e^{-\left(\frac{q_i}{N_{pi}}\right)_2 t} \quad \ldots \quad (35)$$

or

$$q_T(t) = q_1\,(t) + q_2\,(t) \quad \ldots \quad (36)$$

The total production from both layers then is simply the sum of two separate forecasts. Except for the special case of the ratio q_i/N_{pi} being equal for both layers, the sum of two exponentials will not in general result in another exponential.

In attempting to match the rate-time data to a type curve, it was found that the late time data can be matched to the exponential (b = 0) type curve. Fig. 13 shows this match of the late time data designated as layer 1. With this match, the curve was extrapolated backwards in time and the departure, or difference, between the actual rates determined from the extrapolated curve was replotted on the same log-log scale. See TABLE 1 for a

Fetkovich, M.J.: "Decline Curve Analysis Using Type Curves," Paper SPE 4629 presented at the 1973 SPE Annual Technical Conference and Exhibition held in Las Vegas, NV 30 Sep-03 Oct 1973.

summary of the departure curve results. The difference or first departure curve, layer 2, itself resulted in a unique fit of the exponential type curve, thus satisfying Eq. 35 which can now be used to forecast the future production. Using the match points indicated on Fig. 13 to evaluate q_i and D_i for each layer the predictive equation becomes

$$q_T(t) = 58{,}824 \text{ BOPY } e^{-(0.200)t} + 50{,}000 \text{ BOPY } e^{-(0.535)t}$$

where t is in years.

Higgins and Lechtenberg[30] named the sum of two exponentials the double semilog. They reasoned that the degree of fit of empirical data to an equation increases with the number of constants.

This interpretation is not claimed to be the only interpretation possible for this set of data. A match with b = 0.2 can be obtained fitting nearly all of the data points but can not be explained by any of the drive mechanisms so far discussed. The layered concept fits the geologic description and also offered the opportunity to demonstrate the departure curve method. The departure curve method essentially places an infinite amount of combinations of type curves at the disposal of the engineer with which to evaluate rate-time data.

EFFECT OF A CHANGE IN BACK-PRESSURE

The effect of a change in back-pressure is best illustrated by a hypothetical single well problem. The reservoir variables and conditions used for this example are given in Table 2. The analytical single-phase liquid solution of Fig. 3 is used to illustrate a simple graphical forecasting superposition procedure. The inverse procedure, the departure or differencing method can be used to analyze decline-curve data affected by back-pressure changes.

After Hurst[12], superposition for the constant-pressure case for a simple single pressure change can be expressed by

$$q(t) = \frac{kh\,(p_i - p_{wf1})}{141.3(\mu B)\left[\ln\left(\frac{r_e}{r_w}\right) - \frac{1}{2}\right]} q_{Dd}(t_{Dd}) + \frac{kh\,(p_{wf1} - p_{wf2})}{141.3(\mu B)\left[\ln\left(\frac{r_e}{r_w}\right) - \frac{1}{2}\right]} q_{Dd}(t_{Dd} - t_{Dd1})$$

or

$$q(t) = \frac{kh\,(p_i - p_{wf1})}{141.3(\mu B)\left[\ln\left(\frac{r_e}{r_w}\right) - \frac{1}{2}\right]} \cdot \left[q_{Dd}(t_{Dd}) + \left[\frac{p_{wf1} - p_{wf2}}{p_i - p_{wf1}}\right] q_{Dd}(t_{Dd} - t_{Dd1}) \right] \quad \ldots\ldots\ldots (37)$$

Up to the time of the pressure change p_{wf2} at t_{Dd1} the well production is simply q_1 as depicted on Fig. 14. The q_1 forecast as a function of time is simply made by evaluating a single set of match points using the reservoir variables given in Table 2. At p_{wf1} and $r_e/r_w' = 100$

$$t = 1 \text{ DAY}; \quad t_{Dd} = 0.006967$$

$$q_1(t) = 697 \text{ BOPD}; \quad q_{Dd} = 2.02$$

Plot the rate 697 BOPD and time of 1 day on log-log tracing paper on the same size cycle as Fig. 3. Locate the real-time points over the dimensionless time points on Fig. 3 and draw in the r_e/r_w' curve of 100 on the tracing paper. Read flow rates as a function of time directly from the real time scale.

When a change in pressure is made to p_{wf2} at t_1, t equal zero for the accompanying change in rate q_2, (really a Δq for superpostion), this rate change retraces the q_{Dd} vs. t_{Dd} curve and is simply a constant fraction of q_1

$$q_2 = q_1 \left[\frac{p_{wf1} - p_{wf2}}{p_i - p_{wf1}}\right]$$

or q_2 at t - 1 day after the rate change is equal to

$$q_2 = 697 \text{ BOPD } \frac{1000 \text{ psi} - 50 \text{ psi}}{4000 \text{ psi} - 1000 \text{ psi}} = 221 \text{ BOPD}$$

The total rate q_T after the pressure change is $q_T = q_1 + q_2$ as depicted in Fig. 14. All rates of flow for this example were read directly from the curves on Fig. 14 and summed at times past the pressure change p_{wf2}.

The practical application of this example in decline-curve analysis is that the departure or difference method can be used on rate-time data affected by a change in

back-pressure. The departure curve represented by q_2 on Fig. 14 should exactly overlay the curve represented by q_1. If it does in an actual field example, the future forecast is correctly made by extending both curves and summing them at times beyond the pressure change.

CALCULATION OF kh FROM DECLINE-CURVE DATA

Pressure build-up and decline-curve data were available from a high-pressure, highly undersaturated, low-permeability sandstone reservoir. Initial reservoir pressure was estimated to be 5790 psia at -9300 ft. with a bubble-point pressure of 2841 psia. Two field-wide pressure surveys were conducted while the reservoir was still undersaturated. Table 3 summarizes the reservoir properties and basic results obtained from the pressure build-up analysis on each well. Note that nearly all wells had negative skins as a result of hydraulic fracture treatments. Also, appearing on this table are results obtained from an attempt to calculate kh using decline-curve data available for each of the wells.

Ten of the twenty-two wells started on decline when they were first placed on production. As a result, the early production decline data existed in the transient period and a type curve analysis using Fig. 3 was matched to one of the r_e/r_w stems. Other wells listed on the table, where an r_e/r_w match is not indicated, were prorated wells and began their decline several months after they were first put on production. For the decline-curve determination of kh, the reservoir pressure existing at the beginning of decline for each well was taken from the pressure history match of the two field-wide pressure surveys. The constant bottom hole flowing pressure for the wells ranged between 800 and 900 psia.

A type curve match using decline-curve data to calculate kh for well No. 13 is illustrated on Fig. 15. A type curve match using pressure build-up data obtained on this same well is illustrated on Fig. 16. The constant-rate type curve of Gringarten et.al.[8] for fractured wells was used for matching the pressure build-up data. The build-up kh of 47.5 md.-ft. compares very well with the kh of 40.5 MD-FT determined by using the rate-time decline-curve data.

In general, the comparison of kh determined from decline-curve data and pressure build-up data tabulated on Table 3 is surprisingly good. (The pressure build-up analysis was performed independently by another engineer.) One fundamental observation to be made from the results obtained on wells where a match of r_e/r_w was not possible is that the effective wellbore radius r_w' (obtained from the build-up analysis) is used to obtain a good match between build-up and decline-curve calculated kh.

TYPE CURVES FOR KNOWN RESERVOIR AND FLUID PROPERTIES

All the type curves so far discussed were developed for decline-curve analysis using some necessary simplifying assumptions. For specific reservoirs, when PVT data, reservoir variables, and back-pressure tests are available, type curves could be generated for various relative permeability curves and back-pressures. These curves developed for a given field would be more accurate for analyzing decline data in that field. Conventional material balance programs or more sophisticated simulation models could be used to develop dimensionless constant-pressure type curves as was done by Levine and Fratts[31] (See their Fig. 11).

CONCLUSIONS

Decline-curve analysis not only has a solid fundamental base, but provides a tool with more diagnostic power than has previously been suspected. The type curve approach provides unique solutions upon which engineers can agree, or shows when a unique solution is not possible with a type curve only. In the event of a non-unique solution, a most probable solution can be obtained if the producing mechanism is known or indicated.

NOMENCLATURE

b	=	Reciprocal of decline curve exponent (1/b)
B	=	Formation volume factor, res. vol./ surface vol.
c_t	=	Total compressibility, psi^{-1}
C_g	=	Gas well back-pressure curve coefficient
D_i	=	Initial Decline rate, t^{-1}
e	=	Natural logarithm base 2.71828
G	=	Initial gas-in-place, surface measure
G_p	=	Cumulative gas production, surface measure
h	=	Thickness, ft.
J_o	=	Productivity index, STK BBL/DAY/PSI
J'_o	=	Productivity index (back-pressure curve coefficient) STK BBL/DAY/$(psi)^{2n}$
k	=	Effective permeability, md.
n	=	Exponent of back-pressure curve
N_p	=	Cumulative oil production, STK BBL

Fetkovich, M.J.: "Decline Curve Analysis Using Type Curves," Paper SPE 4629 presented at the 1973 SPE Annual Technical Conference and Exhibition held in Las Vegas, NV 30 Sep-03 Oct 1973.

N_{pi} = Cumulative oil production to a reservoir shut-in pressure of 0, STK BBL

P_i = Initial pressure, psia

$\bar{P}_R$ = Reservoir average pressure (shut-in pressure), psia

P_{wf} = Bottom-hole flowing pressure, psia

q_i = Initial surface rate of flow at t = 0

$(q_i)_{max}$ = Initial wide-open surface flow rate at $P_{wf} = 0$

$q(t)$ = Surface rate of flow at time t

q_D = Dimensionless rate, (Eq. 6)

q_{Dd} = Decline curve dimensionless rate, (Eq. 4)

Q_D = Dimensionless cumulative production

r_e = External boundary radius, ft.

r_w = Wellbore radius, ft.

r'_w = Effective wellbore radius, ft.

t = Time, (Days for t_D)

t_D = Dimensionless time, (Eq. 7)

t_{Dd} = Decline curve dimensionless time, (Eq. 5)

ϕ = Porosity, fraction of bulk volume

μ = Viscosity, cp.

REFERENCES

1. Ramsay, H. J., Jr.: "The Ability of Rate-Time Decline Curves to Predict Future Production Rates", M.S. Thesis, U. of Tulsa, Tulsa, Okla. (1968).

2. Slider, H. C.: "A Simplified Method of Hyperbolic Decline Curve Analysis", J. Pet. Tech. (March, 1968), 235.

3. Gentry, R. W.: "Decline-Curve Analysis", J. Pet. Tech. (Jan., 1972) 38.

4. Arps, J. J.: "Analysis of Decline Curves", Trans. AIME (1945) 160, 228.

5. Ramey, H. J., Jr.: "Short-Time Well Test Data Interpretation in the Presence of Skin Effect and Wellbore Storage", J. Pet. Tech. (Jan., 1970) 97.

6. Agarwal, R., Al-Hussainy, R. and Ramey, H. J., Jr.: "An Investigation of Wellbore Storage and Skin Effect in Unsteady Liquid Flow: I. Analytical Treatment:, Soc. Pet. Eng. J. (Sept., 1970) 279.

7. Raghavan, R., Cady, G. V. and Ramey, H. J., Jr.: "Well-Test Analysis for Vertically Fractured Wells", J. Pet. Tech. (Aug. 1972) 1014.

8. Gringarten, A. C., Ramey, H. J., Jr. and Raghavan, R.: "Pressure Analysis for Fractured Wells", Paper SPE 4051 presented at the 47th Annual Fall Meething, San Antonio, Texas, (Oct 8-11, 1972).

9. McKinley, R. M.: "Wellbore Transmissibility from Afterflow-Dominated Pressure Buildup Data", J. Pet. Tech. (July, 1971) 863.

10. Moore, T. V., Schilthuis, R. J. and Hurst, W.: "The Determination of Permeability from Field Data", Bull. API (May, 1933) 211, 4.

11. Hurst, W.: "Unsteady Flow of Fluids in Oil Reservoirs", Physics, (Jan., 1934) 5, 20.

12. Hurst, W.: "Water Influx into a Reservoir and Its Application to the Equation of Volumetric Balance", Trans., AIME (1943) 151, 57.

13. van Everdingen, A. F. and Hurst, W.: "The Application of the Laplace Transformation to Flow Problems in Reservoirs", Trans. AIME (1949) 186, 305.

14. Fetkovich, M. J.: "The Isochronal Testing of Oil Wells", Paper SPE 4529 presented at the 48th Annual Fall Meeting, Las Vegas, Nevada, (Sept. 30-Oct. 3, 1973).

15. Ferris, J., Knowles, D. B., Brown, R. H., and Stallman, R. W.: "Theory of Aquifer Tests", U. S. Geol. Surv., Water Supply Paper 1536E (1962), 109.

16. Tsarevich, K. A. and Kuranov, I. F.: "Calculation of the Flow Rates for the Center Well in a Circular Reservoir Under Elastic Conditions", Problems of Reservoir Hydrodynamics Part I, Leningrad, (1966), 9-34.

17. Fetkovich, M. J.: "A Simplified Approach to Water Influx Calculations-Finite Aquifer Systems", J. Pet. Tech. (July, 1971) 814.

18. Cuttler, W. W., Jr.: "Estimation of Underground Oil Reserves by Oil-Well Production Curves", Bull., USBM (1924)228.

19. Stewart, P. R.: "Low-Permeability Gas Well Performance at Constant Pressure", J. Pet. Tech. (Sept. 1970) 1149.

20. Gurley, J.: "A Productivity and Economic Projection Method-Ohio Clinton Sand Gas Wells", Paper SPE 686 presented at the 38th Annual Fall Meeting, New Orleans, La., (Oct. 6-9, 1963).

21. van Poollen, H. K.: "How to Analyze Flowing Well-Test Data... with Constant Pressure at the Well Bore", Oil and Gas Journal (Jan. 16, 1967).

22. Witherspoon, P. A., Javandel, I., Neuman, S. P. and Freeze, P. A.: "Interpretation of Aquifer Gas Storage Conditions from Water Pumping Tests", Monograph AGA, New York (1967) 110.

23. Matthews, C. S., Brons, F. and Hazebroek, P.: "A Method for Determination of Average Pressure in a Bounded Reservoir", Trans., AIME (1954) 201, 182.

24. Marsh, H. N.: "Method of Appraising Results of Production Control of Oil Wells", Bull., API (Sept., 1928) 202, 86.

25. Stewart, P. R.: "Evaluation of Individual Gas Well Reserves", Pet. Eng. (May, 1966) 85.

26. Lefkovits, H. C. and Matthews, C. S.: "Application of Decline Curves to Gravity-Drainage Reservoirs in the Stripper Stage", Trans., AIME (1958) 213, 275.

27. Russel, D. G. and Prats, M.: "Performance of Layered Reservoirs with Crossflow---- Single-Compressible Fluid Case", Soc. Pet. Eng. J. (March, 1962) 53.

28. Matthews, C. S. and Lefkovits, H. C.: "Gravity Drainage Performance of Depletion-Type Reservoirs in the Stripper Stage", Trans., AIME (1956) 207, 265.

29. Ambrose, A. W.: "Underground Conditions in Oil Fields", Bull., USBM (1921) 195, 151.

30. Higgins, R. V. and Lechtenberg, H. J.: "Merits of Decline Equations Based on Production History of 90 Reservoirs", Paper SPE 2450 presented at the Rocky Mt. Regional Meeting, Denver, Colo., (May 25-27, 1969).

31. Levine, J. S. and Prats, M.: "The Calculated Performance of Solution-Gas Drive Reservoirs", Soc. Pet. Eng. J. (Sept., 1961) 142.

ACKNOWLEDGEMENT

I wish to thank Phillips Petroleum Co. for permission to publish this paper.

NOTE: The author has a limited quantity of full size type curves with grid suitable for actual use which are available on written request.

Fetkovich, M.J.: "Decline Curve Analysis Using Type Curves," Paper SPE 4629 presented at the 1973 SPE Annual Technical Conference and Exhibition held in Las Vegas, NV 30 Sep-03 Oct 1973.

TABLE 1 - SUMMARY OF RATE-TIME DATA FROM EAST SIDE COALINGA FIELD[7] WITH THE RESULTS FROM THE DEPLETION CURVE METHOD

Time Yrs.	(1) Total Field Rate-q_T BOPY	(2) Layer 1 Rate-q_1 BOPY	(1)-(2) Layer 2 Rate-q_2 BOPY
0.5	90,000	52,000*	38000
1.5	64,000	42,500*	21500
2.5	48,000	34,500*	13500
3.5	36,000	28,500*	7500
4.5	27,500	23,000*	4500
5.5	21,250	18,600*	2650
6.5	16,250	15,000*	1250
7.5	13,000	12,500*	500
8.5	10,500	10,500	0
9.5	8,500	8,500	
10.5	6,900	6,900	
11.5	5,600	5,600	
12.5	4,550	4,550	
13.5	3,800	3,800	
14.5	3,200	3,200	
15.5	2,750	2,750	

* Taken from layer 1 curve Fig. 13.

TABLE 1 - DATA FOR EXAMPLE PROBLEM OF A GAS WELL

P_i = 4000 psia

$P_{wf(1)}$ = 1000 psia

$P_{wf(2)}$ = 50 psia

k = 1 md

h = 100 FT

μ_o = 1 cps.

B_o = 1.50 RB/STB BBL

c_t = 20 X 10^{-6} psi^{-1}

r_e = 1053 FT. (80 acres)

r_w' = 10.53 FT (stimulated Well)

$$t_D = \frac{.00634\,kt}{\phi \mu c_t r_w'^2} = \frac{.00634\,(1)\,t}{(.20)(1.0)(20\times10^{-6})(10.53)^2} = 14.20\,t$$

$$t_{Dd} = \frac{14.2\,t}{\frac{1}{2}[(10.5)^2-1][\ln(10.5)-.5]} = .0047\,t_{Days}$$

$$q_{Dd} = \frac{q(t)}{kh(P_i-P_{wf})} \Big/ \frac{q(t)}{1.127(3000)} = \frac{q(t)}{(141.3)(1)(.5)(4.20)} = \frac{q(t)}{345}$$

$q(t) = q_{Dd}(t_{DA})\,345$ or $q(t) = 345\,q_{Dd}(t_{DA})$ at $t = 1$ yr

$q(t) = 650$ BOPD

TABLE 2 - [illegible]

Well No.	h FT.	ϕ %	S_{we} %	Pressure Build-Up Results Skin S	r_w' FT.	kh Md. FT.	Decline Curve Analysis Results $\frac{r_e}{r_w'}$ Matched	q_{Dd} 10,000 FGHK	$\frac{P_i - P_{wf}}{(\mu_o B_o)}$	[illegible] MMcf	[illegible] Bcf
1	34	9.4	32.9	-0.73	0.3	170.5	*	.52	6658	.68	3.10
2	120	10.5	18.3	-2.65	3.5	56.7	*	.68	7575	.42	0.38
3	32	9.9	20.4	-3.71	10.3	63.0	*	.43	8240	.61	3.07
4	63	9.5	18.6	-3.41	7.6	28.5	40	.58	8273	.3[illegible]	3.47
5	67	10.2	15.1	-4.29	18.3	44.4	70	.57	6856	.3[illegible]	3.[illegible]
6	78	10.3	12.6	-2.67	2.6	57.9	*	.56	7674	.6[illegible]	[illegible]
7	37	10.0	17.5	-3.41	7.6	16.8	30	1.30	7788	.[illegible]	3.46
8	47	9.1	24.2	-3.74	10.6	16.6	30	1.14	7375	.3[illegible]	0.[illegible]
9	89	10.2	18.0	-4.19	16.5	164.7	*	.435	5642	.7[illegible]	[illegible]
10	46	10.4	21.7	-5.8[illegible]	82.6	363.2	*	.36	1211	.05[illegible]	[illegible]
11	25	11.5	19.2	-1.06	2.0	59.9	*	.56	7669	.6[illegible]	[illegible]
12	35	12.1	17.0	-3.67	13.3	8.9	50	3.30	5045	9.5	0.50
13	121	10.1	18.8	-3.85	11.8	47.5	50	.54	7259	40.5	0.53
14	71	9.4	20.4	-4.10	15.0	224.8	*	.32	5737	1.04	2.42
15	49	10.9	28.6	-3.59	9.1	101.9	*	.43	4312	11.[illegible]	2.[illegible]
16	35	10.0	25.6	-4.57	24.2	14.3	20	.95	5110	.24	0.09
17	62	8.8	22.4	-3.12	5.7	27.2	*	.82	8198	.3[illegible]	0.[illegible]
18	75	9.4	18.1	-1.56	1.2	65.1	*	.52	6344	.93	1.24
19	38	8.9	19.2	-2.11	2.1	40.5	20	.54	6728	.32	0.64
20	60	9.6	24.6	-5.48	66.1	88.1	*	.34[illegible]	5[illegible]	.6[illegible]	3.67
21	56	11.1	16.5	-2.19	2.2	39.1	20	.72	5428	.20	0.54
22	40	8.9	22.5	-3.79	11.[illegible]	116.0	100	.40	8114	.5[illegible]	1.28

* r_w' used from build-up analysis with r_e of 1490 Ft.

Fetkovich, M.J.: "Decline Curve Analysis Using Type Curves," Paper SPE 4629 presented at the 1973 SPE Annual Technical Conference and Exhibition held in Las Vegas, NV 30 Sep-03 Oct 1973.

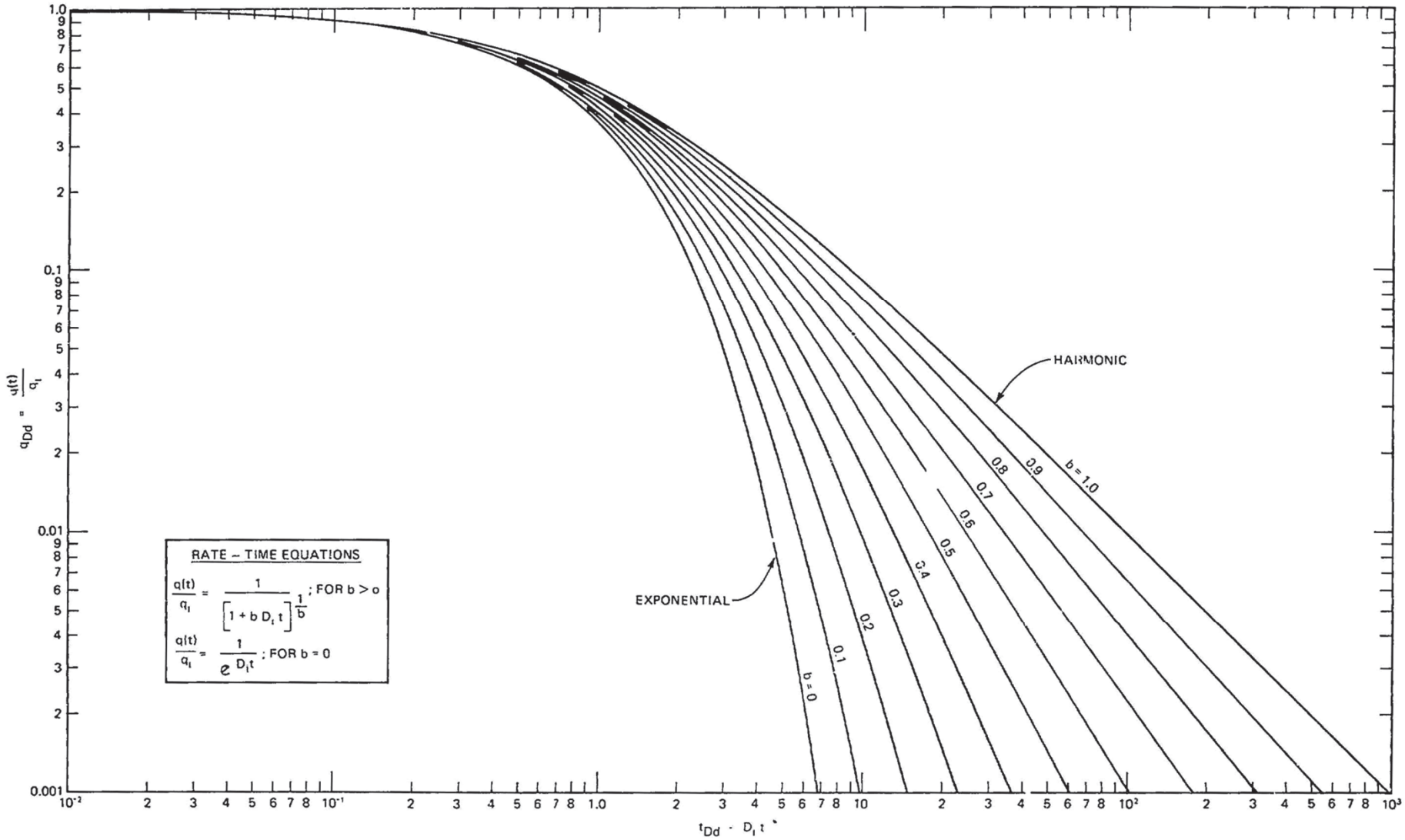

Fig. 1 - Type curves for Arps empirical rate-time decline equations, unit solution ($D_i = 1$).

Fetkovich, M.J.: "Decline Curve Analysis Using Type Curves," Paper SPE 4629 presented at the 1973 SPE Annual Technical Conference and Exhibition held in Las Vegas, NV 30 Sep-03 Oct 1973.

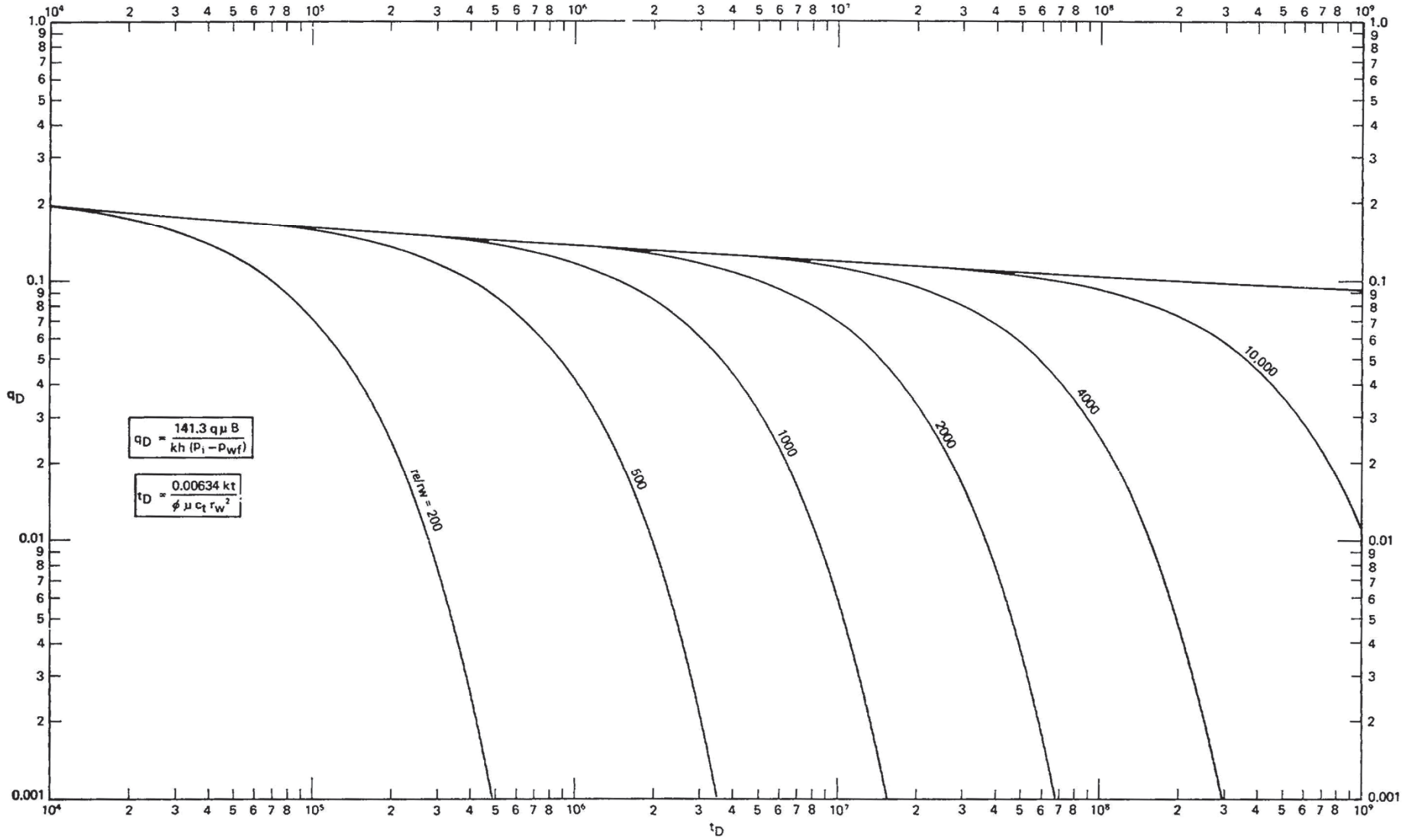

Fig. 2B - Dimensionless flow rate functions plane radial system infinite and finite outer boundary, constant pressure at inner boundary.[10,11,15,16]

Fetkovich, M.J.: "Decline Curve Analysis Using Type Curves," Paper SPE 4629 presented at the 1973 SPE Annual Technical Conference and Exhibition held in Las Vegas, NV 30 Sep-03 Oct 1973.

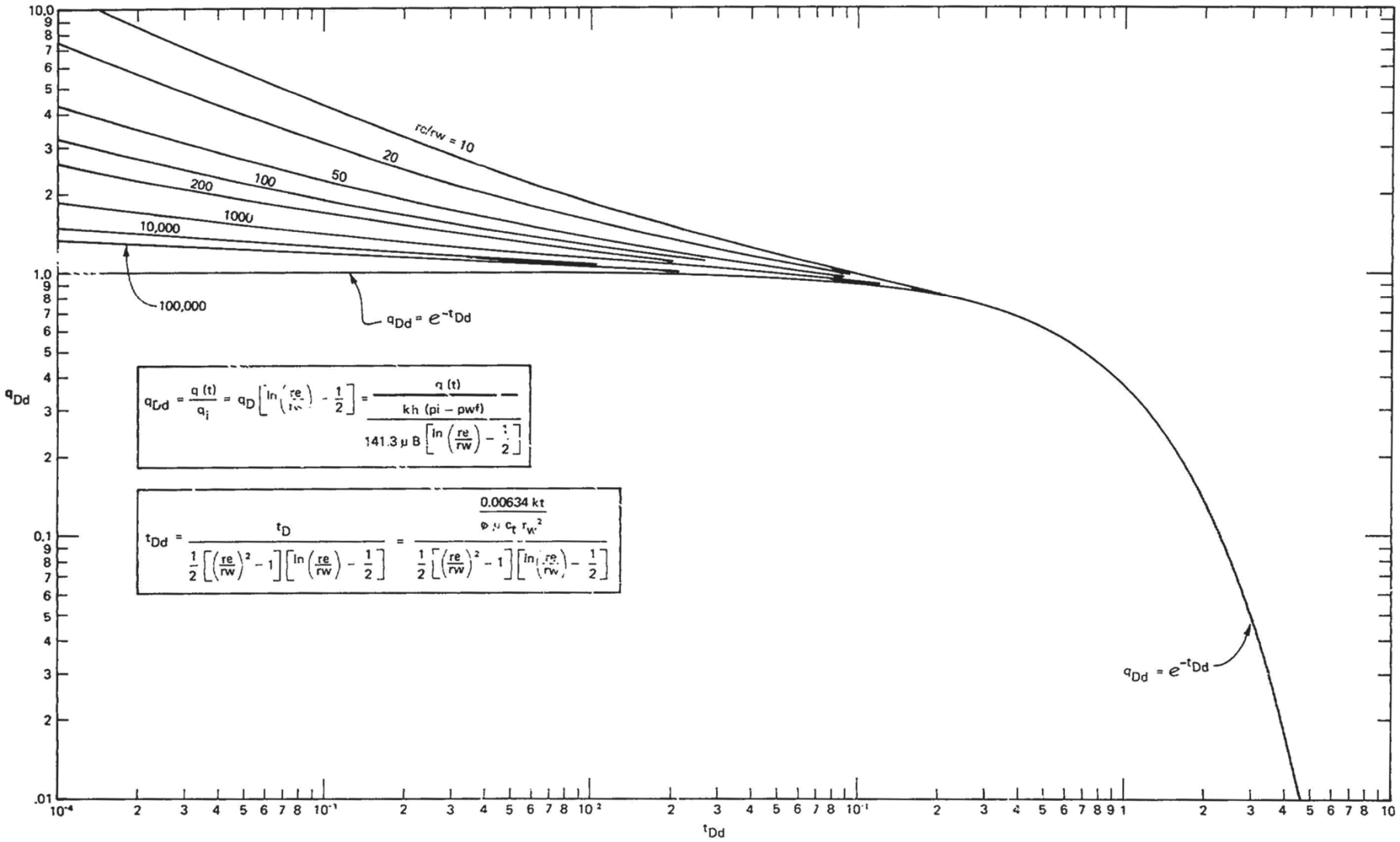

Fig. 3 - Dimensionless flow rate functions for plane radial system, infinite and finite outer boundary, constant pressure at inner boundary.

Fetkovich, M.J.: "Decline Curve Analysis Using Type Curves," Paper SPE 4629 presented at the 1973 SPE Annual Technical Conference and Exhibition held in Las Vegas, NV 30 Sep-03 Oct 1973.

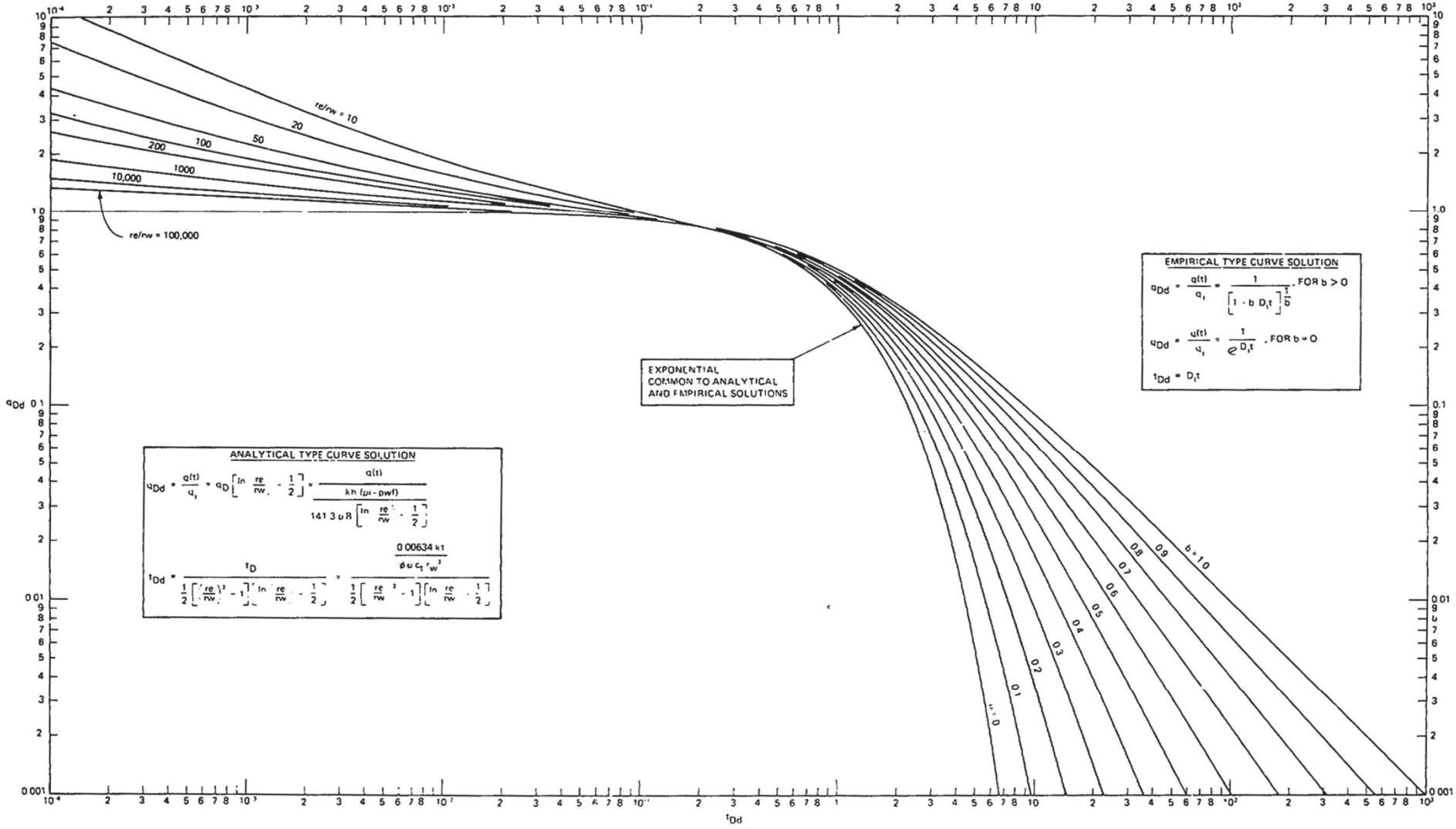

Fig. 4 - Composite of analytical and empirical type curves of Figs. 1 and 3.

Fetkovich, M.J.: "Decline Curve Analysis Using Type Curves," Paper SPE 4629 presented at the 1973 SPE Annual Technical Conference and Exhibition held in Las Vegas, NV 30 Sep-03 Oct 1973.

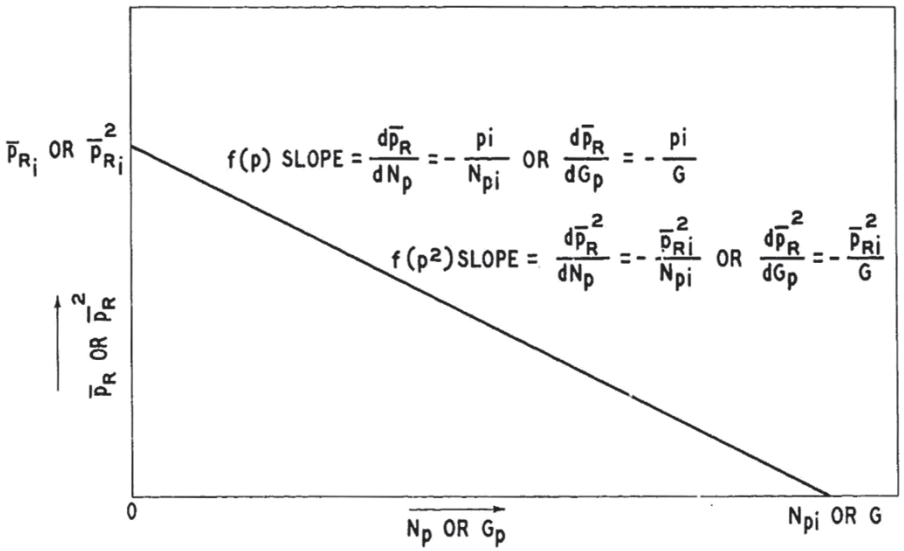

Fig. 5A - Graphical representation of material balance equation.

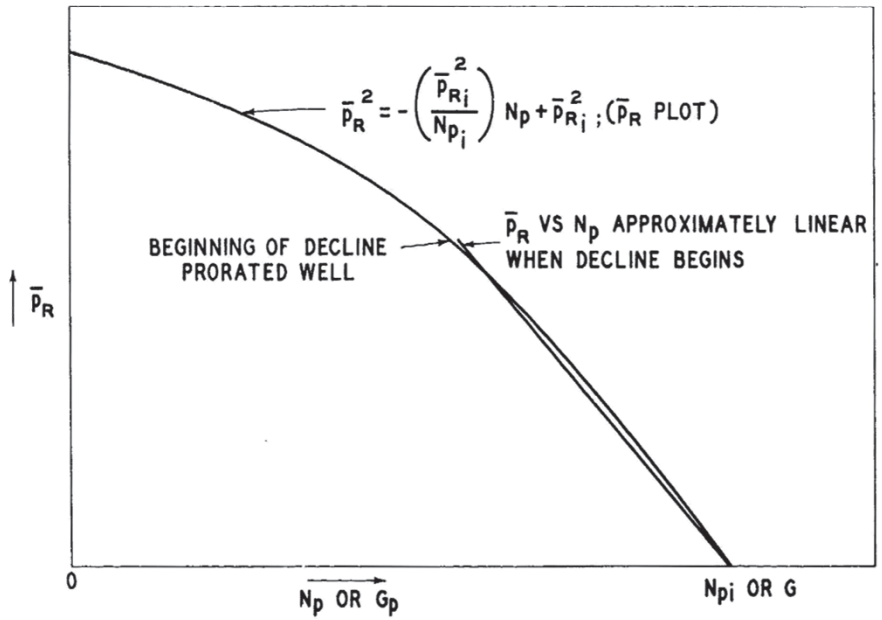

Fig. 5B - Graphical representation of material balance equation.

Fetkovich, M.J.: "Decline Curve Analysis Using Type Curves," Paper SPE 4629 presented at the 1973 SPE Annual Technical Conference and Exhibition held in Las Vegas, NV 30 Sep-03 Oct 1973.

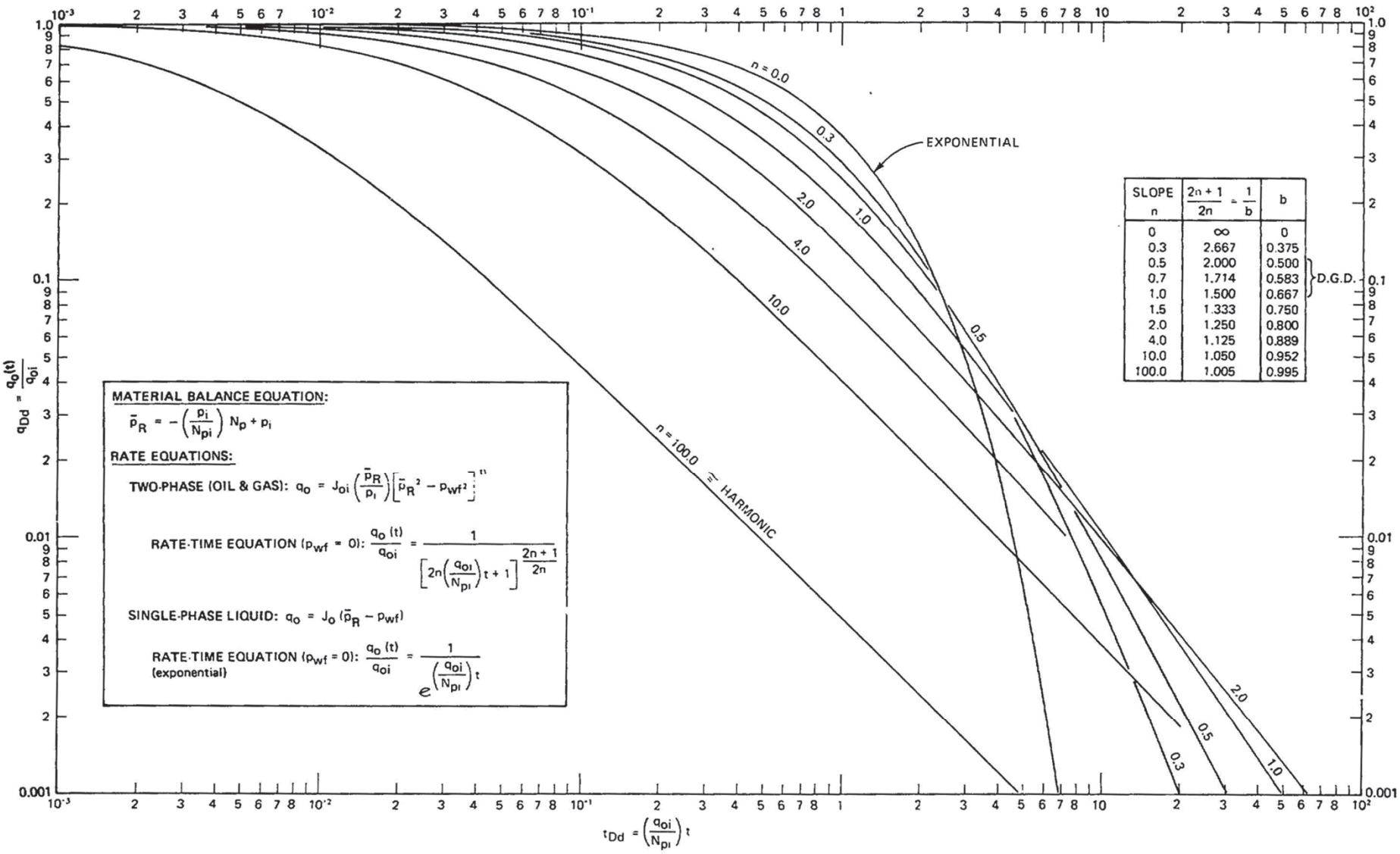

Fig. 6 - Dissolved gas drive reservoir rate - decline type curves finite system with constant pressure at inner boundary (p_{wf} = 0 @ r_w). Early transient effects not included.

Fetkovich, M.J.: "Decline Curve Analysis Using Type Curves," Paper SPE 4629 presented at the 1973 SPE Annual Technical Conference and Exhibition held in Las Vegas, NV 30 Sep-03 Oct 1973.

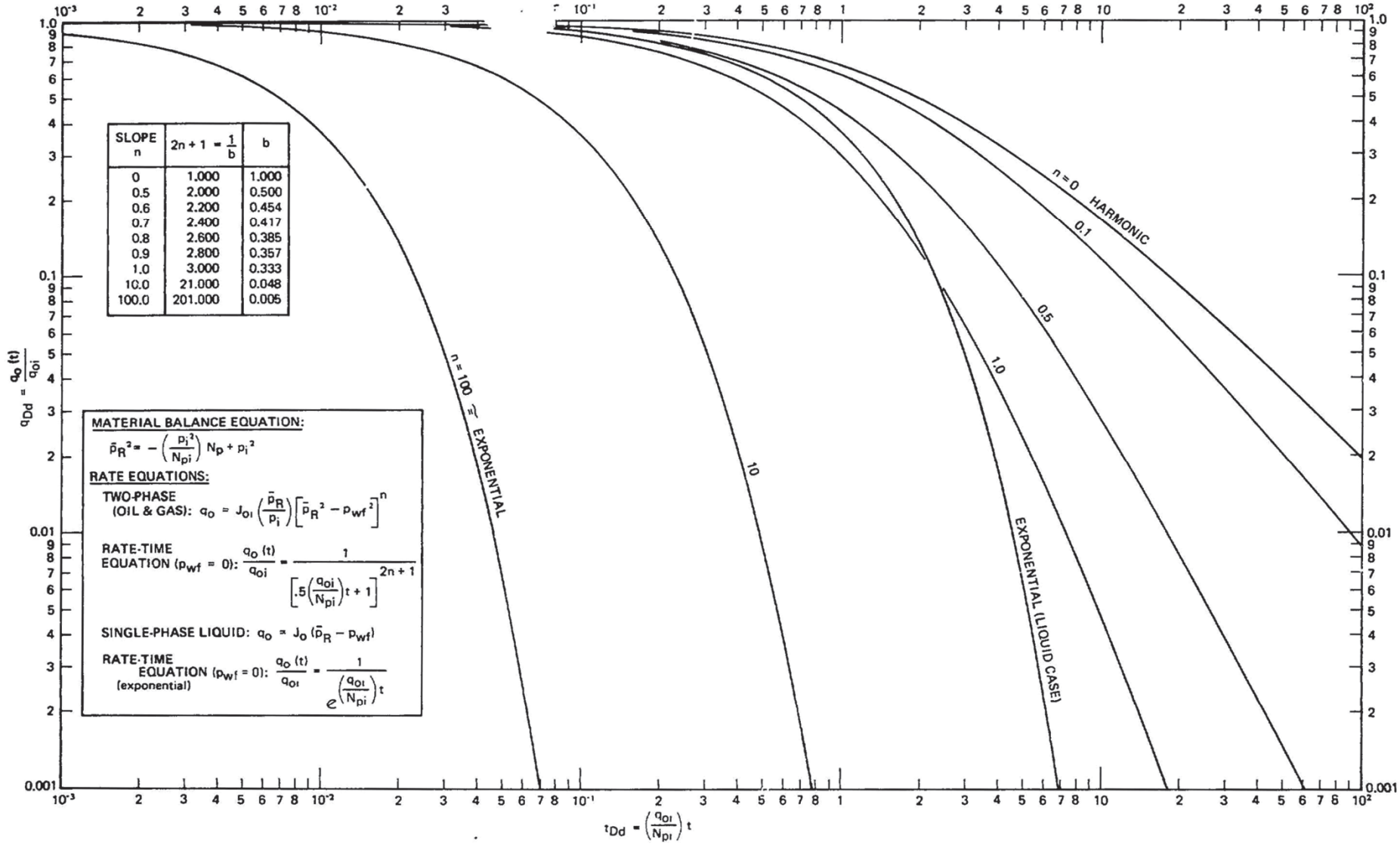

Fig. 7 - Dissolved gas drive reservoir rate - decline type curves finite system with constant pressure at inner boundary (p_{wf} = 0 @ r_w). Early transient effects not included.

Fetkovich, M.J.: "Decline Curve Analysis Using Type Curves," Paper SPE 4629 presented at the 1973 SPE Annual Technical Conference and Exhibition held in Las Vegas, NV 30 Sep-03 Oct 1973.

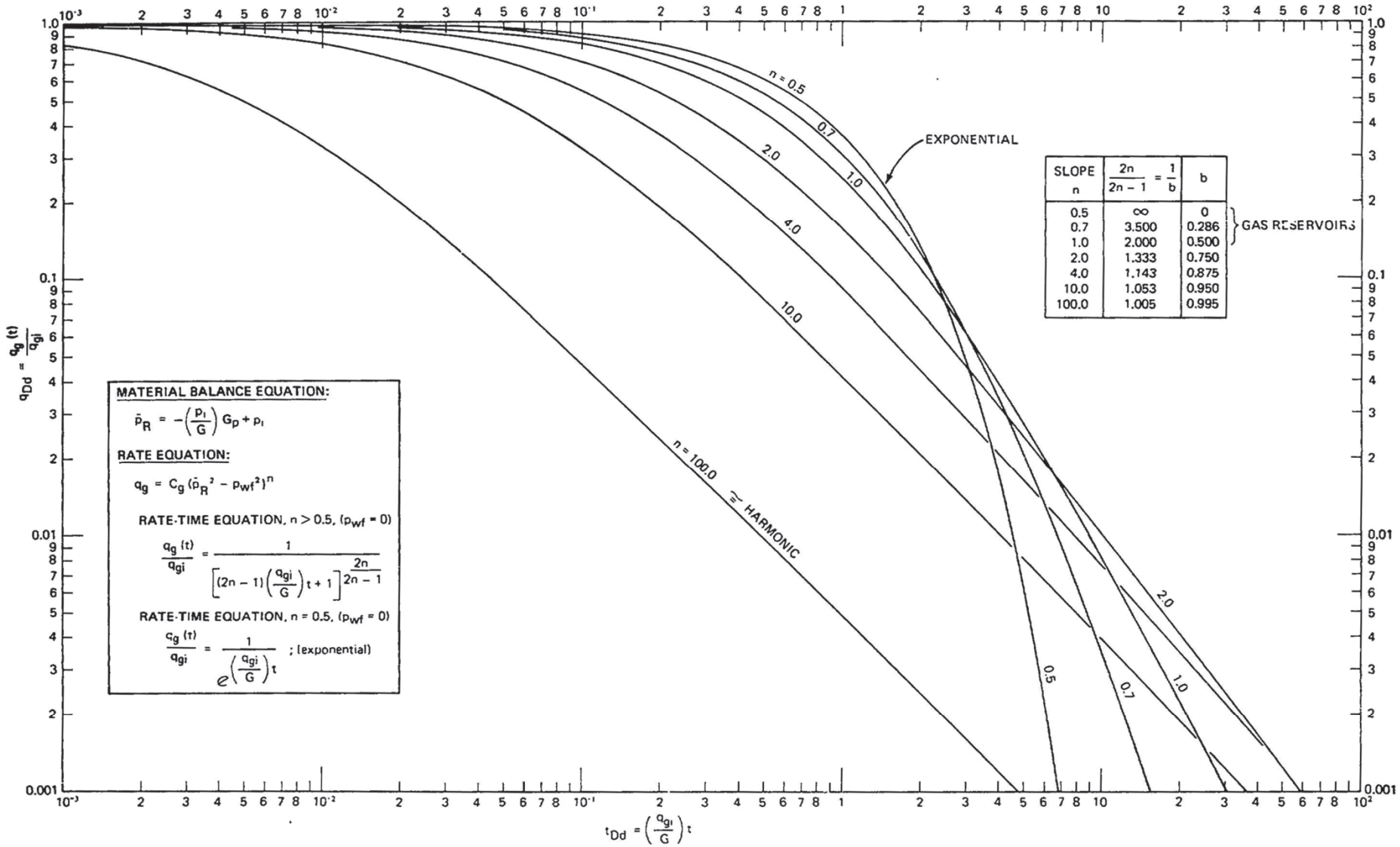

Fig. 8 - Gas reservoir rate - decline type curves finite system with constant pressure at inner boundary (p_{wf} = 0 @ r_w). Early transient effects not included.

Fetkovich, M.J.: "Decline Curve Analysis Using Type Curves," Paper SPE 4629 presented at the 1973 SPE Annual Technical Conference and Exhibition held in Las Vegas, NV 30 Sep-03 Oct 1973.

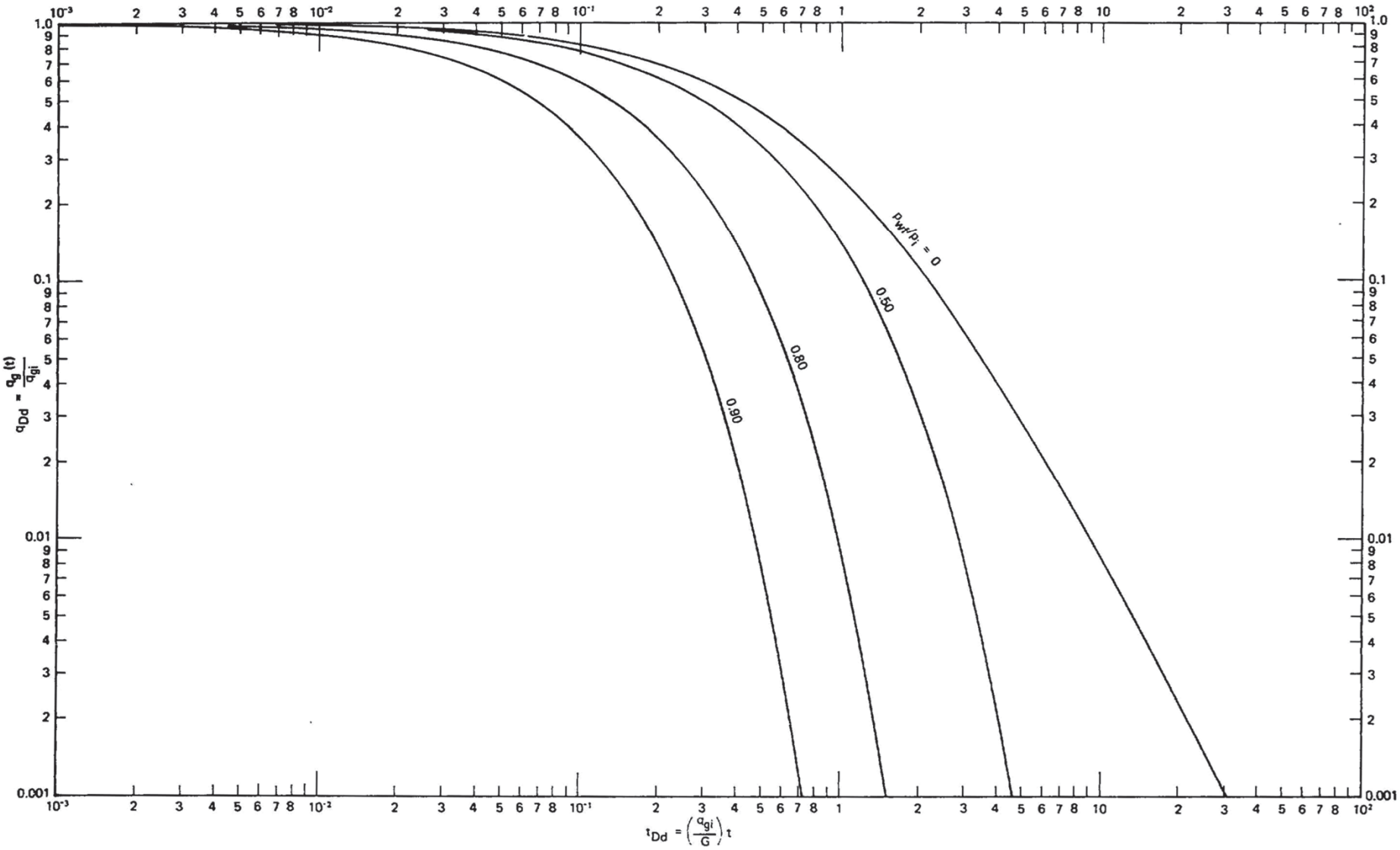

Fig. 9 - Gas reservoir rate decline type curves with back pressure finite system with constant pressure at inner boundary (p_{wf} = constant @ r_w). Early transient effects not included and z = 1 (based on gas well back pressure curve slope, n = 1.

Fetkovich, M.J.: "Decline Curve Analysis Using Type Curves," Paper SPE 4629 presented at the 1973 SPE Annual Technical Conference and Exhibition held in Las Vegas, NV 30 Sep-03 Oct 1973.

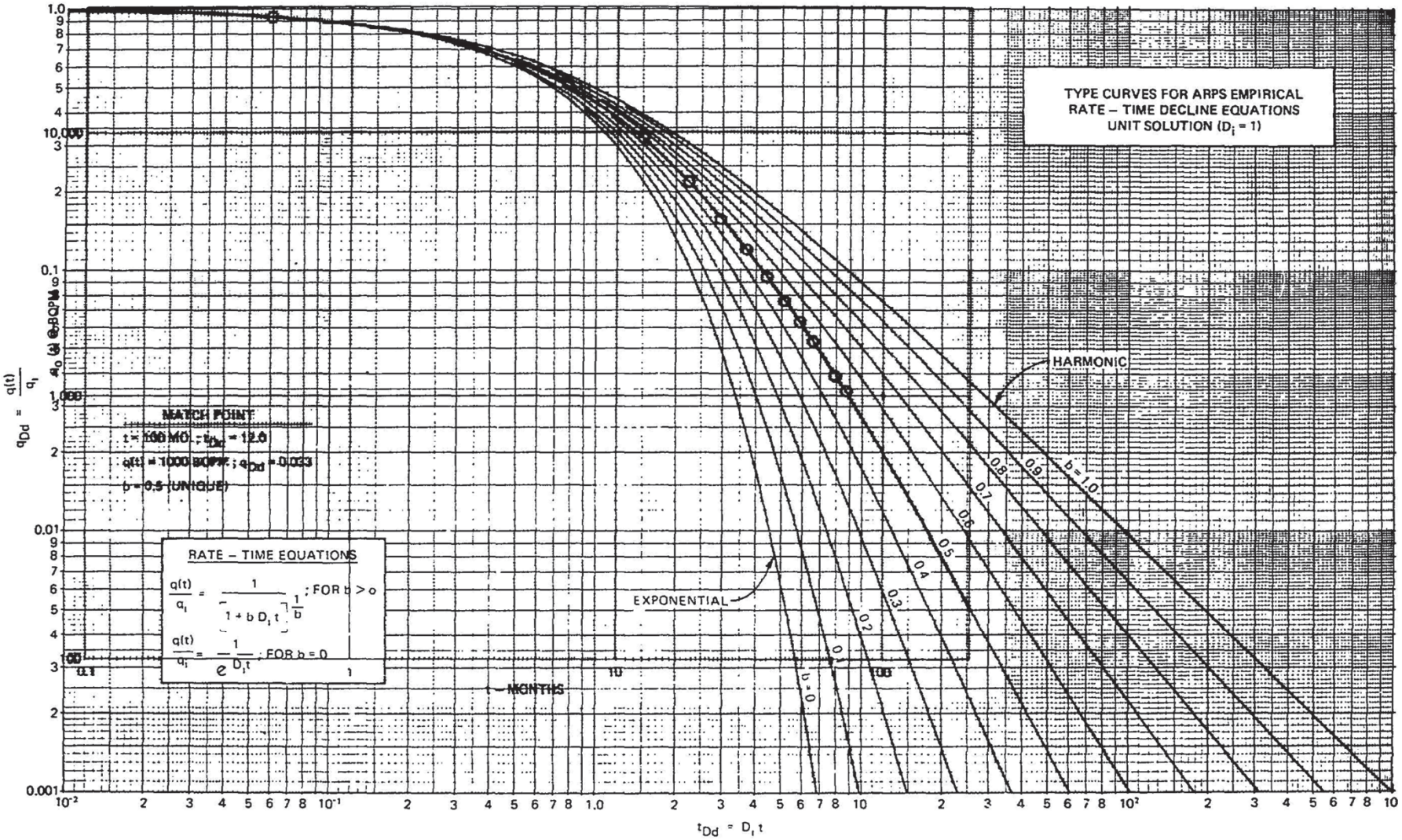

Fig. 10 - Type-curve match of Arps' hyperbolic decline example,[4] (unique match).

Fetkovich, M.J.: "Decline Curve Analysis Using Type Curves," Paper SPE 4629 presented at the 1973 SPE Annual Technical Conference and Exhibition held in Las Vegas, NV 30 Sep-03 Oct 1973.

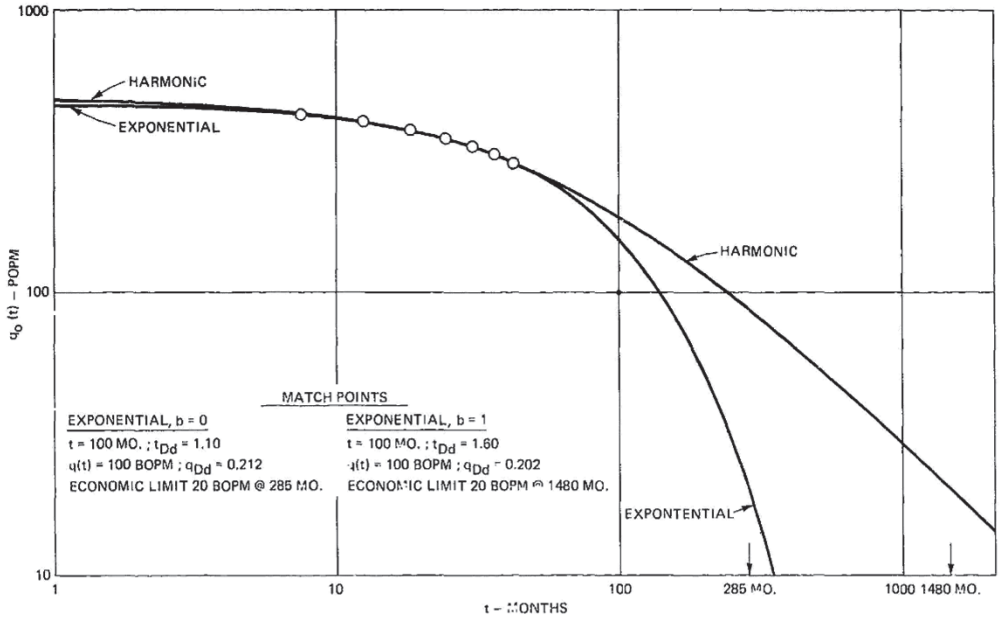

Fig. 11 - Type-curve analysis of Arps' exponential decline example.

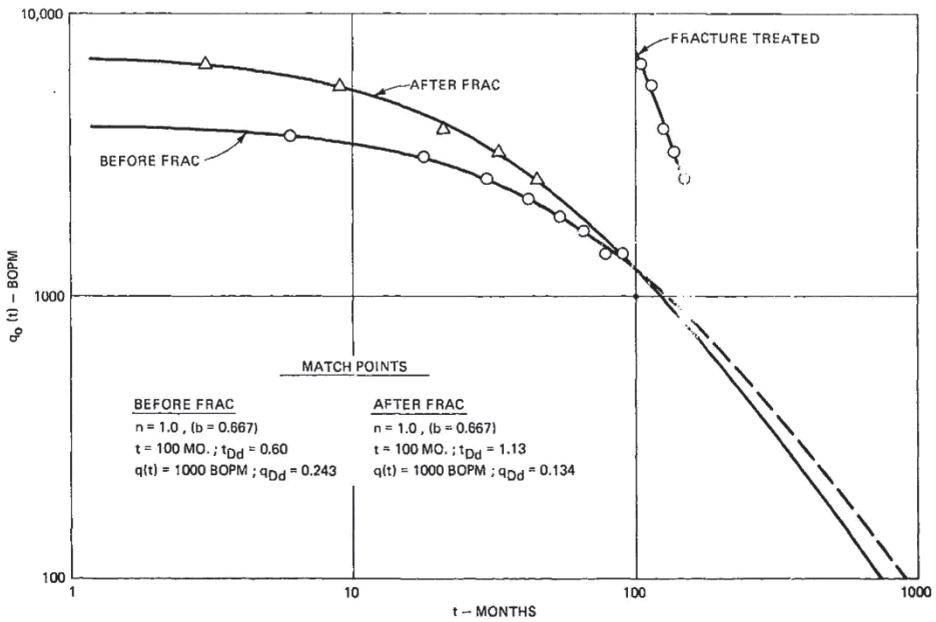

Fig. 12 - Type-curve analysis of a stimulated well before and after fracture treatment.

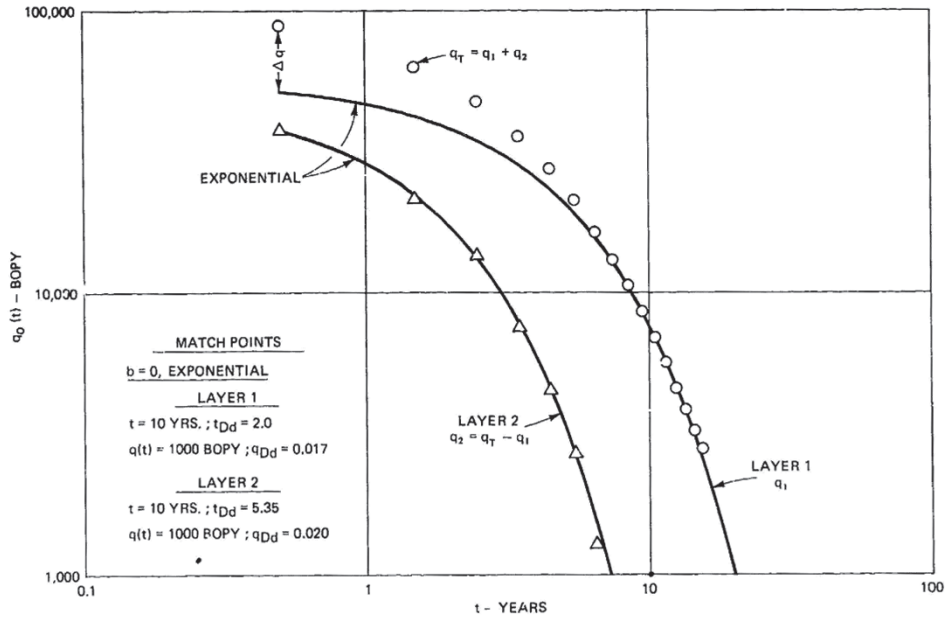

Fig. 13 - Type-curve analysis of a layered reservoir (no crossflow) by differencing.

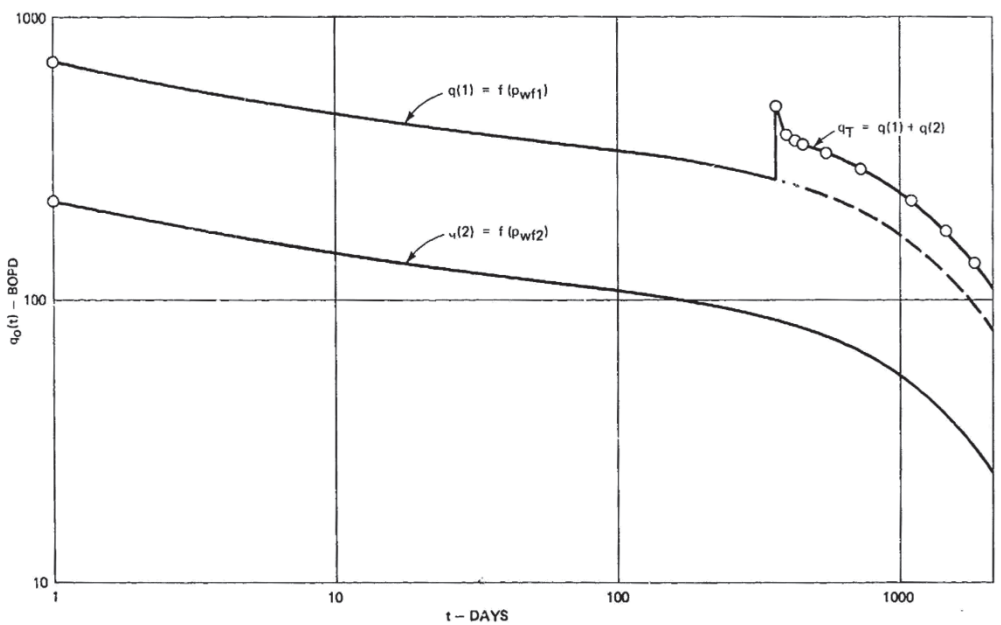

Fig. 14 - Effect of a change in back pressure on decline using graphical superposition.

Fetkovich, M.J.: "Decline Curve Analysis Using Type Curves," Paper SPE 4629 presented at the 1973 SPE Annual Technical Conference and Exhibition held in Las Vegas, NV 30 Sep-03 Oct 1973.

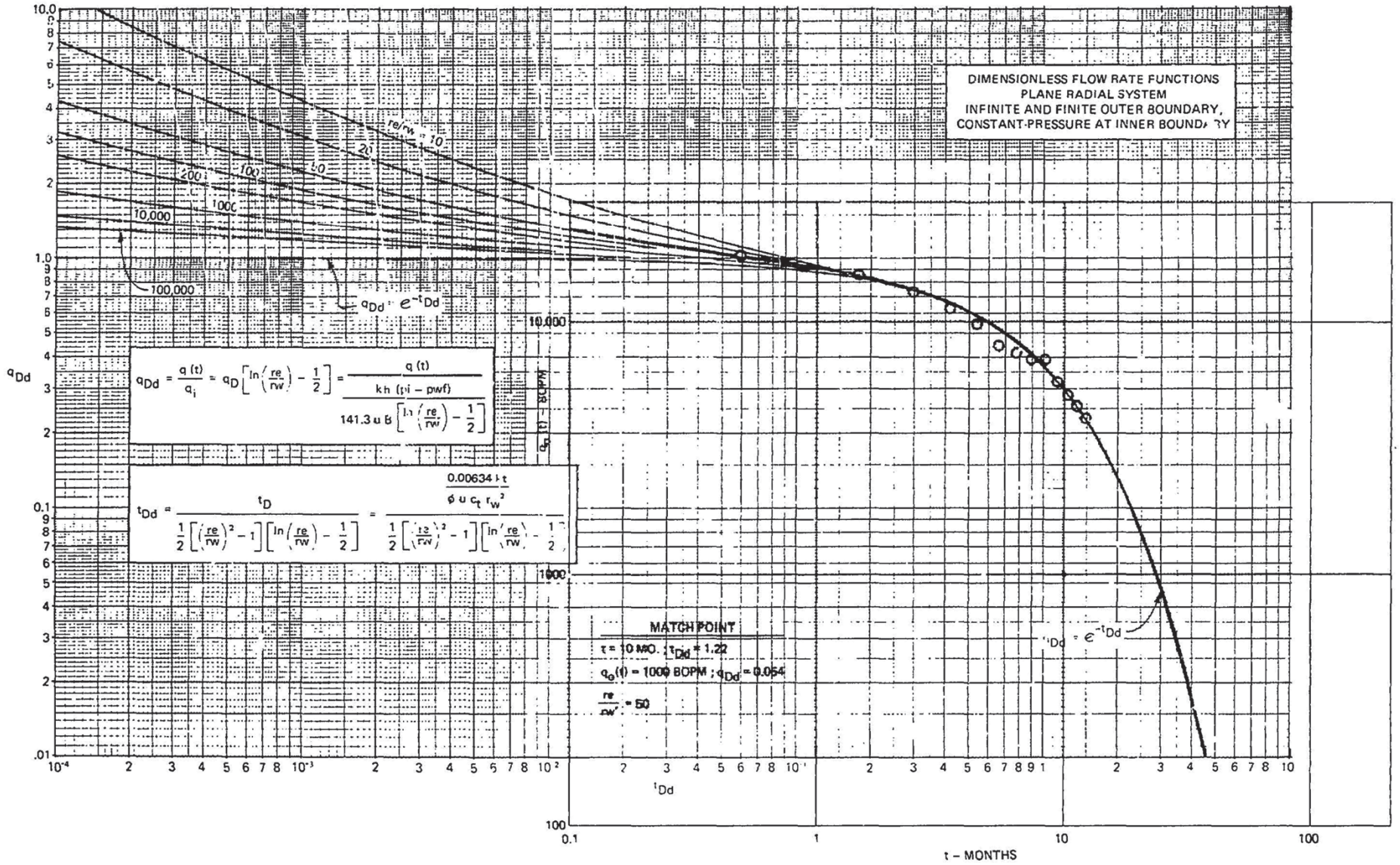

Fig. 15 - Type-curve matching example for calculating Kh using decline curve data, Well 13, Field A.

Fetkovich, M.J.: "Decline Curve Analysis Using Type Curves," Paper SPE 4629 presented at the 1973 SPE Annual Technical Conference and Exhibition held in Las Vegas, NV 30 Sep-03 Oct 1973.

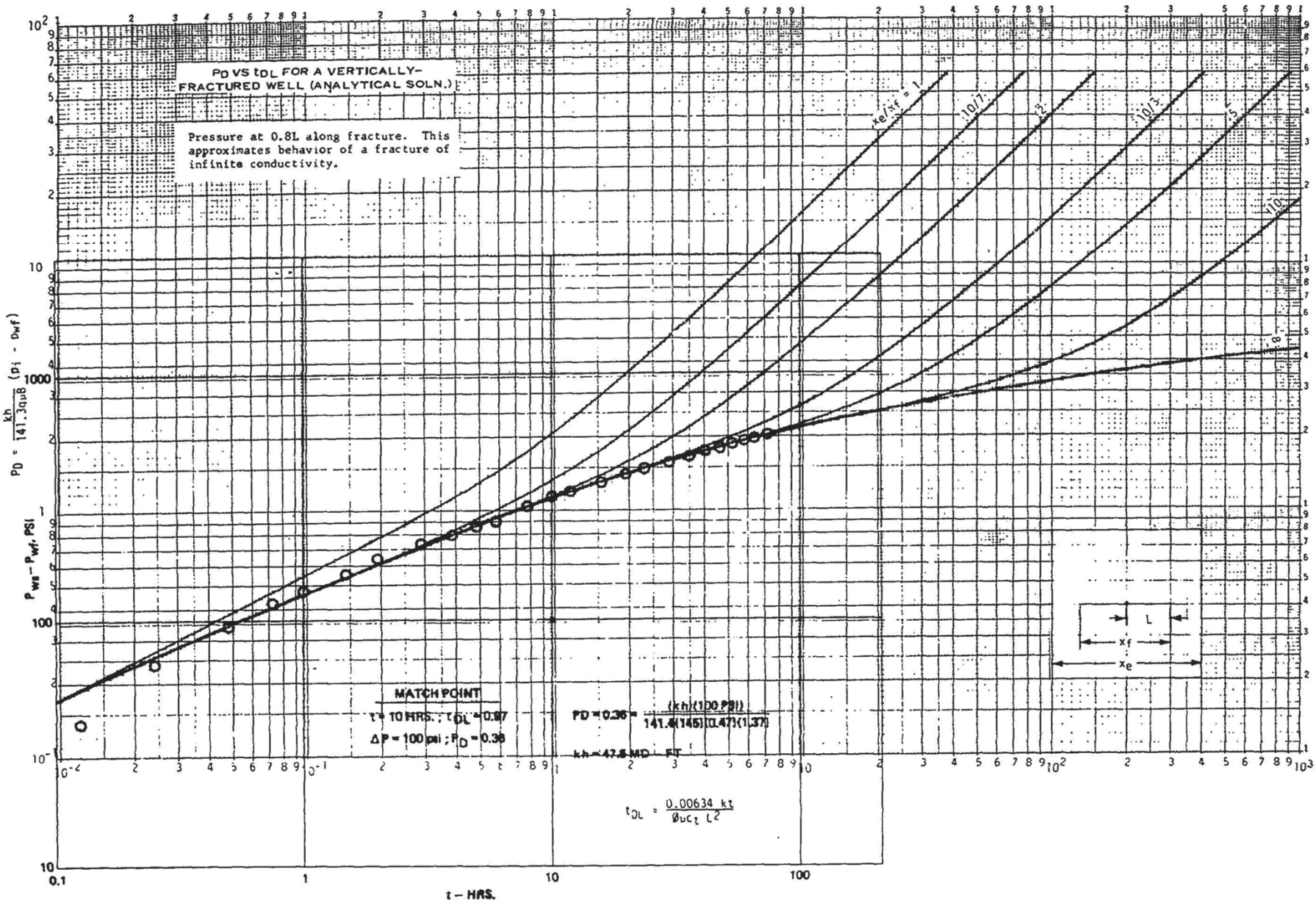

Fig. 16 - Type-curve matching example for calculating Kh from pressure buildup data, Well 13, Field A (type curve from Ref. 8).

Fetkovich, M.J.: "Decline Curve Analysis Using Type Curves," Paper SPE 4629 presented at the 1973 SPE Annual Technical Conference and Exhibition held in Las Vegas, NV 30 Sep-03 Oct 1973.

SPE 4629

Decline Curve Analysis Using Type Curves

M.J. Fetkovich, SPE, Phillips Petroleum Co.

Fetkovich, M.J.: "Decline Curve Analysis Using Type Curves," JPT (March 1980) 1065-1077.

SPE 4629

Decline Curve Analysis Using Type Curves

M.J. Fetkovich, SPE, Phillips Petroleum Co.

Introduction

Rate-time decline curve extrapolation is one of the oldest and most often used tools of the petroleum engineer. The various methods used always have been regarded as strictly empirical and generally not scientific. Results obtained for a well or lease are subject to a wide range of alternate interpretations, mostly as a function of the experience and objectives of the evaluator. Recent efforts in the area of decline curve analysis have been directed toward a purely computerized statistical approach, its basic objective being to arrive at a unique "unbiased" interpretation. As pointed out in a comprehensive review of the literature by Ramsay,[1] "In the period from 1964 to date (1968), several additional papers were published which contribute to the understanding of decline curves but add little new technology."

A new direction for decline curve analysis was given by Slider[2] with his development of an overlay method to analyze rate-time data. Because his method was rapid and easily applied, it was used extensively by Ramsay in his evaluation of some 200 wells to determine the distribution of the decline curve exponent b. Gentry's[3] Fig. 1 displaying the Arps'[4] exponential, hyperbolic, and harmonic solutions all on one curve also could be used as an overlay to match all of a well's decline data. However, he did not illustrate this in his example application of the curve.

The overlay method of Slider is similar in principle to the log-log type curve matching procedure presently being employed to analyze constant-rate pressure buildup and drawdown data.[5-9] The exponential decline, often used in decline curve analysis, readily can be shown to be a long-time solution of the *constant-pressure* case.[10-13] It followed then that a log-log type curve matching procedure could be developed to analyze decline curve data.

This paper demonstrates that both the analytical constant-pressure infinite (early transient period for finite systems) and finite reservoir solutions can be placed on a common dimensionless log-log type curve with all the standard "empirical" exponential, hyperbolic, and harmonic decline curve equations developed by Arps. Simple combinations of material balance equations and new forms of oilwell rate equations from the recent work of Fetkovich[14] illustrate under what circumstances specific values of the hyperbolic decline exponent b should result in dissolved-gas-drive reservoirs. Log-log type curve analysis then is performed using these curves with declining rate data completely analogous to the log-log type curve matching procedure presently being employed with constant-rate case pressure transient data.

0149-2136/80/0006-4629$00.25

Note: The author's full-size type curves with grid suitable for actual use are available on written request from SPE Book Order Dept., 6200 N. Central Expwy., Dallas, TX 75206. Specify SPE 9086 and include $3 prepayment for each order of "Types Curves for Decline Curve Analysis Using Type Curves."

This paper demonstrates that decline curve analysis not only has a solid fundamental base but also provides a tool with more diagnostic power than has been suspected previously. The type curve approach provides unique solutions on which engineers can agree or shows when a unique solution is not possible with a type curve only.

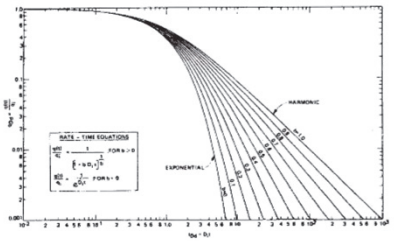

Fig. 1 — Type curves for Arps' empirical rate-time decline equations, unit solution (D_i = 1).

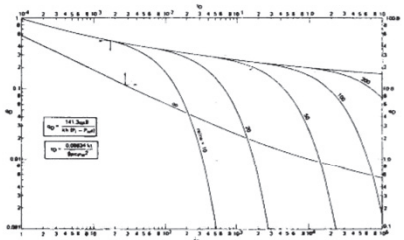

Fig. 2A — Dimensionless flow rate functions for plane radial system, infinite and finite outer boundary, constant pressure at inner boundary.[10,11,15,16]

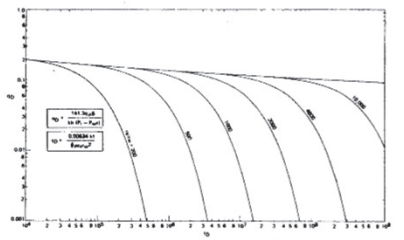

Fig. 2B — Dimensionless flow rate functions for plane radial system, infinite and finite outer boundary, constant pressure at inner boundary.[10,11,15,16]

Arps' Rate-Time Equations

Nearly all conventional decline curve analysis is based on the empirical rate-time equations given by Arps[4] as

$$\frac{q(t)}{q_i} = \frac{1}{\left[1+bD_it\right]^{1/b}} \quad \ldots\ldots\ldots\ldots\ldots\ldots (1)$$

For $b = 0$, we can obtain the exponential decline equation from Eq. 1,

$$\frac{q(t)}{q_i} = \frac{1}{e^{D_it}} \quad \ldots\ldots\ldots\ldots\ldots\ldots (2)$$

and for $b = 1$, referred to as harmonic decline, we have

$$\frac{q(t)}{q_i} = \frac{1}{[1+D_it]} \quad \ldots\ldots\ldots\ldots\ldots\ldots (3)$$

A unit solution ($D_i = 1$) of Eq. 1 was developed for values of b between 0 and 1 in 0.1 increments. The results are plotted as a set of log-log type curves (Fig. 1) in terms of a decline curve dimensionless rate,

$$q_{Dd} = \frac{q(t)}{q_i} \quad \ldots\ldots\ldots\ldots\ldots\ldots (4)$$

and a decline curve dimensionless time,

$$t_{Dd} = D_it \quad \ldots\ldots\ldots\ldots\ldots\ldots (5)$$

From Fig. 1 we see that when all the basic decline curves and normal ranges of b are displayed on a single graph, all curves coincide and become indistinguishable at $t_{Dd} \cong 0.3$. Any data existing before a t_{Dd} of 0.3 will *appear* to be an exponential decline regardless of the true value of b and, thus, plot as a straight line on semilog paper. A statistical or least-squares approach could calculate any value of b between 0 and 1.

Analytical Solutions (Constant-Pressure at Inner Boundary)

Constant well pressure solutions to predict declining production rates with time were published first in 1933 by Moore, Schilthuis and Hurst,[10] and Hurst.[11] Results were presented for infinite and finite, slightly compressible, single-phase plane radial flow systems. The results were presented in graphical form in terms of a dimensionless flow rate and a dimensionless time. The dimensionless flow rate q_D can be expressed as

$$q_D = \frac{141.3\, q(t)\, \mu B}{kh(p_i - p_{wf})} \quad \ldots\ldots\ldots\ldots\ldots\ldots (6)$$

and the dimensionless time t_D as

$$t_D = \frac{0.00634\, kt}{\phi\mu c_t r_w^2} \quad \ldots\ldots\ldots\ldots\ldots\ldots (7)$$

The original publications did not include tabular values of q_D and t_D. For use in this paper infinite

Fetkovich, M.J.: "Decline Curve Analysis Using Type Curves," JPT (March 1980) 1065-1077.

solution values were obtained from Ref. 15, while the finite values were obtained from Ref. 16. The infinite solution and finite solutions for r_e/r_w from 10 to 100,000 are plotted in Figs. 2a and 2b.

Most engineers utilize the constant-pressure solution not in a single constant-pressure problem but as a series of constant-pressure step functions to solve water influx problems using the dimensionless cumulative production Q_D.[13] The relationship between Q_D and q_D is

$$\frac{d(Q_D)}{dt_D} = q_D \quad \ldots\ldots\ldots\ldots\ldots\ldots\ldots\ldots (8)$$

Fetkovich[17] presented a simplified approach to water influx calculations for finite systems that gave results that compared favorably with the more rigorous analytical constant-pressure solutions. Eq. 3 of his paper, for a constant-pressure p_{wf}, can be written as

$$q(t) = \frac{J_o(p_i - p_{wf})}{e^{\left[\frac{(q_i)_{max}}{N_{pi}}\right]t}} \quad \ldots\ldots\ldots\ldots\ldots\ldots (9)$$

but

$$q_i = J_o(p_i - p_{wf}) \quad \ldots\ldots\ldots\ldots\ldots\ldots\ldots (10)$$

and

$$J_o = \frac{(q_i)_{max}}{p_i} \quad \ldots\ldots\ldots\ldots\ldots\ldots\ldots (11)$$

Substituting Eq. 11 into Eq. 10 we can write

$$(q_i)_{max} = \frac{q_i}{\left[1 - \frac{p_{wf}}{p_i}\right]} \quad \ldots\ldots\ldots\ldots\ldots\ldots (12)$$

Now substituting Eqs. 10 and 12 into Eq. 9 we obtain

$$\frac{q(t)}{q_i} = e^{-\left[\frac{q_i t}{\left(1 - \frac{p_{wf}}{p_i}\right)N_{pi}}\right]} \quad \ldots\ldots\ldots\ldots\ldots\ldots (13)$$

Eq. 13 can be considered as a derivation of the exponential decline equation in terms of reservoir variables and the constant-pressure imposed on the well. For the same well, different values of a single constant backpressure p_{wf} always will result in an exponential decline – i.e., the level of backpressure does not change the type of decline. For $p_{wf} = 0$, a more realistic assumption for a well on true wide-open decline, we have

$$\frac{q(t)}{q_i} = e^{-\left[\frac{(q_i)_{max}}{N_{pi}}\right]t} \quad \ldots\ldots\ldots\ldots\ldots\ldots\ldots (14)$$

In terms of the empirical exponential decline curve, Eq. 2, D_i is then defined as

$$D_i = \frac{(q_i)_{max}}{N_{pi}} \quad \ldots\ldots\ldots\ldots\ldots\ldots\ldots (15)$$

In terms of a dimensionless time for decline curve

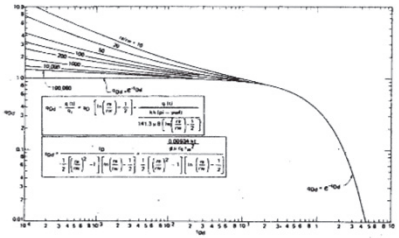

Fig. 3 – Dimensionless flow rate functions for plane radial system, infinite and finite outer boundary, constant pressure at inner boundary.

analysis we have from Eqs. 5 and 15

$$t_{Dd} = \left[\frac{(q_i)_{max}}{N_{pi}}\right]t \quad \ldots\ldots\ldots\ldots\ldots\ldots\ldots (16)$$

Defining N_{pi} and $(q_i)_{max}$ in terms of reservoir variables

$$N_{pi} = \frac{\pi(r_e^2 - r_w^2)\phi c_t h p_i}{5.615\,B} \quad \ldots\ldots\ldots\ldots\ldots\ldots (17)$$

and

$$(q_i)_{max} = \frac{khp_i}{141.3\mu B\left[\ln\left(\frac{r_e}{r_w}\right) - \frac{1}{2}\right]} \quad \ldots\ldots\ldots\ldots (18)$$

The decline curve dimensionless time, in terms of reservoir variables, becomes

$$t_{Dd} = \frac{0.00634\,kt}{\phi\mu c_t r_w^2} \cdot \frac{1}{\frac{1}{2}\left[\left(\frac{r_e}{r_w}\right)^2 - 1\right]\left[\ln\left(\frac{r_e}{r_w}\right) - \frac{1}{2}\right]} \quad \ldots (19)$$

or

$$t_{Dd} = \frac{t_D}{\frac{1}{2}\left[\left(\frac{r_e}{r_w}\right)^2 - 1\right]\left[\ln\left(\frac{r_e}{r_w}\right) - \frac{1}{2}\right]} \quad \ldots\ldots (20)$$

To obtain a decline curve dimensionless rate q_{Dd} in terms of q_D,

$$q_{Dd} = \frac{q(t)}{q_i} = q_D\left[\ln\left(\frac{r_e}{r_w}\right) - \frac{1}{2}\right], \quad \ldots\ldots\ldots (21)$$

or

$$q_{Dd} = \frac{q(t)}{\frac{kh(p_i - p_{wf})}{141.3\mu B\left[\ln\left(\frac{r_e}{r_w}\right) - \frac{1}{2}\right]}} \quad \ldots\ldots\ldots (22)$$

Thus, the published values of q_D and t_D for the infinite and finite constant-pressure solutions were transformed into a decline curve dimensionless rate and time, q_{Dd} and t_{Dd}, using Eqs. 20 and 21. Fig. 3

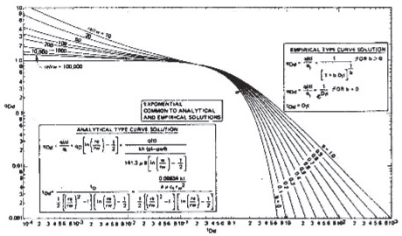

Fig. 4 – Composite of analytical and empirical type curves of Figs. 1 and 3.

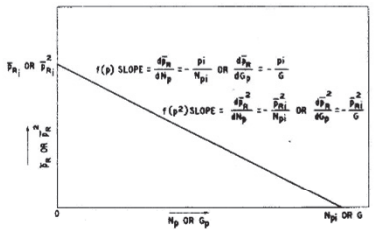

Fig. 5A – Graphical representation of material balance equation.

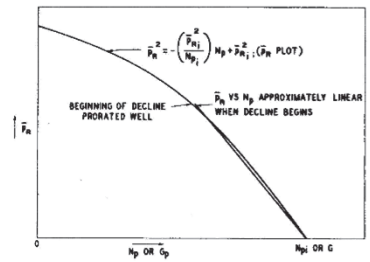

Fig. 5B – Graphical representation of material balance equation.

is a plot of the newly defined dimensionless rate and time, q_{Dd} and t_{Dd}, for various values of r_e/r_w.

At the onset of depletion (a type of pseudosteady state), all solutions for various values of r_e/r_w develop exponential decline and converge to a single curve. Fig. 4 is a combination of the constant-pressure analytical solutions and the standard "empirical" exponential, hyperbolic, and harmonic decline curve solutions on a single dimensionless curve. The exponential decline is common to both the analytical and empirical solutions. Note from the composite curve that rate data existing only in the transient period of the constant terminal pressure solution, if analyzed by the empirical Arps approach, would require values of b much greater than 1 to fit the data.

Solutions From Rate and Material Balance Equations

The method of combining a rate equation and material balance equation for finite systems to obtain a rate-time equation was outlined in Ref. 17. The rate-time equation obtained using this simple approach, which neglects early transient effects, yielded surprisingly good results when compared with those obtained using more rigorous analytical solutions for finite aquifer systems. This rate-equation material balance approach was used to derive some useful and instructive decline curve equations for solution-gas-drive reservoirs and gas reservoirs.

Rate Equations

Until recently, no simple form of a rate equation existed for solution-gas-drive reservoirs with which to predict rate of flow as a function of both flowing pressure and declining reservoir shut-in pressure. Fetkovich[14] has proposed a simple empirical rate equation for solution-gas-drive reservoirs that yields results that compare favorably with computer results obtained using two-phase flow theory. The proposed rate equation was given as

$$q_o = J'_{oi}\left(\frac{\bar{p}_R}{\bar{p}_{Ri}}\right)(\bar{p}_R^2 - p_{wf}^2)^n, \quad \ldots\ldots\ldots (23a)$$

where n will be assumed to lie between 0.5 and 1.0.

Although the above equation has not been verified by field results, it offers the opportunity to define the decline exponent $(1/b)$ in terms of the backpressure curve slope (n) and to study its range of expected values. Also, the initial decline rate D_i can be expressed in terms of reservoir variables. One further simplification used in the derivations is that $p_{wf} = 0$. For a well on decline, p_{wf} usually will be maintained at or near zero to maintain maximum flow rates. Eq. 23a then becomes

$$q_o = J'_{oi}\left(\frac{\bar{p}_R}{\bar{p}_{Ri}}\right)(\bar{p}_R^{2n}), \quad \ldots\ldots\ldots\ldots (23b)$$

The form of Eqs. 23a and 23b also could be used to represent gas-well behavior with a pressure dependent *interwell* permeability effect defined by the ratio $(\bar{p}_R/\bar{p}_{Ri})$. The standard form of the gas-well rate

Fetkovich, M.J.: "Decline Curve Analysis Using Type Curves," JPT (March 1980) 1065-1077.

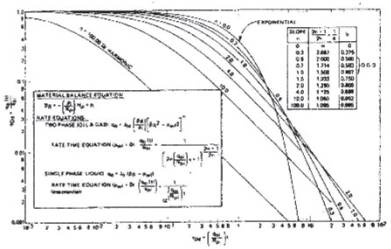

Fig. 6 – Dissolved-gas-drive reservoir rate decline type curves for finite system with constant pressure at inner boundary ($p_{wf} = 0$ @ r_w); early transient effects not included.

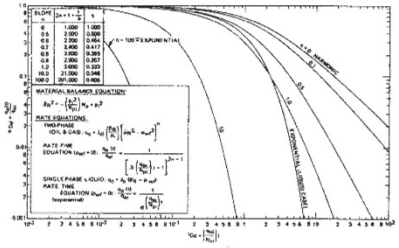

Fig. 7 – Dissolved-gas-drive reservoir rate decline type curves for finite system with constant pressure at inner boundary ($p_{wf} = 0$ @ r_w); early transient effects not included.

equation usually is given as

$$q_g = C_g\left(\bar{p}_R^2 - p_{wf}^2\right)^n. \quad \ldots\ldots\ldots\ldots\ldots (24)$$

Material Balance Equations

Two basic forms of a material balance equation are investigated in this study: $\bar{p}_R$ is linear with N_p or G_p, and $\bar{p}_R^2$ is linear with N_p or G_p (Figs. 5A and 5B). The linear $\bar{p}_R$ relationship for oil is

$$\bar{p}_R = -\left(\frac{\bar{p}_{Ri}}{N_{pi}}\right)N_p + \bar{p}_{Ri}, \quad \ldots\ldots\ldots\ldots (25)$$

and for gas

$$\bar{p}_R = -\left(\frac{\bar{p}_{Ri}}{G}\right)G_p + \bar{p}_{Ri}. \quad \ldots\ldots\ldots\ldots (26)$$

Eq. 25 is a good approximation for totally undersaturated oil reservoirs or is simply assuming that *during the decline period* $\bar{p}_R$ vs. N can be approximated by a straight line. For gas reservoirs, Eq. 26 is correct for the assumption of gas compressibility $Z = 1$.

In terms of $\bar{p}_R^2$ being linear with cumulative production, we would have

$$\bar{p}_R^2 = -\left(\frac{\bar{p}_{Ri}^2}{N_{pi}}\right)N_p + \bar{p}_{Ri}^2. \quad \ldots\ldots\ldots\ldots (27)$$

This form of equation results in the typical shape of the pressure $\bar{p}_R$ vs. cumulative production N_p relationship of a solution-gas-drive reservoir as depicted in Fig. 5B. Applications would be more appropriate in nonprorated fields – i.e., wells are produced wide open and go on decline from initial production. This more likely would be the case for much of the decline curve data analyzed by Cutler[18] obtained in the early years before proration.

Rate-Time Equations for Oil Wells

Rate-time equations using various combinations of material balance and rate equations were derived as outlined in Appendix B of Ref. 17. Using Eqs. 23b and 25, the resulting rate-time equation is

$$\frac{q_o(t)}{q_{oi}} = \frac{1}{\left[2n\left(\frac{q_{oi}}{N_{pi}}\right)t+1\right]^{\frac{2n+1}{2n}}}. \quad \ldots\ldots\ldots (28)$$

A unit solution, $q_{oi}/N_{pi} = 1$, of Eq. 28 is plotted as a log-log type curve for various values of n (Fig. 6) in terms of the decline curve dimensionless time t_{Dd}. For these derivations with $p_{wf} = 0$, $q_{oi} = (q_{oi})_{max}$. For the limiting range of backpressure curve slopes n of 0.5 and 1.0, the Arps empirical decline curve exponent $1/b$ is 2.0 and 1.5, respectively, or b = 0.500 and 0.667, respectively – a surprisingly narrow range. To achieve an exponential decline, n must be equal to zero, and a harmonic decline requires $n \to \infty$. In practical applications, if we assume an n of 1.0 dominates in solution-gas (dissolved-gas) drive reservoirs and $\bar{p}_R$ vs. N is linear for nonuniquely defined rate-time data, we simply would fit the rate-time data to the $n = 1.0$ curve. On the Arps' solution type curves (Fig. 1), we would use $(1/b) = 3/2$ or $b = 0.667$.

The rate-time equation obtained using Eqs. 23b and 27 is

$$\frac{q_o(t)}{q_{oi}} = \frac{1}{\left[0.5\left(\frac{q_{oi}}{N_{pi}}\right)t+1\right]^{2n+1}}. \quad \ldots\ldots\ldots (29)$$

The unit solution of Eq. 29 is plotted as a log-log type curve for various values of n (Fig. 7). This solution results in a complete reversal from that of the previous one; $n = 0$ yields the harmonic decline and $n \to \infty$ gives the exponential decline. For the limiting range of backpressure curve slopes n of 0.5 and 1.0, the decline curve exponent $1/b$ is 2.0 and 3.0 or b = 0.500 and 0.333, respectively. This range of b values fits Arps' findings using Cutler's decline curve data. He found that more than 90% of the values of b lie in the range $0 \le b \le 0.5$. Ramsay[1] found a different distribution of the value of b analyzing modern rate decline data from some 202 leases. His distribution may be more a function of analyzing wells that have been subject to proration and are better represented

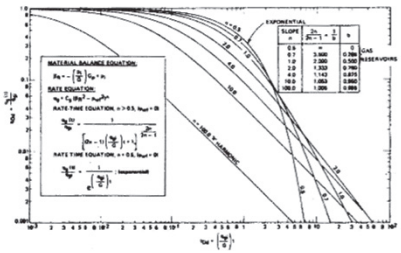

Fig. 8 – Gas reservoir rate decline type curves for finite system with constant pressure at inner boundary ($p_{wf} = 0$ @ r_w); early transient effects not included.

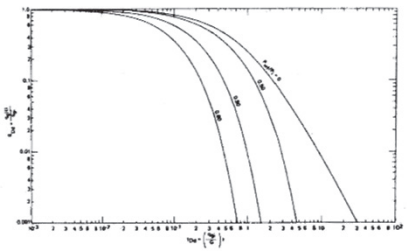

Fig. 9 – Gas reservoir rate decline type curves with backpressure for finite system with constant pressure at inner boundary (p_{wf} = constant @ r_w); early transient effects not included and $Z = 1$ (based on gas well backpressure curve slope, $n = 1$).

by the assumptions underlying the rate-time solution given by Eq. 28 – i.e., $\bar{p}_R$ vs. N_p was linear over the decline period.

Decline Curve Analysis of Gas Wells

Decline curve analysis of rate-time data obtained from gas wells has been reported in only a few instances.[19,20] Using Eq. 24 with $p_{wf} = 0$ and Eq. 26, the rate-time equation for a gas well is

$$\frac{q_g(t)}{q_{gi}} = \frac{1}{\left[(2n-1)\left(\frac{q_{gi}}{G}\right)t+1\right]^{\frac{2n}{2n+1}}}. \quad \ldots\ldots (30)$$

for all backpressure curve slopes where $n > 0.5$.

For $n = 0.5$, the exponential decline is obtained:

$$\frac{q_g(t)}{q_{gi}} = e^{-\left(\frac{q_{gi}}{G}\right)t}. \quad \ldots\ldots\ldots\ldots (31)$$

The unit solutions of Eqs. 30 and 31 are plotted as a log-log type curve in Fig. 8. For the limiting range of backpressure curve slopes n of 0.5 and 1.0, the Arps decline curve exponent $(1/b)$ is ∞ and 2, or $b = 0$ (exponential) and 0.500, respectively.

The effect of backpressure on a gas well is demonstrated for a backpressure curve slope $n = 1.0$ in Fig. 9. The backpressure is expressed as a ratio of p_{wf}/p_i. Note that as $p_{wf} \to p_i$ ($\Delta p \to 0$), the type curve approaches exponential decline, the liquid case solution. Whereas backpressure does not change the type of decline for the liquid case solution, it does change the type of decline in this case.

Using the more familiar rate and material balance equations for gas wells, we can obtain the cumulative-time relationship by integrating the rate-time Eqs. 30 and 31 with

$$G_p = \int_0^t q_g(t)\,dt. \quad \ldots\ldots\ldots\ldots (32)$$

For $n > 0.5$ we obtain

$$\frac{G_p}{G} = 1 - \left[1 + (2n-1)\left(\frac{q_{gi}}{G}\right)t\right]^{\frac{1}{(1-2n)}}, \quad \ldots. (33)$$

and for $n = 0.5$,

$$\frac{G_p}{G} = 1 - e^{-\left(\frac{q_{gi}}{G}\right)t}. \quad \ldots\ldots\ldots\ldots (34)$$

Log-log type curves of Eqs. 33 and 34 could be prepared for convenience in obtaining cumulative production.

Type Curve Analysis

Recent papers by Agarwal *et al.*,[5] Ramey,[6] Raghavan *et al.*,[7] and Gringarten *et al.*,[8] have demonstrated or discussed the application and usefulness of a type curve matching procedure to interpret constant-rate pressure buildup and drawdown data. Van Poollen[21] demonstrated the application of the type curve procedure in analyzing flow-rate data obtained from an oil well producing with a constant pressure at the wellbore. All of his data, however, were in the early transient period. No depletion was evident in his examples. This same type curve matching procedure can be used for decline curve analysis.

The basic steps used in type curve matching of declining rate-time data are as follows.

1. Plot the actual rate vs. time data in any convenient units on log-log tracing paper of the same size cycle as the type curve to be used. (For convenience all type curves should be plotted on the same log-log scale so that various solutions can be tried.)
2. The tracing paper data curve is placed over a type curve, the coordinate axes of the two curves being kept parallel and shifted to a position that represents the best fit of the data to a type curve. More than one of the type curves presented in this paper may have to be tried to obtain a best fit of all the data.
3. Draw a line through and extending beyond the rate-time data overlain along the uniquely matched type curves. Future rates then simply are read from the real-time scale on which the rate data is plotted.
4. To evaluate decline curve constants or reservoir variables, a match point is selected anywhere on the

Fetkovich, M.J.: "Decline Curve Analysis Using Type Curves," JPT (March 1980) 1065-1077.

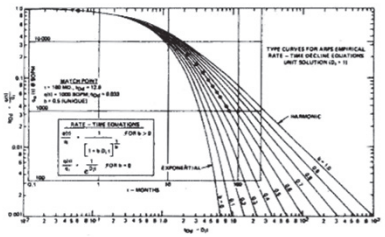

Fig. 10 – Type curve match of Arps' hyperbolic decline example[4] (unique match).

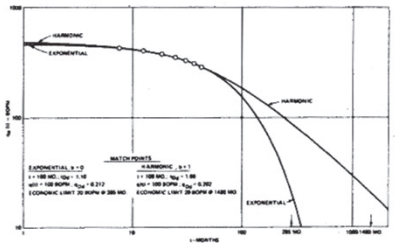

Fig. 11 – Type curve analysis of Arps' exponential decline example.[4]

overlapping portion of the curves, and the coordinates of this common point on both sheets are recorded.

5. If none of the type curves will fit all the data reasonably, the departure curve method[15,22] should be attempted. This method assumes that the data is a composite of two or more different decline curves. After a match of the late time data has been made, the matched curve is extrapolated backward in time and the departure, or difference, between the actual rates and rates determined from the extrapolated curve at corresponding times is replotted on the same log-log scale. An attempt then is made to match the departure curve with one of the type curves. (At all times some consideration of the type of reservoir producing mechanism should be considered.) Future predictions then should be made as the sum of the rates determined from the two (or more if needed) extrapolated curves.

Type Curve Matching Examples

Several examples will be presented to illustrate the method of using type curve matching to analyze typical declining rate-time data. The type curve approach provides solutions on which engineers can agree or shows when a unique solution is not possible with a type curve only. In the event of a nonunique solution, a most probable solution can be obtained if the producing mechanism is known or indicated.

Arps' Hyperbolic Decline Example

Fig. 10 illustrates a type curve match of Arps' example of hyperbolic decline.[4] Every single data point falls on the $b = 0.5$ type curve. This match was found to be unique in that the data would not fit any other value of b. Future producing rates can be read directly from the real-time scale on which the data is plotted. If we wish to determine q_i and D_i, use the match points indicated on Fig. 10 as follows.

$$q_{Dd} = 0.033 = \frac{q(t)}{q_i} = \frac{1{,}000\ \text{BOPM}}{q_i} .$$

$$q_i = \frac{1{,}000\ \text{BOPM}}{0.033} = 30{,}303\ \text{BOPM} .$$

$$t_{Dd} = 12.0 = D_i t = D_i\ 100\ \text{months} .$$

$$D_i = \frac{12.0}{100\ \text{months}} = 0.12\ \text{months}^{-1} .$$

The data also could have been matched using the type curves in Figs. 6 and 7. In both cases the match would have been obtained with a backpressure curve slope $n = 0.5$, which is equivalent to $b = 0.5$. Match points determined from these curves could have been used to calculate q_i and q_i/N_{pi} and finally N_{pi}.

The fact that this example was for a lease, a group of wells, and not an individual well raises an important question. Should there be a difference in results between analyzing each well individually and summing the results or simply adding all wells' production and analyzing the total lease production rate? Consider a lease or field with fairly uniform reservoir properties, b or n is similar for each well, and all wells have been on decline at a similar terminal wellbore pressure p_{wf} for a sufficient period of time to reach pseudosteady state. According to Matthews *et al.*,[23] "at (pseudo) steady state the drainage volumes in a bounded reservoir are proportional to the rates of withdrawal from each drainage volume." It follows then that the *ratio* q_i/N_{pi} will be identical for each well and, thus, the sum of the results from each well will give the same results as analyzing the total lease or field production rate. Some rather dramatic illustrations of how rapidly a readjustment in drainage volumes can take place by changing the production rate of an offset well or drilling an offset well is illustrated in a paper by Marsh.[24] Similar drainage volume readjustments in gas reservoirs also have been demonstrated by Stewart.[25]

For the case where some wells are in different portions of a field separated by a fault or a drastic permeability change, readjustment of drainage volumes proportional to rate cannot take place among *all* wells. The ratio q_i/N_{pi} then may be different for different groups of wells. A total lease or field production analysis then would give different results than summing the results from individual well analysis. A similar situation also can exist for production from stratified reservoirs[26,27] (no crossflow).

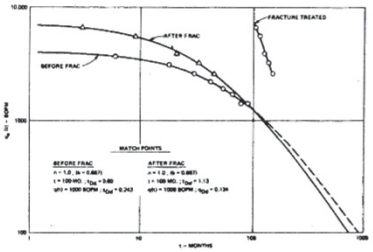

Fig. 12 – Type curve analysis of a stimulated well before and after fracture treatment.

Arps' Exponential Decline Example

Fig. 11 shows the results of a type curve analysis of Arps' example of a well with an apparent exponential decline. In this case, there are not sufficient data to establish uniquely a value of b. The data essentially fall in the region of the type curves where all curves coincide with the exponential solution. As shown in Fig. 11, a value of $b = 0$ (exponential) or $b = 1.0$ (harmonic) appear to fit the data equally well. (Of course all values in between also would fit the data.) The difference in forecasted results from the two extreme interpretations would be great in later years. For an economic limit of 20 BOPM, the exponential interpretation gives a total life of 285 months, the harmonic 1,480 months. This points out yet a further advantage of the type curve approach; all possible alternate interpretations conveniently can be placed on one curve and forecasts made from them. A statistical analysis, of course, would yield a single answer, but it would not be necessarily the correct or most probable solution. Considering the various producing mechanisms, we could select (1) $b = 0$ (exponential) if the reservoir is highly undersaturated, (2) $b = 0$ (exponential) for gravity drainage with no free surface,[28] (3) $b = 0.5$ for gravity drainage with a free surface,[28] (4) $b = 0.667$ for a solution-gas-drive reservoir ($n = 1.0$) if $\bar{p}_R$ vs. N_p is linear, or (5) $b = 0.333$ for a solution-gas-drive reservoir ($n = 1.0$) if $\bar{p}_R^2$ vs. N_p is approximately linear.

Fractured Well Example

Fig. 12 is an example of type curve matching for a well with declining rate data available both before and after stimulation. (The data were obtained from Ref. 1.) This type problem usually presents some difficulties in analysis. Both before- and after-fracture log-log plots are shown in Fig. 12 with the after-fracture data reinitialized in time. These before and after log-log plots will *overlie each other* exactly, indicating that the value of b did not change for the well after the fracture treatment. (The before-fracture plot can be considered as a type curve itself, with the after-fracture data overlaid and matched on it.) Thus, all the data were used in an attempt to define b. When a match is attempted on the Arps unit solution type curves, it was found that a b of between 0.6 and 1.0 could fit the data. Assuming a solution-gas drive, a match of the data was made on the Fig. 6 type curve with $n = 1.0$ and $b = 0.667$.

Using the match points for the before-fracture data, we have from the rate match point

$$q_{Dd} = 0.243 = \frac{q(t)}{q_{oi}} = \frac{1{,}000\ \text{BOPM}}{q_{oi}} ,$$

and

$$q_{oi} = \frac{1{,}000\ \text{BOPM}}{0.243} = 4{,}115\ \text{BOPM} .$$

From the time match point,

$$t_{Dd} = 0.60 = \left(\frac{q_{oi}}{N_{pi}}\right) t$$

$$= \frac{(4{,}115\ \text{BOPM})(100\,\text{months})}{N_{pi}} ,$$

and

$$N_{pi} = \frac{(4{,}115\ \text{BOPM})(100\ \text{months})}{0.60}$$

$$= 685{,}833\ \text{bbl}.$$

Then,

$$\frac{q_{oi}}{N_{pi}} = \frac{4{,}115\ \text{BOPM}}{685{,}833} = 0.006000\ \text{months}^{-1} .$$

Now using the match points for the after-fracture data, we have from the rate match point

$$q_{Dd} = 0.134 = \frac{q(t)}{q_{oi}} = \frac{1{,}000\ \text{BOPM}}{q_{oi}} ,$$

and

$$q_{oi} = \frac{1{,}000\ \text{BOPM}}{0.134} = 7{,}463\ \text{BOPM} .$$

From the time match point,

$$t_{Dd} = 1.13 = \left(\frac{q_{oi}}{N_{pi}}\right) t$$

$$= \frac{(7{,}463\ \text{BOPM})(100\ \text{months})}{N_{pi}} ,$$

and

$$N_{pi} = \frac{7{,}463\ \text{BOPM})(100\ \text{months})}{1.13}$$

$$= 660{,}442\ \text{bbl} .$$

Then,

$$\frac{q_{oi}}{N_{pi}} = \frac{7{,}463\ \text{BOPM}}{660{,}442\ \text{bbl}} = 0.011300\ \text{months}^{-1} .$$

We now can check the two limiting conditions to be considered following an increase in rate after a well stimulation:

1. Did we simply obtain an acceleration of production, the well's reserves remaining the same?
2. Did the reserves increase in direct proportion to the increase in producing rate as a result of a radius of drainage readjustment?[23] Before treatment, N_{pi}

was found to be 685,833 bbl. Cumulative production determined from the rate data before stimulation was 223,500 bbl. Then N_{pi} at the time of the fracture treatment is

$$N_{pi} = 685{,}833 \text{ bbl} - 223{,}500 \text{ bbl}$$
$$= 462{,}333 \text{ bbl}.$$

If only accelerated production was obtained and the reserves remained the same, q_i/N_{pi} after the fracture treatment should have been

$$\frac{7{,}463 \text{ BOPM}}{462{,}333 \text{ bbl}} = 0.016142 \text{ months}^{-1}.$$

Actual q_{oi}/N_{pi} after treatment was 0.011300 months^{-1}. If the reserves increased in direct proportion to the flow rate, the ratio q_{oi}/N_{pi} should have remained the same as that obtained before treatment or 0.006000 months^{-1}. This then would have indicated that

$$N_{pi} = \frac{7{,}463 \text{ BOPM}}{0.006000 \text{ months}^{-1}} = 1{,}243{,}833 \text{ bbl}.$$

Actual increase in reserves as a result of the fracture treatment appears to lie between the two extremes. Based on the method of analysis used, the actual increase in reserves attributable to the fracture treatment is 198,109 bbl (660,442 bbl − 462,333 bbl).

Stratified Reservoir Example

This example illustrates a method of analyzing decline curve data for a layered (no crossflow) or stratified reservoir using type curves. The data are taken from Ref. 18 and are for the East Side Coalinga field. Ambrose[29] presented a cross section of the field, showing an upper and lower oil sand separated by a continuous black shale. This layered description for the field along with the predictive equation for stratified reservoir presented in Ref. 27 led to the idea of using the departure curve method (differencing) to analyze decline curve data.

After Russell and Prats,[27] the production rate of a well (or field) at pseudosteady state producing a single-phase liquid at the same constant wellbore pressure ($p_{wf} = 0$ for simplicity) from two stratified layers is

$$q_T(t) = q_{i1}\, e^{-\left(\frac{q_i}{N_{pi}}\right)_1 t} + q_{i2}\, e^{-\left(\frac{q_i}{N_{pi}}\right)_2 t}, \quad \ldots\ldots\ldots\ldots\ldots\ldots\ldots\ldots (35)$$

or

$$q_T(t) = q_1(t) + q_2(t). \quad \ldots\ldots\ldots\ldots\ldots\ldots (36)$$

The total production from both layers then is simply the sum of two separate forecasts. Except for the special case of the ratio q_i/N_{pi} being equal for both layers, the sum of two exponentials will not result, in general, in another exponential.

In attempting to match the rate-time data to a type curve, it was found that the late time data can be matched to the exponential ($b = 0$) type curve. Fig. 13 shows this match of the late time data designated

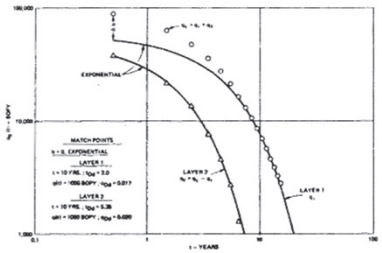

Fig. 13 — Type curve analysis of a layered reservoir (no crossflow) by differencing.

TABLE 1 — SUMMARY OF RATE-TIME DATA FROM EAST SIDE COALINGA FIELD[18] WITH THE RESULTS FROM THE DEPARTURE CURVE METHOD

Time (years)	(1) Total Field Rate, q_T (BOPY)	(2) Layer 1 Rate, q_1 (BOPY)	(1) − (2) Layer 2 Rate, q_2 (BOPY)
0.5	90,000	52,000*	38,000
1.5	64,000	42,500*	21,500
2.5	48,000	34,500*	13,500
3.5	36,000	28,500*	7,500
4.5	27,500	23,000*	4,500
5.5	21,250	18,600*	2,650
6.5	16,250	15,000*	1,250
7.5	13,000	12,500*	500
8.5	10,500	10,500	0
9.5	8,500	8,500	
10.5	6,900	6,900	
11.5	5,600	5,600	
12.5	4,550	4,550	
13.5	3,800	3,800	
14.5	3,200	3,200	
15.5	2,750	2,750	

*Taken from Layer 1 curve in Fig. 13.

as Layer 1. With this match, the curve was extrapolated backward in time, and the departure, or difference between the actual rates determined from the extrapolated curve was replotted on the same log-log scale. See Table 1 for a summary of the departure curve results. The difference or first departure curve, Layer 2, itself resulted in a unique fit of the exponential type curve, thus satisfying Eq. 35, which now can be used to forecast the future production. Using the match points indicated in Fig. 13 to evaluate q_i and D_i for each layer, the predictive equation becomes

$$q_T(t) = 58{,}824 \text{ BOPY}\, e^{-(0.200)t} + 50{,}000 \text{ BOPY}\, e^{-(0.535)t},$$

where t is in years.

Higgins and Lechtenberg[30] named the sum of two exponentials the double semilog. They reasoned that the degree of fit of empirical data to an equation increases with the number of constants.

This interpretation is not claimed to be the only

TABLE 2 — DATA FOR EXAMPLE PROBLEM OF A CHANGE IN BACKPRESSURE

$p_i = 4{,}000$ psia
$p_{wf1} = 1{,}000$ psia
$p_{wf2} = 50$ psia
$k = 1$ md
$h = 100$ ft
$\mu_o = 1$ cp
$B_o = 1.50$ RB/STB
$c_t = 20 \times 10^{-6}$ psi^{-1}
$r_e = 1{,}053$ ft (80 acres)
$r_w' = 10.53$ ft (stimulated well)

$$t_D = \frac{0.00634\, kt}{\phi \mu c_t r_w'^2} = \frac{0.00634\,(1)\, t}{(0.20)(1.0)(20 \times 10^{-6})(10.53)^2} = 14.30\, t$$

$$t_{Dd} = \frac{14.30\, t}{\tfrac{1}{2}\left[(100)^2 - 1\right]\left[\ln(100) - 0.5\right]} = 0.0006967\, t_{\text{days}}$$

$$q_{Dd} = \frac{q(t)}{\dfrac{kh(p_i - p_{wf})}{141.3(\mu B)\left[\ln\left(\frac{r_e}{r_w}\right) - \frac{1}{2}\right]}} = \frac{q(t)}{\dfrac{100\,(3{,}000)}{141.3(1)(1.5)(4.105)}} = \frac{q(t)}{345}$$

$q(t) = q_{Dd}(t_{Dd})\, 345$ or $q(t) = 2.02\,(345)$ at $t = 1$ day
$q(t) = 697$ BOPD

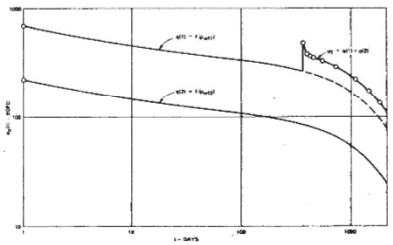

Fig. 14 — Effect of a change in backpressure on decline using graphical superposition.

interpretation possible for this set of data. A match with $b = 0.2$ can be obtained fitting nearly all of the data points but cannot be explained by any of the drive mechanisms so far discussed. The layered concept fits the geologic description and offered the opportunity to demonstrate the departure curve method. The departure curve method essentially places an infinite amount of combinations of type curves at the disposal of the engineer with which to evaluate rate-time data.

Effect of a Change in Backpressure

The effect of a change in backpressure is illustrated best by a hypothetical single-well problem. The reservoir variables and conditions used for this example are given in Table 2. The analytical single-phase liquid solution of Fig. 3 is used to illustrate a simple graphical forecasting superposition procedure. The inverse procedure, the departure or differencing method, can be used to analyze decline-curve data affected by backpressure changes.

After Hurst,[12] superposition for the constant-pressure case for a simple single-pressure change can be expressed by

$$q(t) = \frac{kh(p_i - p_{wf1})}{141.3(\mu B)\left[\ln\left(\frac{r_e}{r_w}\right) - \frac{1}{2}\right]} q_{Dd}(t_{Dd}) + \frac{kh(p_{wf1} - p_{wf2})}{141.3(\mu B)\left[\ln\left(\frac{r_e}{r_w}\right) - \frac{1}{2}\right]} q_{Dd}(t_{Dd} - t_{Dd1}),$$

or

$$q(t) = \frac{kh(p_i - p_{wf1})}{141.3(\mu B)\left[\ln\left(\frac{r_e}{r_w}\right) - \frac{1}{2}\right]} \cdot \left\{ q_{Dd}(t_{Dd}) + \left[\frac{p_{wf1} - p_{wf2}}{p_i - p_{wf1}}\right] q_{Dd}(t_{Dd} - t_{Dd1}) \right\}. \quad \ldots\ldots\ldots\ldots\ldots\ldots (37)$$

Up to the time of the pressure change p_{wf2} at t_{Dd1}, the well production is simply q_1 as depicted on Fig. 14. The q_1 forecast as a function of time is made simply by evaluating a single set of match points using the reservoir variables given in Table 2. At p_{wf1} and $r_e/r_w' = 100$: $t = 1$ day, $t_{Dd} = 0.006967$, $q_1(t) = 697$ BOPD, and $q_{Dd} = 2.02$.

Plot the rate 697 BOPD and time of 1 day on log-log tracing paper on the same size cycle as Fig. 3. Locate the real-time points over the dimensionless time points in Fig. 3 and draw in the r_e/r_w' curve of

Fetkovich, M.J.: "Decline Curve Analysis Using Type Curves," JPT (March 1980) 1065-1077.

TABLE 3 – COMPARISONS OF *kh* DETERMINED FROM BUILDUP AND DECLINE CURVE ANALYSIS, FIELD A (SANDSTONE RESERVOIR); 160-ACRE SPACING, r_e = 1,490 ft, r_w = 0.25 ft

				Pressure Buildup Results			Decline Curve Analysis Results				
Well No.	h (ft)	ϕ (%)	S_{wc} (%)	Skin s	r_w' (ft)	kh (md-ft)	r_e/r_w' Matched	q_{Dd} (10,000 BOPM)	$\frac{p_i - p_{wf}}{(\mu_o B_o)}$	kh (md-ft)	k (md)
1	34	9.4	32.9	−0.23	0.3	120.5	*	0.52	6658	108	3.18
2	126	10.5	18.3	−2.65	3.5	56.7	*	0.68	7979	48	0.38
3	32	9.9	20.4	−3.71	10.3	63.0	*	0.43	8048	60	1.88
4	63	9.5	18.6	−3.41	7.6	28.5	40	0.58	8273	31	0.49
5	67	10.2	15.1	−4.29	18.3	44.4	20	0.57	6296	32	0.48
6	28	10.3	12.6	−2.07	2.0	57.9	*	0.60	7624	62	2.21
7	17	10.0	17.5	−3.41	7.6	16.8	10	1.30	7761	8.3	0.49
8	47	9.1	24.2	−3.74	10.6	16.6	10	1.14	7375	10	0.21
9	87	10.2	18.0	−4.19	16.5	104.7	*	0.435	5642	76	0.87
10	40	10.4	21.7	−5.80	82.9	363.2	*	0.36	1211	255	6.38
11	29	11.5	19.2	−1.00	2.0	59.9	*	0.56	7669	66	2.28
12	19	11.1	17.0	−3.97	13.3	8.9	50	3.30	5045	9.5	0.50
13	121	10.1	18.8	−3.85	11.8	47.5	50	0.54	7259	40.5	0.33
16	74	9.4	20.4	−4.10	15.0	224.8	*	0.32	5737	104	1.41
15	49	10.9	28.6	−3.59	9.1	101.9	*	0.43	4312	115	2.35
16	35	10.0	25.6	−4.57	24.2	14.3	20	0.96	5110	24	0.69
17	62	8.8	22.4	−3.12	5.7	27.2	*	0.82	8198	35	0.56
18	75	9.4	18.1	−1.50	1.2	65.1	*	0.52	6344	93	1.24
19	38	8.9	19.2	−2.11	2.1	40.5	20	0.54	6728	32	0.84
20	60	9.6	24.6	−5.48	60.1	88.1	*	0.345	5690	64	1.07
21	56	11.1	16.5	−2.19	2.2	39.1	20	0.72	5428	30	0.54
22	40	8.9	22.5	−3.79	11.1	116.0	100	0.46	8114	51	1.28

*r_w' used from buildup analysis with r_e of 1,490 ft.

100 on the tracing paper. Read flow rates as a function of time directly from the real-time scale.

When a change in pressure is made to p_{wf2} at t_1, $t = 0$ for the accompanying change in rate q_2 (really a Δq for superposition), this rate change retraces the q_{Dd} vs. t_{Dd} curve and is simply a constant fraction of q_1:

$$q_2 = q_1\left[\frac{p_{wf1} - p_{wf2}}{p_i - p_{wf1}}\right],$$

or at t − 1 day after the rate change,

$$q_2 = 697 \text{ BOPD}\left[\frac{1{,}000 \text{ psi} - 50 \text{ psi}}{4{,}000 \text{ psi} - 1{,}000 \text{ psi}}\right]$$
$$= 221 \text{ BOPD}.$$

The total rate q_T after the pressure change is $q_T = q_1 + q_2$ as depicted in Fig. 14. Flow rates for this example were read directly from the curves in Fig. 14 and summed at times past the pressure change p_{wf2}.

The practical application of this example in decline curve analysis is that the departure or difference method can be used on rate-time data affected by a change in backpressure. The departure curve represented by q_2 in Fig. 14 should overlie exactly the curve represented by q_1. If it does in an actual field example, the future forecast is made correctly by extending both curves and summing them at times beyond the pressure change.

Calculation of *kh* From Decline Curve Data

Pressure buildup and decline curve data were available from a high-pressure, highly undersaturated, low-permeability sandstone reservoir. Initial reservoir pressure was estimated to be 5,790

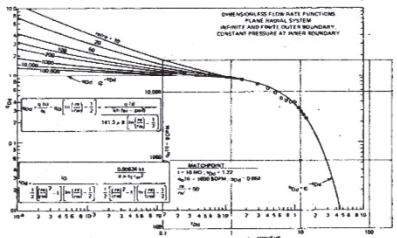

Fig. 15 – Type curve matching example for calculating *kh* using decline curve data, Well 13, Field A.

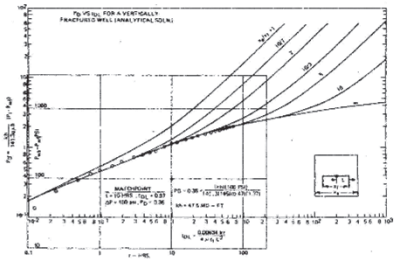

Fig. 16 – Type curve matching example for calculating *kh* from pressure buildup data, Well 13, Field A (type curve from Ref. 8).

psia at −9,300 ft with a bubble-point pressure of 2,841 psia. Two fieldwide pressure surveys were conducted while the reservoir was still undersaturated. Table 3 summarizes the reservoir properties and basic results obtained from the pressure buildup analysis on each well. Note that nearly all wells had negative skins as a result of hydraulic fracture treatments. Also appearing in this table are results obtained from an attempt to calculate *kh* using decline curve data available for each of the wells.

Ten of the 22 wells started on decline when they first were placed on production. As a result, the early production decline data existed in the transient period, and a type curve analysis using Fig. 3 was matched to one of the r_e/r_w stems. Other wells listed on the table, where an r_e/r_w match is not indicated, were prorated wells and began their decline several months after they first were put on production. For the decline curve determination of *kh*, the reservoir pressure existing at the beginning of decline for each well was taken from the pressure history match of the two fieldwide pressure surveys. The constant bottomhole flowing pressure for the wells ranged between 800 and 900 psia.

A type curve match using decline curve data to calculate *kh* for Well 13 is illustrated in Fig. 15. A type curve match using pressure buildup data obtained on this same well is illustrated in Fig. 16. The constant-rate type curve of Gringarten *et al.*[8] for fractured wells was used for matching the pressure buildup data. The buildup *kh* of 47.5 md-ft compares very well with the *kh* of 40.5 md-ft determined by using the rate-time decline curve data.

In general, the comparison of *kh* determined from decline curve data and pressure buildup data tabulated in Table 3 is surprisingly good. (The pressure buildup analysis was performed independently by another engineer.) One fundamental observation to be made from the results obtained on wells where a match of r_e/r_w was not possible is that the effective wellboore radius r_w' (obtained from the buildup analysis) is used to obtain a good match between buildup and decline curve calculated *kh*.

Type Curves for Known Reservoir and Fluid Properties

All the type curves discussed so far were developed for decline curve analysis using some necessary simplifying assumptions. For specific reservoirs, where PVT data, reservoir variables, and backpressure tests are available, type curves could be generated for various relative permeability curves and backpressure. These curves developed for a given field would be more accurate for analyzing decline data in that field. Conventional material balance programs or more sophisticated simulation models could be used to develop dimensionless constant-pressure type curves as was done by Levine and Pratts[31] (see their Fig. 11).

Conclusions

Decline curve analysis not only has a solid fundamental base but provides a tool with more diagnostic power than has been suspected previously. The type curve approach provides unique solutions upon which engineers can agree or shows when a unique solution is not possible with a type curve only. In the event of a nonunique solution, a most probable solution can be obtained if the producing mechanism is known or indicated.

Nomenclature

b = reciprocal of decline curve exponent $(1/b)$
B = formation volume factor, res vol/surface vol
c_t = total compressibility, psi^{-1} (pa^{-1})
C_g = gas-well backpressure curve coefficient
D_i = initial decline rate, t^{-1}
e = natural logarithm base 2.71828
G = initial gas-in-place, surface measure
G_p = cumulative gas production, surface measure
h = thickness, ft (m)
J_o = productivity index, STB/D/psi (stock-tank m^3/d/kPa)
J_o' = productivity index (backpressure curve coefficient) STB/D/(psi)^{2n} [stock-tank m^3/d/(kPa)^{2n}]
k = effective permeability, md
n = exponent of backpressure curve
N_p = cumulative oil productive, STB (stock-tank m^3)
N_{pi} = cumulative oil production to a reservoir shut-in pressure of 0, STB (stock-tank m^3)
p_i = initial pressure, psia (kPa)
$\bar{p}_R$ = reservoir average pressure (shut-in pressure), psia (kPa)
p_{wf} = bottomhole flowing pressure, psia (kPa)
q_D = dimensionless rate (Eq. 6)
q_{Dd} = decline curve dimensionless rate (Eq. 4)
q_i = initial surface rate of flow at $t = 0$
$(q_i)_{max}$ = initial wide-open surface flow rate at $p_{wf} = 0$
$q(t)$ = surface rate of flow at time t
Q_D = dimensionless cumulative production
r_e = external boundary radius, ft (m)
r_w = wellbore radius, ft (m)
r_w' = effective wellbore radius, ft (m)
t = time, days for t_D
t_D = dimensionless time (Eq. 7)
t_{Dd} = decline curve dimensionless time (Eq. 5)
Z = gas compressibility factor
μ = viscosity, cp (Pa·s)
ϕ = porosity, fraction of bulk volume

Acknowledgment

I thank Phillips Petroleum Co. for permission to publish this paper.

Fetkovich, M.J.: "Decline Curve Analysis Using Type Curves," JPT (March 1980) 1065-1077.

References

1. Ramsay, H.J. Jr.: "The Ability of Rate-Time Decline Curves to Predict Future Production Rates," MS thesis, U. of Tulsa, Tulsa, OK (1968).
2. Slider, H.C.: "A Simplified Method of Hyperbolic Decline Curve Analysis," *J. Pet. Tech.* (March 1968) 235-236.
3. Gentry, R.W.: "Decline-Curve Analysis," *J. Pet. Tech.* (Jan. 1972) 38-41.
4. Arps, J.J.: "Analysis of Decline Curves," *Trans.*, AIME (1945) **160**, 228-247.
5. Ramey, H.J. Jr.: "Short-Time Well Test Data Interpretation in the Presence of Skin Effect and Wellbore Storage," *J. Pet. Tech.* (Jan. 1970) 97-104; *Trans.*, AIME, **249**.
6. Agarwal, R., Al-Hussainy, R., and Ramey, H.J. Jr.: "An Investigation of Wellbore Storage and Skin Effect in Unsteady Liquid Flow: I. Analytical Treatment," *Soc. Pet. Eng. J.* (Sept. 1970) 279-290; *Trans.*, AIME, **249**.
7. Raghavan, R., Cady, G.V., and Ramey, H.J. Jr.: "Well-Test Analysis for Vertically Fractured Wells," *J. Pet. Tech.* (Aug. 1972) 1014-1020; *Trans.*, AIME, **253**.
8. Gringarten, A.C., Ramey, H.J. Jr., and Raghavan, R.: "Unsteady-State Pressure Distributions Created by a Well With a Single Infinite-Conductivity Vertical Fracture," *Soc. Pet. Eng. J.* (Aug. 1974) 347-360; *Trans.*, AIME, **257**.
9. McKinley, R.M.: "Wellbore Transmissibility from Afterflow-Dominated Pressure Buildup Data," *J. Pet. Tech.* (July 1971) 863-872; *Trans.*, AIME, **251**.
10. Moore, T.V., Schilthuis, R.J., and Hurst, W.: "The Determination of Permeability from Field Data," *Bull.*, API (May 1933) **211**, 4.
11. Hurst, R.: "Unsteady Flow of Fluids in Oil Reservoirs," *Physics* (Jan. 1934) **5**, 20.
12. Hurst, W.: "Water Influx into a Reservoir and Its Application to the Equation of Volumetric Balance," *Trans.*, AIME (1943) **151**, 57-72.
13. van Everdingen, A.F. and Hurst, W.: "The Application of the Laplace Transformation to Flow Problems in Reservoirs," *Trans.*, AIME (1949) **186**, 305-324.
14. Fetkovich, M.J.: "The Isochronal Testing of Oil Wells," paper SPE 4529 presented at the SPE 48th Annual Fall Meeting, Las Vegas, Sept. 30-Oct. 3, 1973.
15. Ferris, J., Knowles, D.B., Brown, R.H., and Stallman, R.W.: "Theory of Aquifer Tests," *U.S. Geol. Surv.*, Water Supply Paper 1536E (1962) 109.
16. Tsarevich, K.A. and Kuranov, I.F.: "Calculation of the Flow Rates for the Center Well in a Circular Reservoir Under Elastic Conditions," *Problems of Reservoir Hydrodynamics*, Leningrad (1966) Part I, 9-34.
17. Fetkovich, M.J.: "A Simplified Approach to Water Influx Calculations-Finite Aquifer Systems," *J. Pet. Tech.* (July 1971) 814-823.
18. Cuttler, W.W. Jr.: "Estimation of Underground Oil Reserves by Oil-Well Production Curves," *Bull.*, USBM (1924) **228**.
19. Stewart, P.R.: "Low-Permeability Gas Well Performance at Constant Pressure," *J. Pet. Tech.* (Sept. 1970) 1149-1156.
20. Gurley, J.: "A Productivity and Economic Projection Method – Ohio Clinton Sand Gas Wells," *J. Pet. Tech.* (Nov. 1963) 1183-1185.
21. van Poollen, H.K.: "How to Analyze Flowing Well-Test Data...with Constant Pressure at the Well Bore," *Oil and Gas J.* (Jan. 16, 1967) 98-101.
22. Witherspoon, P.A., Javandel, I., Neuman, S.P., and Freeze, P.A.: *Interpretation of Aquifer Gas Storage Conditions from Water Pumping Tests*, Monograph, AGA, New York City (1967) 110.
23. Matthews, C.S., Brons, F., and Hazebroek, P.: "A Method for Determination of Average Pressure in a Bounded Reservoir," *Trans.*, AIME (1954) **201**, 182-191.
24. Marsh, H.N.: "Method of Appraising Results of Production Control of Oil Wells," *Bull.*, API (Sept. 1928) **202**, 86.
25. Stewart, P.R.: "Evaluation of Individual Gas Well Reserves," *Pet. Eng.* (May 1966) 85.
26. Lefkovits, H.C. and Matthews, C.S.: "Application of Decline Curves to Gravity-Drainage Reservoirs in the Stripper Stage," *Trans.*, AIME (1958) **213**, 275-284.
27. Russel, D.G. and Prats, M.: "Performance of Layered Reservoirs With Crossflow – Single-Compressible Fluid Case," *Soc. Pet. Eng. J.* (March 1962) 53-67.
28. Matthews, C.S. and Lefkovits, H.C.: "Gravity Drainage Performance of Depletion-Type Reservoirs in the Stripper Stage," *Trans.*, AIME (1956) **207**, 265-274.
29. Ambrose, A.W.: "Underground Conditions in Oil Fields," *Bull.*, USBM (1921) **195**, 151.
30. Higgins, R.V. and Lechtenberg, H.J.: "Merits of Decline Equations Based on Production History of 90 Reservoirs," paper SPE 2450 presented at the SPE Rocky Mountain Regional Meeting, Denver, May 25-27, 1969.
31. Levine, J.S. and Prats, M.: "The Calculated Performance of Solution-Gas Drive Reservoirs," *Soc. Pet. Eng. J.* (Sept. 1961) 142-152.

SI Metric Conversion Factors

acre	×	4.046 873	E+03	= m^2
bbl	×	1.589 873	E−01	= m^3
cp	×	1.0*	E−03	= Pa·s
ft	×	3.048*	E−01	= m
md-ft	×	3.008 142	E+02	= μm^2.
psi	×	6.894 757	E+00	= kPa
psi^{-1}	×	1.450 377	E−04	= Pa^{-1}

*Conversion factor is exact.

JPT

Original manuscript received in Society of Petroleum Engineers office Aug. 3, 1973. Paper accepted for publication Aug. 7, 1974. Revised manuscript received March 31, 1980. Paper (SPE 4529) first presented at the SPE 48th Fall Meeting, held in Las Vegas, Sept. 30-Oct. 3, 1973.

Fetkovich, M.J.: "Decline Curve Analysis Using Type Curves," JPT (March 1980) 1065-1077.

Fetkovich, M.J., Vienot, M.E., Bradley and M.D., Kiesow, U.G.: "Decline Curve Analysis Using Type Curves – Case Histories," SPEFE (Dec. 1987) 637-656.

Decline-Curve Analysis Using Type Curves—Case Histories

M.J. Fetkovich, SPE, Phillips Petroleum Co.
M.E. Vienot, SPE, Phillips Petroleum Co.
M.D. Bradley, SPE, Phillips Petroleum Co.
U.G. Kiesow, SPE, Phillips Petroleum Co.

SPE Formation Evaluation, December 1987

Decline-Curve Analysis Using Type Curves—Case Histories

M.J. Fetkovich, SPE, Phillips Petroleum Co.
M.E. Vienot, SPE, Phillips Petroleum Co.
M.D. Bradley, SPE, Phillips Petroleum Co.
U.G. Kiesow, SPE, Phillips Petroleum Co.

Summary. Case-history studies demonstrate methods of analyzing rate-time data to determine reservoir variables and to predict future production. Constant-wellbore-pressure analysis techniques use existing q_{dD}-t_{dD} type curves and new q_{dD}-τ_{dD} type curves from actual field data.

Introduction

Since Fetkovich's[1] original presentation in 1973, many successful applications have been made with declining rate-time data using the type-curve approach. Case-history studies of individual oil and gas wells, groups of wells in a field, and total fields are presented in this follow-up paper. Additional papers[2-7] dealing with the constant-wellbore-pressure solution (which also include the depletion period) have since been published to aid analysis and understanding of what is now called "advanced decline-curve analysis."

In essence, decline-curve analysis is a forecasting technique: rate-time data are history-matched on an appropriate type curve, and then a forecast is made. Complex simulation studies proceed similarly. By *using basic reservoir engineering concepts and knowledge*, we know what direction to take, what type curve(s) to choose, and where the rate-time data should fit.

Decline-curve analysis must work because it is founded on basic fluid-flow principles—the same principles used in pressure-transient analysis. The problem most engineers have had and will continue to have with decline-curve analysis is bad, erratic, or insufficient data. Careful attention to obtaining accurate flow rates, flowing pressures, and downtime should help solve the problem. A good rate-time analysis not only will give the same results as conventional pressure-transient analysis, but also will allow a forecast to be made directly at no cost in lost production. For low-permeability stimulated wells, in particular, pressure-buildup testing could be eliminated in many cases as being of little value or economically unjustifiable because of the resulting production loss when compared with what can be obtained from properly conducted constant-wellbore-pressure drawdown tests.

Rate-Time Type-Curve Analysis Concepts

The Radial Flow Solution. The fundamental basis of advanced decline-curve analysis is an understanding of the constant-wellbore-pressure solutions and their corresponding log-log type-curve plots, which are the inverse of the constant-rate solution. Fig. 1 is a composite of the analytic constant-wellbore-pressure solution and the Arps[8] exponential, hyperbolic, and harmonic decline-curve solutions on a single dimensionless type curve. The depletion stem values of b range between 0 (exponential) and 1 (harmonic), which are the normally accepted limits. The exponential-depletion stem ($b=0$) is common to the analytic solution and to the Arps equation.

Decline-curve dimensionless rate and dimensionless time in terms of reservoir variables are defined for the type curve as

$$q_{dD}=q_D\left[\ln\left(\frac{r_e}{r_w}\right)-\tfrac{1}{2}\right] \quad \ldots\ldots\ldots\ldots\ldots\ldots\ldots\ldots\ldots\ldots (1)$$

or

$$q_{dD}=\frac{q(t)}{\dfrac{kh(p_i-p_{wf})}{141.2\mu B\left[\ln\left(\dfrac{r_e}{r_w}\right)-\tfrac{1}{2}\right]}} \quad \ldots\ldots\ldots\ldots\ldots\ldots\ldots\ldots\ldots\ldots (2)$$

and

$$t_{dD}=\frac{0.00634kt}{\phi(\mu c_t)_i r_w^2}\,\frac{1}{\tfrac{1}{2}\left[\left(\dfrac{r_e}{r_w}\right)^2-1\right]\left[\ln\left(\dfrac{r_e}{r_w}\right)-\tfrac{1}{2}\right]} \quad \ldots\ldots\ldots\ldots\ldots\ldots\ldots\ldots (3)$$

or

$$t_{dD}=\frac{t_D}{\tfrac{1}{2}\left[\left(\dfrac{r_e}{r_w}\right)^2-1\right]\left[\ln\left(\dfrac{r_e}{r_w}\right)-\tfrac{1}{2}\right]} \quad \ldots\ldots\ldots\ldots\ldots\ldots\ldots\ldots\ldots\ldots (4)$$

Published values of q_D and t_D for the infinite and finite constant-pressure solutions for single-phase radial flow were transformed into a defined decline-curve dimensionless rate and time, q_{dD} and t_{dD}, by Eqs. 1 and 4. The values in Fig. 2 were used to generate Fig. 3, which is a plot of the decline-curve dimensionless rate and time, q_{dD} and t_{dD}, for various values of r_e/r_w down to 10.

The constant ½ was used in the final equations with p_i (after ½, ⅝, and ¾ were tried), because a better correlation was obtained, particularly at small r_e/r_w stems; the constant-pressure-outer-boundary case during the transient period also overlies the closed-outer-boundary-case type curve.

The plotted type curves (Figs. 1 and 3) generated from the *exact* q_D-t_D constant-wellbore-pressure solution are also exact by definition, although they were generated with the ½ value. The curves cannot be used by simply changing ½ to ¾. One can only back-calculate the correct q_D-t_D from these curves with the value of ½. The r_e/r_w stems were discontinued at a value of 10 because the correlation begins to break down as linear instead of radial flow develops—i.e., as r_e approaches r_w.

In Fig. 1, note that a t_{dD} between 0.2 and 0.3 separates the transient period from the depletion period. Fitting rate-time data to the Arps equation is valid only when depletion sets in and the transient period is over. If flowing pressures are available and are not reasonably constant but smooth and monotonically decreasing, the pressure-normalized rate, log $q/\Delta p$ vs. log t, should be used for analysis.

Rapidly declining rate data fitting the early transient r_e/r_w stems are characteristic of low-permeability stimulated wells and often result in a unique fit. Stimulation causes the rate data to appear

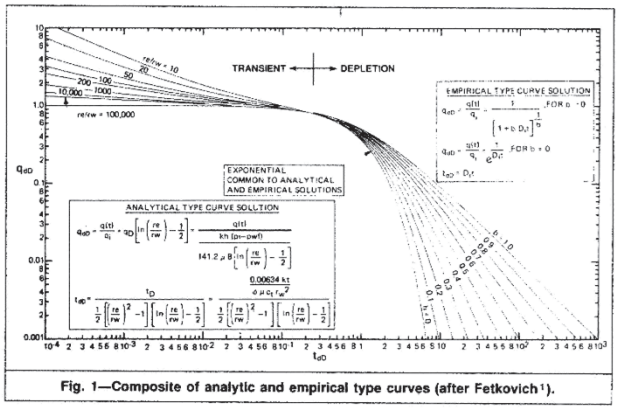

Fig. 1—Composite of analytic and empirical type curves (after Fetkovich[1]).

on a small r_e/r_w stem, and the low permeability then allows them to remain on the stem for real-time periods. Data for high-permeability stimulated wells leave the transient stems and go to pseudosteady state almost immediately. Conversely, a well with a large positive skin producing at a truly constant wellbore pressure will yield very flat rate declines, indistinguishable from $b=0$ to ∞, and will also look like a constant-rate situation. Just as we make a log Δp-log Δt type-curve plot to find the semilog straight line in pressure-buildup analysis, in decline-curve analysis we must make a log q-log Δt type-curve plot of rate-time data to see whether the data are transient.

With regard to the r_e/r_w transient stems, we will repeat a statement from the original paper[1]: "Note from the composite curve [Fig. 1] that rate data existing only in the transient period of the constant terminal pressure solution, if analyzed by the empirical Arps approach, would require values of b much greater than 1 to fit the data." The principal objective of that paper was the development of Fig. 1, which provided a method of analysis for transient data. Transient data should not be interpreted by the Arps equation.

Fig. 4 illustrates the effect of transposing the r_e/r_w stem of 10, indicative of a low-permeability stimulated well response, and the r_e/r_w stem of 10,000, indicative of a large positive skin or damaged well, to the depletion state where the Arps equation is applicable. An equivalent Arps $b=10$ approximates the r_e/r_w stem of 10,000; a $b=3$ approximates the r_e/r_w stem of 10. They appear equivalent and on log-log type-curve matching would be indistinguishable if the Arps exponent b were left unbounded. The same data, if fit on the transient portion to the left of $t_{dD}=0.2$ and then extrapolated, must ultimately go down a depletion stem. The same data fit to an Arps equation with $b>1$ will extrapolate to infinity with no rational basis of terminating the forecast. The exponent b must be bound between 0 and 1.

If we rearrange Eq. 2, we can evaluate the productivity factor from the q_{dD}-$q(t)$ match point:

$$\frac{kh}{\left[\ln\left(\dfrac{r_e}{r_{wa}}\right)-\tfrac{1}{2}\right]}=\left[\frac{141.2\mu B}{(p_i-p_{wf})}\right]\left[\frac{q(t)}{q_{dD}}\right]. \quad \ldots\ldots\ldots\ldots (5)$$

where r_{wa} is the effective wellbore radius determined from the skin effect, $r_{wa}=r_w e^{-s}$. The skin term can also include the effect of the shape factor C_A (see Ref. 9).

Assuming that $(r_e/r_w)^2$ is large compared with 1 in the term $[(r_e/r_w)^2-1]$, reintroducing thickness, h, in the t_{dD} equation, Eq. 3, thus $(kh/\phi h)$, and substituting Eq. 5 into Eq. 3, we can obtain the following equation in terms of the match point q_{dD}-$q(t)$ and t_{dD}-t:

$$V_p=\pi r_e^2 h\phi=\left[\frac{\overline{\mu B}}{(\mu c_t)_i(p_i-p_{wf})}\right]\left(\frac{t}{t_{dD}}\right)\left[\frac{q(t)}{q_{dD}}\right]. \quad \ldots\ldots\ldots\ldots (6)$$

This equation gives the PV at the start of the decline analysis.

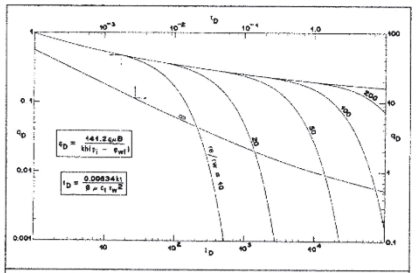

Fig. 2—Dimensionless flow-rate functions, q_D-t_D, for plane radial system, infinite and finite outer boundary, constant pressure at inner boundary (after Fetkovich[1]).

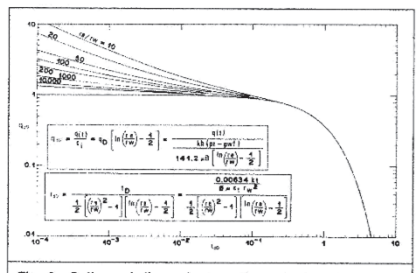

Fig. 3—Collapsed dimensionless flow-rate functions, q_{dD}-t_{dD}, for plane radial system, infinite and finite outer boundary, constant pressure at inner boundary (after Fetkovich[1]).

Fetkovich, M.J., Vienot, M.E., Bradley and M.D., Kiesow, U.G.: "Decline Curve Analysis Using Type Curves – Case Histories," SPEFE (Dec. 1987) 637-656.

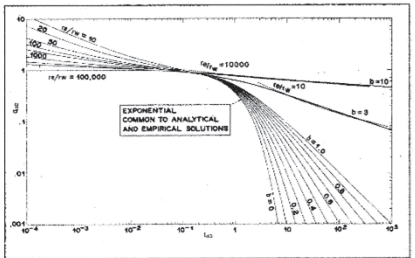

Fig. 4—Apparent *b* values in excess of 1 because of transient flow data.

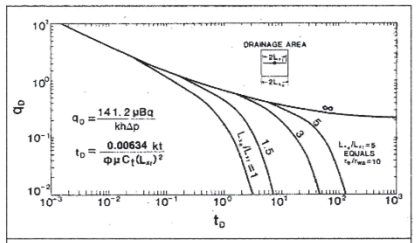

Fig. 5—Dimensionless flow-rate function for infinite-conductivity, vertical-fracture, constant-wellbore-pressure solution (after Locke and Sawyer[2]).

It must be pointed out that Eq. 6 is valid only for closed-outer-boundary situations when the onset of depletion is indicated by the data showing evidence of starting down one of the depletion stems. In the case of water-drive reservoirs, there might be a sufficient delay in aquifer movement to detect depletion, which could then be evaluated. Transient data alone with no indication of depletion are not unique on the q_{dD}-t_{dD} type curve of Fig. 1 or 3. Data only in the transient stage could fit on every stem. This is more easily seen if transient data were fit only on the q_D-t_D type curve (Fig. 2) to the left of $r_e/r_w = 10$. Clearly, this portion of the curve is common to all r_e/r_w depletion stems from 10 to infinity.

Single-Vertical-Fracture Solution. The 1975 Locke and Sawyer constant-wellbore-pressure, infinite-conductivity, vertical-fracture solution type curve (Fig. 5) begins, with regard to depletion stems, where the radial-flow solutions illustrated in Figs. 1 through 3 leave off. In terms of effective wellbore radius ($r_{wa} = L_{x_f}/2$), r_e/r_{wa} of 10 approximately equals $L_{x_e}/L_{x_f} = 5$, where the single-vertical-fracture solution more closely represents the physical situation.

With improved stimulation techniques, hydraulic fracture lengths, L_{x_f}, can and do start approaching L_{x_e} for 5- and 10-acre [2- and 4-ha] spacings—i.e., $L_{x_e}/L_{x_f} \rightarrow 1$. The r_e/r_w stems could easily be extended to include values less than 10 with little loss in the type-curve evaluation accuracy; see Ref. 10 for q_D-t_D values of r_e/r_w less than 10.

In our experience, the basic type curves of Figs. 1 through 3 and 5 have solved most of our decline-curve analysis problems.

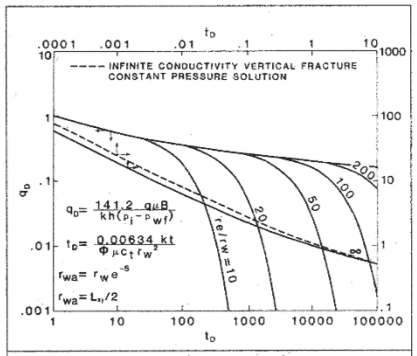

Fig. 6—Comparison of dimensionless flow rate for plane radial flow and infinite-conductivity, vertical-fracture, constant-pressure solutions.

With regard to the early transient period, the dashed line of Fig. 6 illustrates the infinite-conductivity, vertical-fracture solution expressed in terms of $r_{wa} = L_{x_f}/2$—i.e., t_{xfD} converted to t_{rwaD} by the following equation:

$$t_{rwaD} = 4t_{xfD} \quad \ldots\ldots\ldots\ldots\ldots\ldots\ldots\ldots\ldots\ldots\ldots\ldots\ldots\ldots\ldots\ldots\ldots\ldots (7)$$

Rate-time data for a stimulated well can be matched and forecast on either the infinite-conductivity, vertical-fracture solution or the plane-radial-flow solution with r_{wa} or effective wellbore radius for skin, with little practical difference in the resulting forecast. A rapid decline in rate with time usually identifies a stimulated low-permeability well. Data fit on a single-vertical-fracture solution do not identify fracture volume depletion or a naturally fractured reservoir. Whether or not an induced stimulation fracture is propagated down a natural fracture is irrelevant in identifying a naturally fractured system.

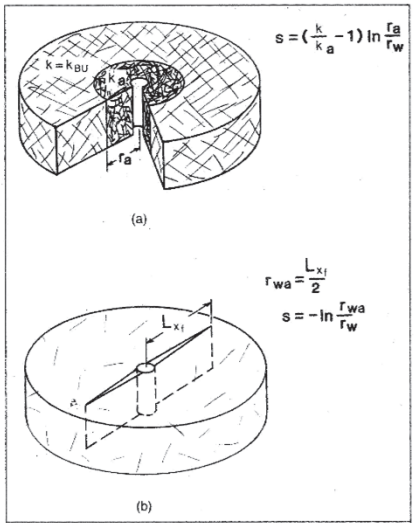

Fig. 7—Comparison of natural fracture and single-vertical-fracture models: (a) intense natural fracturing and matrix acid effect; (b) induced single vertical fracture from acid fracture.

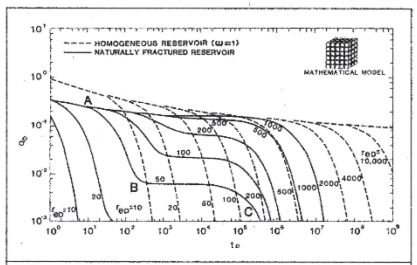

Fig. 8—q_d vs. t_d for constant-pressure production (after Da Prat *et al.*[6]).

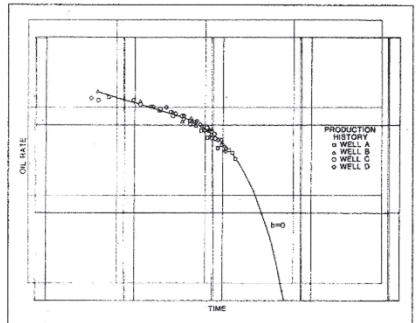

Fig. 9—Overlay of log-rate-vs.-log-time data for individual Wells A, B, C, and D.

The question of whether naturally fractured reservoirs can initially have negative values of skin without stimulation needs to be addressed because the rapid decay in rate resulting from a negative skin effect can be and has been misinterpreted as identifying a naturally fractured reservoir. We will discuss this again later with examples. If we examine Fig. 7a, representing an intensely naturally fractured reservoir (similar to the Warren and Root[12] model), we see from the definition of skin that for a well drilled in a naturally fractured reservoir to have a negative skin, it must penetrate a region near the wellbore that has a permeability greater than that in the interwell region. The likelihood is remote that we could be so fortunate every time we drill a well in a naturally fractured hydrocarbon reservoir. Cutting a single vertical natural fracture with a vertical or subvertical well is equally remote. Wells drilled in a naturally fractured reservoir will initially have large positive skins because of heavy mud losses around the wellbore into the natural fractures. In an intensely naturally fractured limestone reservoir, an acid treatment generally removes the mud damage and results in good negative skins. Pressure-transient data obtained after such a stimulation fit the van Everdingen and Meyer[11] matrix-acid solution (a situation where the permeability near the wellbore is truly altered) as opposed to the single-vertical-fracture solution based on the model shown in Fig. 7b. In the case of the Greater Ekofisk development, the type-curve characteristics are noticeably different after stimulation. Data fit to the single-vertical-fracture solution usually result in a low fracture intensity index (FI), whereas data fit to the matrix-acid solution result in a high FI. The fracture volume associated with Fig. 7a will be connected to the wellbore; in contrast, any fracture volume associated with Fig. 7b may not be connected. In our experience, wells have never obtained a negative skin in a naturally fractured reservoir except after a stimulation treatment.

Naturally Fractured Reservoir (Warren and Root Model) Type Curves. Dual-porosity or naturally-fractured-reservoir type curves developed by Da Prat *et al.*[6] were a significant and timely contribution to decline-curve analysis concepts. The unsupported statement "fracture depletion" with rapidly declining rate-time data is widely used. Careless use of the word "fractured" when dealing with hydraulically fractured wells and the corresponding rapid decline in rate associated with these successful fracture jobs have helped perpetuate the fracture-volume-depletion myth.

On the basis of the Da Prat *et al.* naturally fractured (Warren and Root model), dual-porosity, constant-wellbore-pressure type curves, the only identifying characteristic is the double-exponential decline: depletion of the fracture volume followed by depletion of the matrix volume. Segments A to B in Fig. 8 represent fracture depletion, and Segments B to C represent matrix depletion. This behavior is not equivalent to the two parallel straight lines from the constant-rate solution of Warren and Root[12] because theirs was an infinite-reservoir solution. Two semilog force-fits (double exponential) of early-time data can be and have been manufactured by unsuspecting engineers trying to smooth the rate-time data. There is no indication from the dual-porosity type curves of a $b > 1$ any-

where, except again in the transient portion, which is identical in character to the homogeneous-reservoir solution. The transient portion can yield only *apparent* values of $b > 1$. Also, the matrix-depletion stem can be so flat as to be easily misinterpreted as having a b much greater than 1 (see the misplaced r_e/r_w stem of 10,000 in Fig. 4). Gas saturations within the matrix block for solution-gas-drive systems along with end effects (little or no oil flow from the matrix blocks) would appear as large positive skins with respect to oil flow, further creating long, flat, transient r_e/r_w stems. Stimulation or removal of matrix skins is not possible.

Log-Log Decline-Curve Plot. If we closely examine Eqs. 2 and 3 expressing q_{dD}-t_{dD} and consider the nature of the log q_{dD}-log t_{dD} plot, we should recognize that real rate-time data, in any convenient units, when plotted as log q-log t can look exactly like one of the q_{dD}-t_{dD} type-curve plots previously discussed. The data in rate and time will be shifted from the unit solution only by the coefficient of q and t in q_{dD} and t_{dD}, respectively. Some basic reservoir knowledge usually suggests with which type curve, and where on the curve, we should expect to obtain a match. By overlaying rate-time data on Fig. 1 or 3, for example, we can obtain a match of q_{dD}, t_{dD}, r_e/r_{wa}, and b and evaluate reservoir variables kh, r_e/r_{wa}, s, r_e, or PV. In a given field, all wells should normally be expected to match the same depletion type curve, although skins could be different; the axis will be shifted in time and rate for each well only by the coefficient of q_{dD} and t_{dD}. For q_{dD}, the coefficient is

$$\frac{141.2\mu B\left[\ln\left(\frac{r_e}{r_{wa}}\right) - \frac{1}{2}\right]}{kh(p_i - p_{wf})},$$

and for t_{dD}, the coefficient is

$$\left[\frac{0.00634k}{\phi(\mu c_t)_i r_{wa}^2}\right]\left\{\frac{1}{\frac{1}{2}\left[\left(\frac{r_e}{r_{wa}}\right)^2 - 1\right]\left[\ln\left(\frac{r_e}{r_{wa}}\right) - \frac{1}{2}\right]}\right\}.$$

The overlaying technique is a fundamental concept that leads to the idea of developing a field type curve from rate-time data alone. The type curve so developed may or may not appear anything like an existing solution. Fig. 9 is the log q-log t plots of Wells A through D in the same field; the match results are given in Table 3 of Ref. 1. First, note that the data from the four wells overlie each other and have developed a single log-log type curve at least to the range

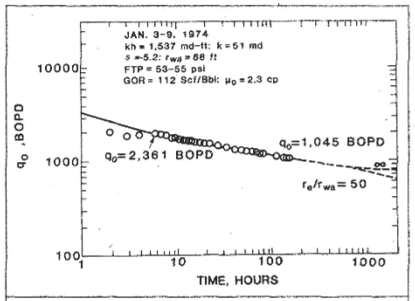

Fig. 10—Log-rate-vs.-log-time data for Well M-4X obtained from long-duration, constant-pressure production test.

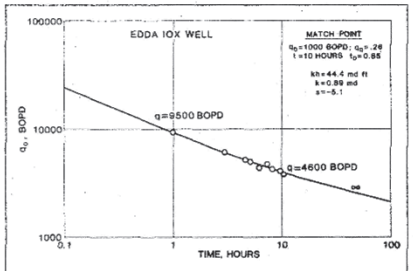

Fig. 11—Well Edda 10X rate-time type-curve match of 10-hour production test after stimulation.

TABLE 1—EDDA 10X WELL: DST 2 SUMMARY OF ANALYSIS RESULTS (POSTACID) AND RESERVOIR DATA

	Horner	q_D-t_D Constant p_{wf} Plane Radial System
k, md	0.95	0.89
s	−4.8	−5.1
r_{wa}, ft	40	54
Reservoir Data		
ϕ	0.25	
S_w	0.35	
μ, cp	0.167	
p_i, psia	7,043	
B_o, RB/STB	1.992	
h, ft	50	
c_t, psi^{-1}	21.6×10^{-6}	

of existing data. Essentially, the shift in the rate axis reflects a different kh, while the shift in the time axis reflects a different k and r_{wa}. We could match and have matched this curve to a known analytic solution (Fig. 3). By knowing or estimating reservoir variables from some source, such as a complete buildup analysis or early-time rate-time decline analysis on at least one of the wells, we can back-calculate values of q_{dD} and t_{dD}. Slight differences in r_e/r_{wa} stems appear to be reflected in the early transient period. The significance of the collapsed q_{dD}-t_{dD} plot (Fig. 3) is illustrated by this example.

The next logical step in the use of type curve and log-log plot concepts is the development of the total field type curve. Total field production can be considered as an "average well" times the number of wells. Wells overlie wells within a field with the same drive mechanism, so why shouldn't field rate-time production data from the same formation with similar drive mechanisms overlie other fields in the same formation? The reservoir and fluid variables [k, h, r_e (spacing), r_{wa}, μ_o, B_o, p_i, p_{wf}, ϕ, s_w, and c_t] can be different for all fields. This concept will be demonstrated with the development of the Monterey type curve from historical production data from several Monterey fields in California.

Arps Limits of b. The Arps stems in Fig. 1, $b=0$ to 1, combined with the analytic transient stems, deserve some discussion. First, the data used by Arps to develop and test his original equations were from real fields and wells. They indicate that real-world data most often do not follow the single-phase analytic solution for depletion, the $b=0$ solution. The limits to b that he found by use of Cutler's data were between 0 and 0.7, with over 90% of the cases having values less than 0.5: no case was found with a b in excess of 0.7. Arps' own experience, however, indicated that $b=1$ did occur, but only rarely.

If we consider the initial declining-rate period as nothing more than an extended drawdown test, then matching the early-time data on the rate-time type curve for reservoir parameter evaluation yields initial permeability, k_i, and $(\mu c_t)_i$ at $t=0$, the start of the decline analysis. A value of $b>0$ reflects changing values of $(k_{ro}/\mu_o B_o)_p$ and $(\mu)_p(c_t)_p$ during reservoir depletion. For a given drive mechanism, k_i, $(\mu c_t)_i$, and b should be sufficient to describe a type curve for a given field or formation. Theoretically, an oil pseudopressure, p_{ps}, and a pseudodimensionless time, t_{pdD}, could be developed from a history-matched k_{ro}-k_{rg} relationship to drive the rate-time data to the analytic solution $b=0$; however, this is too complex a procedure and will find little practical use. Nevertheless, the pursuit may be worthwhile, perhaps leading to a better understanding of what causes the different values of b.

Carter's[5] study of the effect of pressure level and drawdown on gas well rate-time behavior provides some insight into what causes b values to be greater than 0. Examination of his Fig. 1 shows that the early transient period is unaffected by a variation in $(\mu c_t)_p$, while the depletion stems increase from $b=0$ for $\lambda=1$ to $b=0.3$ for $\lambda=0.75$, and $b\cong 0.5$ for $\lambda=0.55$. Carter's λ is defined as

$$\lambda=\frac{\mu(p_i)c_g(p_i)}{\overline{\mu c_g}} \quad \ldots\ldots\ldots\ldots\ldots\ldots\ldots\ldots\ldots\ldots (8)$$

or

$$\lambda=\left[\frac{\mu(p_i)c_g(p_i)}{2}\right]\left[\frac{p_{pi}-p_{pwf}}{\left(\frac{p}{z}\right)_i-\left(\frac{p}{z}\right)_{wf}}\right].$$

One could interpolate between his λ values by interpolating between the approximate b values.

A $b>0$ for solution-gas-drive reservoirs should reflect an increasing total compressibility with increasing gas saturation. Later development of other supplemental drives—such as gravity segregation, limited water movement, late-time crossflow from nonwellbore productive layers, and hydrocarbon influx from the periphery of the reservoir—would tend to increase the value of b.

Decline-Curve Analysis Using Type Curves—Individual Well Cases

Well M-4X. Well M-4X was the fourth of five appraisal wells drilled on a carbonate Middle Cretaceous Mishrif structure in the Middle East. In Jan. 1974, data for production rate vs. time, obtained on a long-duration production test after two separate acid treatments totaling 14,000 gal [53 m^3] 20% HCl, indicated a

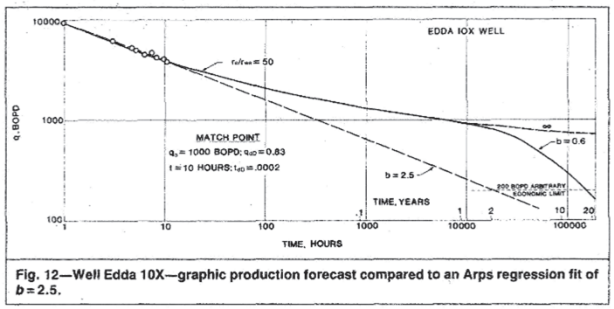

Fig. 12—Well Edda 10X—graphic production forecast compared to an Arps regression fit of $b=2.5$.

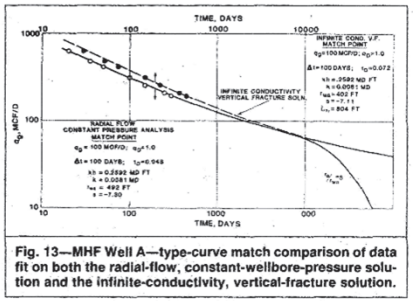

Fig. 13—MHF Well A—type-curve match comparison of data fit on both the radial-flow, constant-wellbore-pressure solution and the infinite-conductivity, vertical-fracture solution.

severe decline in production rate. The initial rate declined steadily from 2,361 to 1,045 BOPD [375 to 166 m^3/d oil] after only 160 hours (6.7 days) of testing (see Fig. 10). This high initial decline rate was generally interpreted to be depletion. More specifically, it was interpreted as fracture and vug porosity depletion because some vugs and fractures were identified in the initial core description.

First and foremost about the test is that it was recognized as a true constant-wellbore-pressure test where the rate must necessarily decline with time. The constant wellhead flowing pressure observed during the test of 53 to 55 psi [365.4 to 379.2 kPa], coupled with the fact that the reservoir fluid was highly undersaturated and should then have an essentially constant oil head, resulted in a constant bottomhole flowing pressure (BHFP) during the entire test. A constant-wellbore-flowing-pressure analysis was made by type-curve matching the rate-time data on Fig. 2. The match shown in Fig. 10 was unique and conclusively established that the rate-time decline was a transient phenomenon and not depletion; i.e., the rate-time data fit the transient portion of the analytic type curve. Depletion would be identified by the rate-time data overlying an r_e/r_w exponential-depletion stem (analogous to the reservoir limit test).

Because the identifying mark of dual-porosity depletion is an exponential-depletion stem (depletion of the fracture/vugs) followed later by another exponential-depletion stem (depletion of the matrix), we clearly cannot attribute the well's rapid decline in rate to the reservoir's being naturally fractured or vuggy. The rapid transient decline rate of the well is the expected behavior of a successfully stimulated well of moderate to low permeability. One should look at the ratio k/μ to see what is moderate or low permeability. For this well,

$$\frac{k_o}{\mu_o}=\frac{51\text{ md}}{2.3\text{ cp}}\cong 25\text{ md/cp [}\sim 25{,}000\text{ md/Pa·s]}.$$

For a gas reservoir of 0.02 cp [0.02 mPa·s], the same ratio of 25 would yield a permeability of 0.5 md. Both would exhibit similar transient behavior.

Using the rate-time data from the 7-day production test, we forecast the well's future production rate as a function of time by drawing a line through the rate-time data overlaid on the uniquely matched portion of the type curve and down a premised r_e/r_{wa} stem for an assumed spacing, r_e. At an appropriate rate, the BHFP was lowered to 500 psia [3447.4 kPa] by use of the superposition method given in Ref. 1.

Well Edda 10X. Well Edda 10X rate-time data taken in Nov. 1973 were obtained on the second appraisal well drilled in the Upper Cretaceous chalk reservoir of the Edda field, one of several fields located in the Greater Ekofisk development of the Norwegian North Sea. A drillstem test taken in Nov. 1973 after an acid fracture treatment, without the use of proppants, indicated a very severe decline in production rate during the drawdown test. The rate declined from 9,500 BOPD [1510 m^3/d oil] at 1 hour to 4,600 BOPD [731 m^3/d oil] after only 10 hours. The flowing tubing pressure varied from 896 psia [6177.9 kPa] at the beginning of the test to 751 psia [5178.1 kPa] at the end, essentially a constant-wellbore-pressure condition. Again, as in the Well M-4X test, the rate decline was incorrectly assumed to be either natural fracture volume depletion, because the Greater Ekofisk development reservoirs are known to be naturally fractured, or closure of the induced fracture as a result of pressure drawdown—both exotic and simplistic explanations.

Fig. 11 illustrates the type-curve match on the plane-radial-flow, constant-wellbore-pressure solution with another unique match on the transient or infinite-acting period. No exponential depletion, fracture volume depletion, or any other type of depletion is indicated. It is not possible to determine whether the reservoir is naturally fractured from the rate-time decline. Again, the rapid decline in rate is the expected behavior of a successfully stimulated low-permeability well.

An Arps depletion stem match of the data gives an apparent $b=2.5$, which, of course, is invalid.

An evaluation of the q_D-t_D match and the results obtained from the pressure-buildup analysis are summarized in Table 1. The values of permeability and skin obtained from the rate-time drawdown analyses and the Horner buildup are essentially the same. To determine whether the reservoir was naturally fractured, a fracture index, I_f, was calculated from a permeability value obtained from a matrix-plug permeability-porosity plot compared with a buildup or drawdown calculated permeability:

$$I_f=\frac{k_{BU}\text{ or }k_{DD}}{k_{(\phi-k)}}=\frac{0.9\text{ md}}{0.66\text{ md}}=1.4. \quad \ldots\ldots\ldots\ldots\ldots (9)$$

For this well, there appears to be little natural fracturing at this location because the index is 1.4. This is not the case, however, for most of the development wells drilled later in this field. We

TABLE 2—MHF GAS WELL A: COMPARISON OF PRODUCTION FORECASTS

Time (months)	Constant-Pressure Solution (Mscf/D)	Infinite-Conductivity Vertical-Fracture Solution (Mscf/D)	Ref. 13 Simulator Results (Mscf/D)
12	182	182	190
18	157	157	165
24	140	136	150
30	130	128	140
36	122	120	135
42	117	112	130
48	110	108	120
54	108	103	110
60	104	100	105
(years)			
6	100	95	
7	96	89	
8	92	86	
9	89	83	
10	86	80	
11	84	78	
12	82	75	
13	80	73	
14	79	71	
15	77	69	
16	76	68	
17	74	67	
18	73	66	
19	72	65	
20	71	64	

will demonstrate this in a full-field rate-time analysis of the total field production.

Fig. 12 illustrates a one-well forecast that was made before any development drilling by extrapolating down an r_e/r_w stem for the premised well spacing. Future rates were read from the real-time scale on which the rate data were plotted. Also shown in Fig. 12 is an extrapolation of the same data fit on an Arps $b=2.5$, which is clearly incorrect. Although one would not attempt an Arps equation fit and extrapolation on only 10 hours of production data, it serves as the only example in which, using transient data, false values of $b>1$ would severely underestimate production.

To summarize, this example illustrated the ability to develop a sound technical decline-curve analysis prediction with basic reservoir engineering principles and only 10 hours of rate-time data.

MHF Well A. Agarwal *et al.*[13] presented 300 days of rate-time data for a massive hydraulically fractured (MHF) well. Fig. 13 illustrates a type-curve match of their data on the radial-flow, constant-wellbore-pressure solution and the infinite-conductivity, single-vertical-fracture, constant-wellbore-pressure solution. Clearly, all the data lie on the transient or infinite-acting period, and there is no evidence of depletion. An evaluation of the match points on the basic radial-flow, constant-wellbore-pressure solution yields $k=0.0081$ md. This value is identical to the Agarwal *et al.* prefracture test result and is the same value obtained from matching on the vertical-fracture, constant-wellbore-pressure solution. Calculated values of skin or L_{x_f} are reasonably close. Table 2 lists the Agarwal *et al.* forecast results obtained when their type-curve analysis and reservoir and fluid properties were entered into their MHF simulator. Listed on the far left is the forecast read directly from the match on the basic radial-flow, constant-wellbore-pressure solution. The middle column is the forecast read directly from the match on the infinite-conductivity, vertical-fracture, constant-wellbore-pressure solution. Note the good agreement between the graphical extrapolation with the radial-flow, constant-wellbore-pressure solution and their simulator results. Our extended forecasts from the type-curve matches are, for practical purposes, the same.

Fitting the transient data to the Arps equation resulted in an apparent value of $b\approx 2.2$; in this case, for the 20-year forecast period, it would not have resulted in as severely different a forecast as in the previous Well Edda 10X example.

This example further serves as a classic graphical illustration of a case for infill drilling—closer spacing than an $r_e=2{,}000$ ft [610 m]—to increase recoverable reserves in a reasonable time period. This example also illustrates that conventional deliverability forecasting of rate-time decline would be grossly in error, even if we correctly estimated a stabilized backpressure curve position from reservoir variables. On the curve of Fig. 14, note the point at which the rate departs from the transient stem and starts down the depletion stem. This point represents the stabilized backpressure curve position. The rate at the given Δp^2 would establish a point on the stabilized backpressure curve.

All early transient production higher than this stabilized rate would be completely ignored in a conventional deliverability rate-time forecast. Further complicating a conventional deliverability approach is the inability to get valid reservoir pressures from reasonable-duration pressure-buildup tests in such a low-permeability well to determine original gas in place from a p/z-vs.-G_p graph. Additional discussion of this point occurs later in the San Juan example.

To illustrate more clearly the shifting of the backpressure curve with time to the stabilized curve position, Cullender's[14] Gas Well No. 3 backpressure curve coefficients—C values for a 214-hour flow and C values from a four-point isochronal test and 72-hour deliverability tests covering a period of 9 years—were plotted and matched on the infinite-conductivity, vertical-fracture, constant-wellbore-pressure solution (Fig. 15). Fig. 16 shows these same data plotted as a series of backpressure curves shifting with time. (See Table 3 of Ref. 14 for the complete set of the data.) This well was initially acid-fractured. Note the near-perfect fit of all the data on the infinite-conductivity, vertical-fracture, constant-wellbore-pressure solution with no indication of wellbore performance deterioration. Even after 9 years of production and a 106-psi [730.9-kPa] reservoir shut-in pressure decline, the 72-hour values of C fall on the original curve trace.

West Virginia Gas Well A. Well A is a low-permeability gas well located in West Virginia. It produces from the Onondaga chert that has been hydraulically fractured with 50,000 gal [189 m³] of 3% gelled acid and 30,000 lbm [13 608 kg] of sand. After initial completion, the well was placed on production for 200 days and then shut in for a 106-day pressure buildup in an attempt to obtain reservoir pressure. A conventional Horner analysis of the buildup data gave $p_R=3{,}268$ psia [22 532 kPa], $k=0.082$ md, and $s=-5.4$. A type-curve analysis of the same data indicated that the correct semilog straight line started at about 600 hours (25 days).

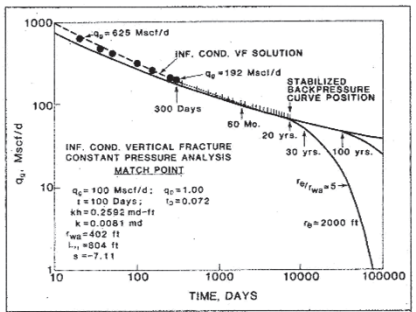

Fig. 14—MHF Well A graphic production forecast.

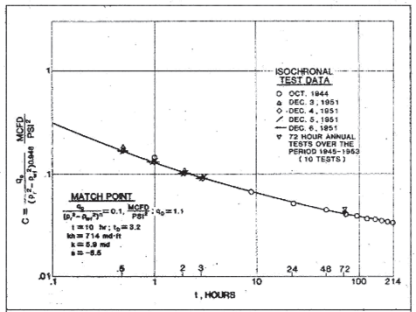

Fig. 15—Type-curve fit of all Cullender's Gas Well 3 data in terms of C, pressure-normalized rate, on the infinite-conductivity, vertical-fracture, constant-wellbore-pressure solution.

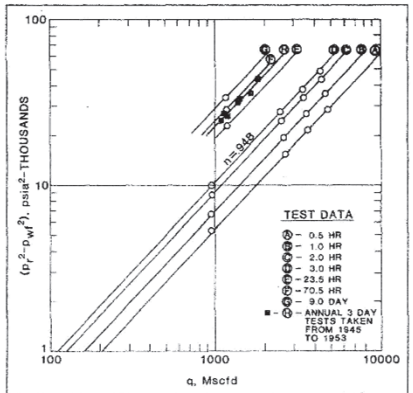

Fig. 16—Cullender's Gas Well 3 data expressed as transient backpressure curves.

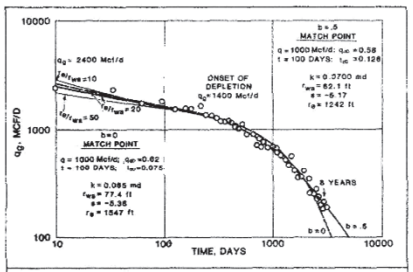

Fig. 17—West Virginia Gas Well A type-curve fit of 8 years of production data fit to a $b=0$ and $b=0.5$.

TABLE 3—WEST VIRGINIA GAS WELL A

Reservoir and Fluid Properties	
Gas specific gravity	0.57 (air = 1.00)
Porosity	0.06
Water saturation	0.35
Original pressure, psia	4,175
Pressure at start of decline, psia	3,268
Viscosity at 3,268 psia, cp	0.0171
System compressibility at 3,268 psia, psi^{-1}	177×10^{-6}
Thickness, ft	70
Temperature, °F	160
Wellbore radius, ft	0.354
Rate before 106-day pressure buildup, Mscf/D	2,181
Δp_p, psi^2/cp	774×10^6
B_g at 3,268 psia, scf/ft^3	208.8
B_g at 4,175 psia, scf/ft^3	253.9

TABLE 4—WEST VIRGINIA GAS WELL A: SENSITIVITY TO r_e/r_w

	$r_e/r_{wa}=10$	$r_e/r_{wa}=20$	$r_e/r_{wa}=50$	Horner Analysis p_p Basis
kh, md-ft	3.542	4.902	6.705	5.635
k, md	0.0506	0.0700	0.0958	0.0805
V_p, 10^6 ft^3	20.36	20.36	20.36	
r_e, ft	1,242	1,242	1,242	
r_{wa}, ft	124.2	62.1	24.8	
s	−5.86	−5.17	−4.25	−5.52
G at 3,268 psia, Bscf	2.763	2.763	2.763	
G_i at 4,175 psia, Bscf	3.360	3.360	3.360	

Fig. 17 is a log-log plot of monthly production data. These are raw monthly production data obtained directly from production files, not data from special tests. The 8 years of rate-time data were matched on the radial-flow, constant-wellbore-pressure solution (dashed line), the r_e/r_{wa} exponential stem of 20, and $b=0$ to yield $k=0.0651$ md, $s=-5.38$, and $r_e=1,547$ ft [472 m]. The solid line through the same data shows a fit on the $b=0.5$ and Carter's $\lambda=0.55$ constant-wellbore-pressure solution on the r_e/r_{wa} stem of 20. Results from the match on a $b=0.5$ resulted in a $k=0.0700$ md, $s=-5.17$, and $r_e=1,242$ ft [379 m]. These results compare closely with those obtained from the match on Carter's type curve, which gave $k=0.0678$ md, $s=-5.17$, and $r_e=1,252$ ft [382 m]. Carter's λ was calculated to be 0.555 for this example. For the pressure ratio $p_{wf}/p_R=500$ psi/3,268 psi=0.15 [3447 kPa/22 532 kPa], Figs. 8 and 9 of Ref. 1 also indicate that the expected depletion stem should have a $b=0.5$ for this gas well.

Occasional shut-ins and blows to the atmosphere for dewatering the wellbore did occur during the normal production of the well. One would expect a $b=0.5$ situation gradually to approach a $b=0$ performance because liquid loading occurs when the flow rate declines and the wellbore deteriorates with time.

Evaluating the Match. The previous discussion of the match to the r_e/r_{wa} stem of 20 leaves some doubt as to whether the match to the 20 stem is unique or the best answer. We will investigate the sensitivity of results to stems of 10, 20, and 50 for the $b=0$ and $b=0.5$ match. To illustrate the complete evaluation of the matching technique, we will use the $b=0.5$ match (Fig. 17) to the composite type curve as an example. Table 3 lists all the pertinent reservoir variables for the well. For the match point of $b=0.5$, $q_{dD}=0.58$, $q(t)=1,000$ Mscf/D [28×10^3 std m^3/d], $t_{dD}=0.126$, and $t=100$ days.

When Eq. 5 is expressed in terms of gas units and pseudopressure, p_p, the productivity factor is

$$\frac{kh}{\left[\ln\left(\frac{r_e}{r_{wa}}\right)-\frac{1}{2}\right]}=\frac{q(t)p_{sc}T}{(19.87\times10^{-6}q_{dD}T_{sc}(p_{pi}-p_{pwf})} \quad \ldots\ldots(10)$$

$$=\frac{1,000(14.7)(620)}{(19.87\times10^{-6})(0.58)(520)(7,948\times10^5-208\times10^5)}$$

$$=1.965 \text{ md-ft [0.599 md·m]}.$$

Also expressing Eq. 6 in terms of gas units and pseudopressure, p_p, we have

$$V_p=\pi r_e^2h\phi=\left[\frac{2,000p_{sc}T}{(\mu c_t)_iT_{sc}(p_{pi}-p_{pwf})}\right]\left(\frac{t}{t_{dD}}\right)\left[\frac{q(t)}{q_{dD}}\right] \quad \ldots\ldots(11)$$

$$=\left[\frac{2,000(14.7)(620)}{0.0172(177\times10^{-6})(520)(7,948\times10^5-208\times10^5)}\right]$$

$$\times\left(\frac{100}{0.126}\right)\left(\frac{1,000}{0.58}\right)$$

$$=20.36\times10^6 \text{ ft}^3 \text{ [0.5765}\times10^6 \text{ m}^3\text{]},$$

and

$$r_e=\sqrt{\frac{V_p}{\pi h\phi}}=\sqrt{\frac{20.36\times10^6}{3.1416(70)(0.06)}}=1,242 \text{ ft [379 m]}. \quad \ldots(12)$$

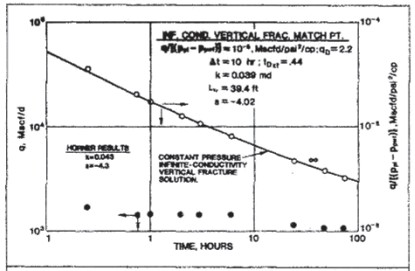

Fig. 18—West Virginia Gas Well B comparison of rate-time plot and pressure-normalized, rate-time plot of same data.[15]

The gas in place, G, at $p_i=3,268$ psia [22 533 kPa], with p_i being the pressure at the start of the decline analysis, is then

$$G=V_p(1-S_w)B_g \quad \ldots\ldots(13)$$

$$=20.36\times10^6(1-0.35)(208.8)$$

$$=2.763 \text{ Bscf [78.2}\times10^6 \text{ std m}^3\text{]}.$$

For comparison purposes, G at $p_i=3,268$ psia [22 533 kPa] from the Carter type-curve match on $\lambda=0.55$ is 2.807 Bscf [79.4×10^6 std m^3], while that obtained from the $b=0$ match is 4.286 Bscf [121.3×10^6 std m^3].

Assuming little or no PV change resulting from rock and water expansion, at the original reservoir pressure of 4,175 psia [28 787 kPa], $B_g=253.9$ scf/ft^3 [std m^3/m^3], an original gas in place, G_i, was then calculated to be 3.360 Bscf [95.1×10^6 std m^3]. The difference of 0.597 Bscf [17×10^6 std m^3] compares well with the measured cumulative production of 0.580 Bscf [16×10^6 std m^3] between the two average reservoir pressure intervals.

With the productivity factor calculated as 1.965 md-ft [0.599 md·m] and r_e calculated as 1,242 ft [379 m], we can now investigate the sensitivity of k and s to r_e/r_{wa} stems (Table 4). Regardless of the r_e/r_{wa} stem chosen, once the depletion stem is established by the rate-time data (the match points from the composite type curve Fig. 1), q_{dD}-$q(t)$ and t_{dD}-t are fixed and the PV is then fixed. The calculated initial permeability and skin are insensitive to the r_e/r_{wa} stem selection. In this case, we have the 106-day pressure-buildup analysis run just before the start of the decline-curve analysis with which to compare. From the Horner results, the correct r_e/r_{wa} stem appears to be ~20. If at early time we had taken more frequent, precise rates and flowing pressures, then we could have uniquely fit the stem. At the very least, kh and s could have been calculated from a short-duration, constant-wellbore-pressure test, as opposed to calculating kh and s from a long-duration buildup test. This was done for West Virginia Gas Well B.[15]* Fig. 18 compares the pressure-normalized, constant-wellbore-pressure analysis (the rate data alone had no character) and the corresponding Horner analysis results for this well. Therefore, one need not have shut in Gas Well A for 106 days to obtain kh and s for selecting the proper r_e/r_{wa} stem.

Table 5 summarizes the pertinent results of matching the rate-time data on $b=0$, $b=0.5$, and Carter's $\lambda=0.55$. By comparing the difference of 0.91 Bscf [25.8×10^6 std m^3] between a calculated $G_i=5.20$ Bscf [147.2×10^6 std m^3] at 4,175 psia [28 787 kPa] and the $G=4.29$ Bscf [121.5×10^6 std m^3] at 3,268 psia [22 533 kPa] with the real cumulative production of 0.58 Bscf [16.4×10^6 std m^3] between the two shut-in pressures, the $b=0$ as a match is ruled out and the $b=0.5$ must be selected.

*Fetkovich, M.J. and Thrasher, T.S.: "Constant Well Pressure Testing and Analysis in Low Permeability Reservoirs," paper 7928 presented at the 1979 SPE Symposium on Low-Permeability Reservoirs, Denver, May 20–22 (available from author).

TABLE 5—WEST VIRGINIA GAS WELL A: SUMMARY OF RATE-TIME ANALYSIS RESULTS

	Match Points			
	Composite Type Curve $b=0$	Composite Type Curve $b=0.5$	Carter Type Curve $\lambda=0.55$ ($b=0.5$)	
	q_{dD} 0.62	q_{dD} 0.58	q_{DR} 0.24	
	t_{dD} 0.075	t_{dD} 0.126	t_{DR} 60	
	$q(t)$, Mscf/D 1,000	$q(t)$, Mscf/D 1,000	$q(t)$, Mscf/D 1,000	
	t, days 100	t, days 100	t, days 100	
	$r_e/r_{wa}=10$	$r_e/r_{wa}=20$	$r_e/r_{wa}=50$	Horner Analysis
	$b=0$ Evaluation			
kh, md-ft	3.292	4.558	6.231	
k, md	0.047	0.065	0.089	0.0805
r_{wa}, ft	154.7	77.4	30.9	
s	−6.08	−5.38	−4.47	−5.52
r_a, ft	1,547	1,547	1,547	
	$b=0.5$ Evaluation			
kh, md-ft	3.542	4.902	6.705	
k, md	0.0506	0.0700	0.0958	
r_{wa}, ft	124.2	62.1	24.8	
s	−5.86	−5.17	−4.25	
r_e, ft	1,242	1,242	1,242	
	Carter's $\lambda=0.55$ Evaluation			
kh, md-ft	3.451	4.746	6.699	
k, md	0.0493	0.0678	0.0957	
r_{wa}, ft	126.4	62.6	24.8	
s	−5.88	−5.17	−4.25	
r_e, ft	1,264	1,252	1,240	

San Juan Example. Early in 1982, a reservoir study of all wells completed in the Blanco Mesaverde pool in one entire township in Rio Arriba County, NM (San Juan basin), was initiated to quantify the reserve increase resulting from the infill drilling program begun in 1975. The initial spacing of 320 acres [130 ha] was halved through infill drilling.

The San Juan basin is located in northwestern New Mexico and extends into southwestern Colorado. The gas-producing formations in the basin are sandstones of Upper Cretaceous Age. The Mesaverde ranges in gross thickness from a few hundred to almost 1,800 ft [550 m]. Average porosity in the Mesaverde is about 10%, and the permeability ranges from 0.02 to 1.0 md. Initial pressure in the study area was about 1,200 psi [8274 kPa].

The area we investigated had 72 original wells, drilled two per section, plus 72 infill wells. Initial pressure for a majority of the infill wells was some 30 to 40% less than original reservoir pressure, indicating that drainage was occurring. A limited number of infill wells had initial pressures essentially equal to original pressure, indicating that drainage was not occurring at these locations.

The reserve determination method used in the past was the p/z plot. This method consisted of plotting annual 7-day shut-in pressures vs. cumulative gas produced. Although annual 7-day shut-ins were taken, the final shut-in pressure was well below the true static reservoir pressure. Because of the low-permeability stimulated character of the wells, the semilog straight line was seldom reached, making the determination of average reservoir pressure difficult. This essentially negated the p/z plot as a useful reservoir analysis tool until infill wells were drilled. Trend plotting of the short-duration shut-in and its corresponding p/z was used without recognizing the need to pass through the initial p/z value (see Fig. 19). The initial p/z value was ignored to prevent an apparent yearly increase in gas reserves.

A majority of the infill wells came in at pressures about 30 to 40% lower than the original reservoir pressure. In these cases, the

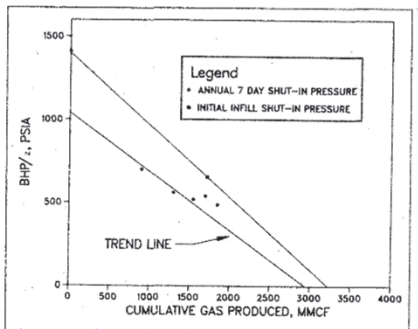

Fig. 19—Trend plot of p/z-vs.-cumulative-gas-production data for San Juan Gas Well 36.

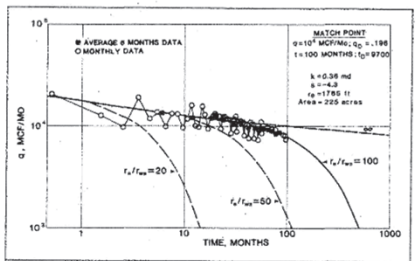

Fig. 20—San Juan Gas Well 58 rate-time type-curve match of production data on the radial-flow, constant-wellbore-pressure solution.

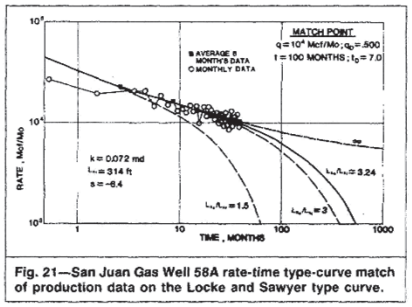

Fig. 21—San Juan Gas Well 58A rate-time type-curve match of production data on the Locke and Sawyer type curve.

TABLE 6—SAN JUAN WELL 58: SENSITIVITY TO r_e/r_w

	$r_e/r_{wa}=100$	$r_e/r_{wa}=200$
k, md	0.34	0.40
s	−4.3	−3.6
r_e, ft	1,765	1,776

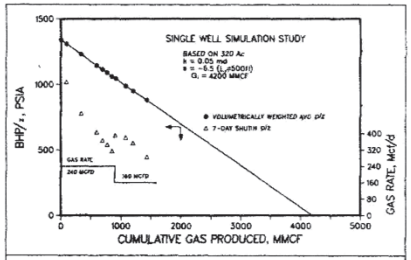

Fig. 22—Single-well simulation study of rate reduction effect on 7-day annual shut-in pressures.

infill original pressure could be used to provide a pressure point on the plot of p/z vs. cumulative gas produced of the original well. A reserve figure was determined for the original well by passing a line from the initial p/z through the infill-well p/z value with an abandonment pressure of 100 psi [690 kPa] assumed. This method could not be used, however, when the infill initial pressure essentially equaled the original reservoir pressure. In such cases, the most practical method available to determine the reserve was decline-curve analysis.

Figs. 20 and 21 present the rate-time data and type-curve match of the original well, Well 58, and the offset infill well, Well 58A. The latter came in at near-original pressure. Data for both wells (as for all wells in the study area) were obtained from a commercially available data base. The character of the monthly rate-time data was erratic—a problem not uncommon in rate-time analysis—and average 6-month rates available from the data base were plotted at midpoint intervals as a form of data smoothing. The average 6-month data points appear as solid squares on the type-curve matches. Notice how the character of the production profile was enhanced by this smoothing technique.

A type-curve match of the rate-time data for Well 58 indicates the well to be on decline and going down a depletion stem. The calculated k and s are 0.36 md and −4.3, respectively, with a calculated drainage area of 225 acres [91 ha]. Although not apparent, a match on different r_e/r_{wa} stems would result in essentially the same calculated value of r_e. The drainage radius is fixed once depletion is evident. Table 6 illustrates this point for Well 58 matched on r_e/r_{wa} stems of 100 and 200. The rate-time data of Well 58A were matched to the Locke and Sawyer type curve and found to be entirely transient. The k and s were calculated to be 0.07 md and −6.4, respectively.

These results are consistent in that one would expect the infill well permeability to be less than the original well permeability, when the infill location had not been drained. The more negative skin factor for the infill well represents the improvement in hydraulic fracturing technology and design, because the original well was stimulated in the late 1950's. A production forecast for the infill well was developed by forecasting down a depletion stem of $L_{x_f}/L_{x_{sf}}=3.2$. This stem corresponds to the skin of −6.4 and a drainage area of 95 acres [38 ha] to keep the total drainage area of 320 acres [130 ha] whole.

A reserve forecast for all wells on decline in the study area was made from a rate-time analysis. These calculated reserves are within 9% of the p/z reserve determined with the infill-well original pressure. The reserve study of the township indicated that infill drilling resulted in an average reserve increase of 11%.

Reserve increases resulting from infill drilling have been postulated as a result of the flattening observed in the p/z trend after infill drilling. If total field production remains essentially constant (fixed market demand) before and after infill drilling, a reduction

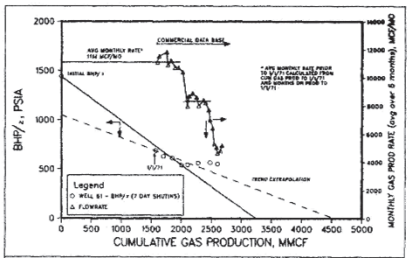

Fig. 23—San Juan field—well example of rate reduction effect on 7-day annual shut-in pressures.

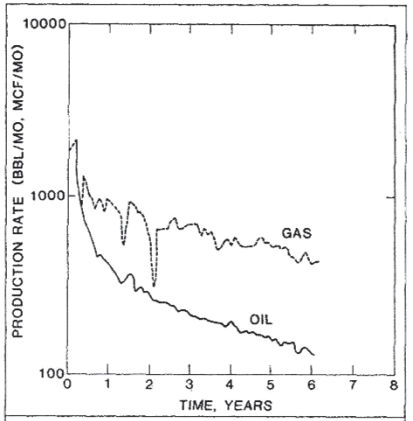

Fig. 24—Semilog plot of production history of Gentry and McCray's Oil Well Example No. 2 data.

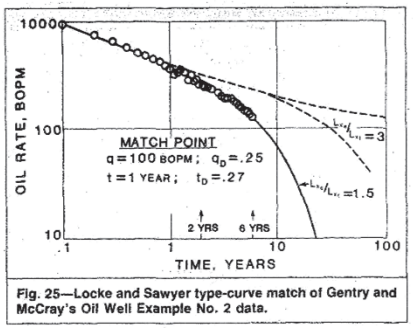

Fig. 25—Locke and Sawyer type-curve match of Gentry and McCray's Oil Well Example No. 2 data.

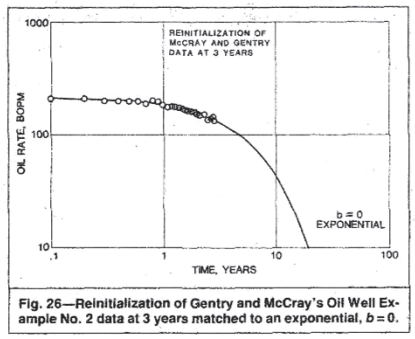

Fig. 26—Reinitialization of Gentry and McCray's Oil Well Example No. 2 data at 3 years matched to an exponential, $b=0$.

in some of the original wells' flow rates will occur after the start of infill drilling. This reduction in flow rate will cause a corresponding increase in flowing pressure. When the well is next shut in for an annual 7-day test, the final buildup pressure will automatically reflect a higher final shut-in pressure than when the well was produced at the previously higher rate. The obvious limiting case is when a well is cut back to zero flow rate, and only then will 7-day shut-ins reflect true reservoir pressure. The rate-reduction effect is demonstrated by a two-dimensional (2D), single-well, transient gas model simulation and actual field data. Also, examination of pressure production data from low-permeability gas wells in fields not subject to infill drilling shows the same increased shut-in pressure trend as a result of reduction in takes resulting from the current oversupply of gas.

The single-well simulation is based on an area of 320 acres [130 ha], a permeability of 0.05 md, and a 500-ft [152-m] infinite-conductivity vertical fracture corresponding to a −6.5 skin. In the simulation, the well produced at a constant rate of 240 Mscf/D [6.80×10^3 std m^3/d] for 10 years and then at 160 Mscf/D [4.53×10^3 std m^3/d] for 10 years. Annual 7-day shut-ins were simulated, and Fig. 22 presents the resulting plot of p/z vs. cumulative gas produced. Note the rise in 7-day p/z values when the rate reduction took effect. It is this rise that can be misinterpreted as a reserve increase. Fig. 23 is an actual well example illustrating the same problem. In this instance, the flow rates of the original wells were reduced because of the production of infill wells. Notice the effect of the reduced flow rate on the p/z plot, which is identical to that shown by the 2D, single-well model study.

In low-permeability reservoirs, transient effects may last for several years. Coupled with this problem are the extreme shut-in times required to establish usable average reservoir pressures and the difficulty in determining the stabilized backpressure curve. Decline type-curve analysis provides a reserve estimate and a production forecast, which can easily be updated without knowledge of reservoir pressures or the stabilized curve.

Reported Cases of $b>1$. Gentry and McCray[16] made a study attempting to determine why some wells exhibit decline-curve values of $b>1$. The reservoir model described in their study did not include the effects of transient flow behavior.

The rate-time data presented as Field Example No. 2 (Fig. 24) were plotted as log q-log t and yielded an almost perfect type-curve match of all the data on the Locke and Sawyer infinite-conductivity, single-vertical-fracture, constant-wellbore-pressure solution (see Fig. 25). Note that the first year of data is in the transient or infinite-acting period.

All the data were expected to match this type curve because the well was described as being completed in the Mississippi limestone and the producing formation was stated to be fractured, with a tight matrix. No evidence of a double-depletion exponential decline indicative of a naturally fractured reservoir appears in the log-log data plot. "Fractured" may have simply meant hydraulically fractured. In any case, a well completed in a limestone reservoir would probably have been stimulated. Because oil wells are generally drilled on small spacing, and because improved stimulation techniques result in hydraulic fracture lengths beginning to approach

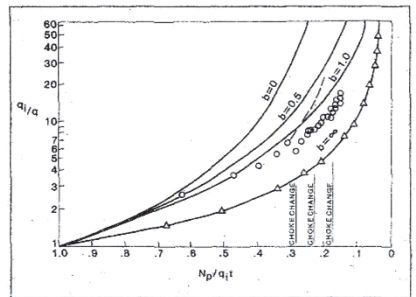

Fig. 27—Dimensionless N_p/q_it plot for Gentry and McCray's Oil Well Example No. 2 data, indicating an apparent b between one and infinity.

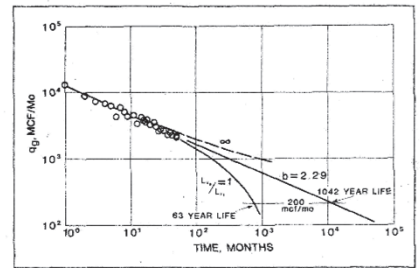

Fig. 28—Wattenberg field—well data matched to the Locke and Sawyer type curve and compared to a regression fit using an Arps equation with $b=2.29$.

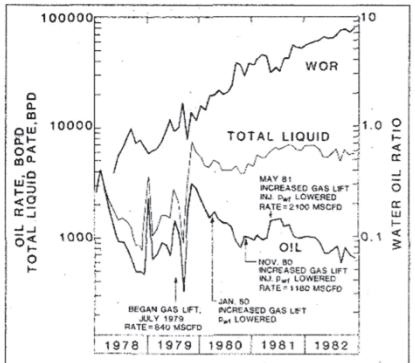

Fig. 29—Production performance of Field E.

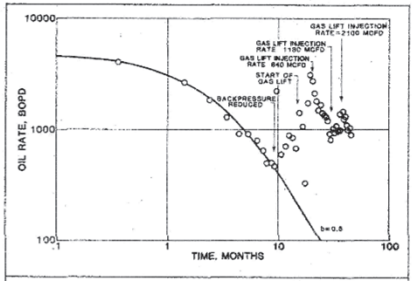

Fig. 30—Log rate vs. log time production performance plot of Field E.

TABLE 7—FIELD E: RESERVOIR DATA AND COMPARISON OF ANALYSIS RESULTS

p_i, psia	2,921
p_{wf}, psia	2,760
μ, cp	0.615
B_o, RB/STB	1.06
c_t, psi^{-1}	12.7×10^{-6}
ϕ	0.18
S_w	0.26
h, ft	100
r_w	0.258

	Early Well Test	q_{dD}-t_{dD} Type-Curve Match
k, md	143	152
s	−3.9	−4.1

spacing, $L_{x_e}/L_{x_f}\rightarrow1$. In the unique match of Fig. 25, $L_{x_e}/L_{x_f}=1.5$. Fig. 26 shows a match of the 2- to 6-year data, but they are reinitialized in time after depletion has clearly set in, at about 2 years. The data fit a decline with $b=0$ and can even be recognized as such on their original semilog plot. Fig. 27 shows the same rate-time data and their use of the Arps equation in a different form, leading to implied values of b between 1 and infinity. Once again, an attempt to fit transient-dominated data to the Arps depletion equation leads to apparent values of $b>1$.

One further example from the literature illustrates a fit of transient data to the Arps equation with a least-squares computer model to "precisely determine optimum values for the coefficients a, b, and q_o."[17] Fig. 28 is a log q-log t plot and match of Well No. 2, Wattenberg field, an example from Ref. 17. The match is again made on the infinite-conductivity, vertical-fracture, constant-wellbore-pressure-solution type curve. The Wattenberg field produces from a tight gas sand and is developed on 160-acre [65-ha] spacing with hydraulic fracture lengths averaging at least 1,500 ft [457 m].[18] Good engineering judgment indicates that with an $L_{x_e}=1{,}320$ ft [402 m] and a fracture length of 1,500 ft [457 m], the data should decline down an $L_{x_e}/L_{x_f}\cong1.0$ stem on the type-curve match, which it does after a nearly 5-year-long transient flow period. The "unique and unbiased"[17] statistical extrapolation of the Arps equation fit of the data with $b=2.29$ yields a life of 1,042 years to an economic limit of 200 Mscf/month [5.66×10^3 std m^3/month], which is unreasonable. The extrapolation of the vertical-fracture-solution type curve on the basis of basic reservoir information with spacing and fracture lengths gives a rational answer.

According to Ref. 17, this application of the regression approach by use of the Arps equation was used on some 200 tight-gas wells. A correlation of b with fracture fluid volume on about 50 Wattenberg wells indicated that in nearly all cases, $b>1$ and was as high as 3.5 in one instance.

All cases we have seen where $b>1$ have been shown to be transient rate-time decline of low-permeability stimulated wells. Statistical approaches to decline-curve analysis that permit $b>1$, the recognized upper limit to the Arps equation, can lead to bad results and bad decisions. The normal range of apparent b, from force fits of transient data to the Arps equation, appears to be between 2.2 and 2.5. To identify transient data and their end, a log-log plot of rate-time data must be made.

Decline-Curve Analysis Using Type-Curves—Field Cases

Field E. One of our earliest field type-curve analysis cases was a one-well field. The depletion mechanism was virtually a full bottomwater drive or, more specifically, a constant-pressure-outer-boundary case. To date, no analytic work concerning the expected value of b with water displacement processes has been done.

Field E is located in the Far East and produces from a carbonate Upper Miocene Kais reef. The reservoir is highly undersaturated with a producing gas/oil ratio (GOR) of ~3 scf/bbl [~0.54 std m^3/m^3] and a gravity of 47°API [0.79 g/cm^3], and is more than likely to be naturally fractured—a typical situation for developing a strong waterdrive. Only the upper 50% of the producing interval was perforated to avoid early water coning. The well was initially completed with 4 shots/ft [13 shots/m] and acidized with 6,100 gal [23 m^3] 30% HCl staged with ball sealers. The initial reservoir pressure was 2,921 psia [20 140 kPa]. As with most of the reef reservoirs in the area, later shut-in pressures return to within 10 to 20 psi [68.9 to 137.9 kPa] of the original reservoir pressure after a 24-hour shut-in.

Fig. 29 is a semilog plot illustrating the production performance of the field in terms of oil production, total fluid production, and WOR. Gas rates were so small that the GOR is not plotted. The initial oil rate decline basically coincides with increasing water production when, after 1 year, gas-lift facilities were installed for all fields in the area. Successful gas lifting in this field began in July 1979 and resulted in the first BHFP change and another decline period. Gas injection rates were increased twice more to lower the BHFP, resulting in yet two more decline periods.

Fig. 30 is the same oil production rate data now placed on a log q_o-log t plot in preparation for type-curve analysis. Each of the three additional decline periods following increased gas injection rates were reinitialized in time and log q-log t plots made for each one. They all exactly overlie the initial decline established during the natural-flow period. This should be expected from superposition principles; i.e., every new transient introduced into the well or field must go back and retrace the original q_{dD}-t_{dD} curve (Fig. 31). (Referring back to the Cullender Gas Well No. 3 data log q-log t plot in Fig. 15, note that the ten 72-hour annual tests taken between 1945 and 1953 with up to 106 psi [730.9 kPa] of pressure depletion exactly overlie the original type-curve match.)

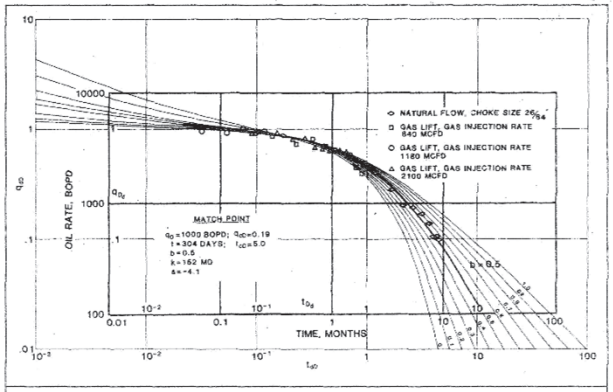

Fig. 31—Field E oil-rate-vs.-time data matched on the q_{dD}-t_{dD} type curve and the transfer of the q_{dD}-t_{dD} axes onto the real-time data plot.

TABLE 8—EDDA RESERVOIR DATA AND TYPE-CURVE MATCHING RESULTS ($r_e/r_{wa}=50$; $b=0.6$)

	Total Production Period	Reinitialized Production Period 3	Reinitialized Production Period 6
kh, md-ft	202	178	127
k, md	2.0	1.8	1.3
r_{wa}, ft	29.62	28.53	29.21
s	−4.4	−4.4	−4.4
r_e, ft	1,481	1,427	1,461
V_p, MMbbl	29.0	27.0	28.0
ϕ	0.236	0.236	0.236
S_w	0.365	0.365	0.365
μ_o, cp	0.185	0.17	0.255
B_o, RB/STB	1.92	1.98	1.67
μB, cp-RB/STB	0.416	0.44	0.50
c_t, psi^{-1}	27×10^{-6}	35×10^{-6}	105×10^{-6}
p_i, psia	6,300	5,200	3,800
p_{wf}, psia	1,500	1,500	1,500
h	100	100	100
r_w	0.354	0.354	0.354

Reservoir Data at Discovery

p_i, psia	7,115
p_b, psia	5,045
μ_{oi}, cp	0.2
B_{oi}, RB/STB	1.895
c_t, psi^{-1}	24×10^{-6}
ϕ	0.236
S_w	0.365
h, ft	100

A match was made with the composite q_{dD}-t_{dD} type curve (Fig. 1) on a value of $b=0.5$. Evaluation of the match point yielded $k=152$ md and $s=-4.1$. This compares well with the initial well test Horner analysis of $k=143$ md and $s=-3.9$. Table 7 compares the results and lists the reservoir and fluid properties used for the well.

Fig. 31 shows the log q-log t match on the q_{dD}-t_{dD} type curve. If we now transfer the q_{dD}-t_{dD} axes onto the tracing paper of the real-time plot, we have a Kais Reef full waterdrive type curve that could be used to predict future performance with backpressure changes for any set of reservoir (k, ϕ, h, p_i) and fluid (μ, B, c_t) parameters with any well spacing (r_e) and any skin effect (r_{wa}) of another Kais Reef reservoir having no performance data at all. This grid transfer is equivalent to back-calculating q_{dD}-t_{dD} values for each of the plotted rate-time data from the known reservoir variables listed in Table 7 and the results obtained from the pressure-buildup analysis.

Edda Field. The Edda field is the smallest of four overpressured volatile oil reservoirs within the Greater Ekofisk development in the Norwegian Sector of the North Sea. Table 8 lists the basic reservoir and fluid properties. Production is from seven wells completed in the Upper Cretaceous chalk (Maastrichtian) or Tor formation. Slight to moderate natural fracturing is indicated from the FI derived from the pressure-buildup analysis (see Table 9). Note that Well C-5 indicates no natural fracturing while Well C-2 has the highest J_f of 28. All wells were acid-fractured without proppants on completion. As indicated by the skin values listed in Table 9, all wells appear to have been successfully stimulated.

Fig. 32 illustrates the production performance of the field with time in terms of monthly average oil and gas production and GOR. Note that the field came on fairly rapidly, resulting in a classic field decline curve. The surface flowing pressure after the first few months has been virtually constant throughout the field's production history. The slight dips in production are a result of field shut-ins. Note also the slight production peaks that follow, discussed in detail later. Of special note is the flattening of the GOR curve starting in about mid-1982.

Fig. 33 is the total field oil production rate plotted in terms of measured daily production rate vs. time on a log q-log t basis. To the best of our knowledge, this is the first time that daily production for a field was measured and available for decline-curve analysis over a 4-year period. Transient spikes after shut-ins are clearly visible and significant on this plot and are used in the decline analysis. There were several field shutdowns followed by an initial transient spike (flush production), as expected for such a low-perme- ability field with successfully stimulated wells. Theoretically, each of the transient spikes (if reinitialized in time) should retrace the field's initial q_{dD}-t_{dD} transient decline. Fig. 34 is a plot of two of the transient spikes obtained after extended shut-ins, and indeed they both virtually overlie the original field transient decline. The rate and time scales shown in Fig. 34 are for the initial production period only; the rate and time scales for Periods A and B have been omitted for clarity of presentation. Note that the field transient appears to end after about 100 days of production. Permeability, skin, and reservoir volumes were calculated for the total field match and each of the two production transients on an average-well basis also—i.e., q_T divided by the number of wells. Table 8 summarizes the

TABLE 9—EDDA: INITIAL-COMPLETION-WELL TEST RESULTS AND FRACTURE INTENSITY INDICES

Well	kh (md-ft)	h (ft)	k (md)	s	ϕ (%)	k matrix (ϕ-k plot) (md)	k well test / k matrix (ϕ-k)
C-2	2,028	110	18.4	−4.9	25.3	0.66	28
C-5	50	70	0.7	−4.0	23.8	0.50	1
C-9	1,119	120	9.3	−4.5	24.6	0.58	16
C-10	218	82	2.7	−4.7	24.0	0.50	5
C-11	510	90	5.7	−4.6	24.1	0.52	11
C-14	298	114	2.6	−3.0	22.6	0.40	7
C-15	201	115	1.7	−3.7	20.8	0.28	6
Total	4,424	701	41.1	−29.4	165.2	3.44	74
Arithmetic Average Value*	632	100	5.9	−4.2	23.6	0.49	11

*$\bar{k}$ = 6.32 md.

match results for $r_e/r_{wa}=50$ and $b=0.6$. Reservoir pressures and gas saturations for total-compressibility calculations for the decline analysis of the transient spikes following shut-ins were estimated from a total field pressure, GOR, and a field-deliverability-matched, compositional material-balance study that is normally updated yearly. Note from the table the slightly declining values of effective permeability to oil values as a result of increasing gas saturation in the reservoir. The calculated reservoir PV's from all three matches are about the same.

A comparison of the calculated PV from the initial match of the total field rate-time data of 202.8×10^6 res bbl [32.2×10^6 res m^3] with that obtained from the total field compositional material-balance performance-matched PV of 201.1×10^6 res bbl [32.0×10^6 res m^3] is excellent.

Material-balance matching of the reservoir consisted of two distinct periods of interest with respect to the decline-curve analysis. The period before the GOR flattened out when forecasted gave rate-time data that fit a $b=0.3$. The period after the flattening, because of more efficient indicated recovery (less gas voidage), now results in a $b=0.6$, the same value of b indicated from the decline-curve match. Al-Kasim,[19] using data we furnished and a one-dimensional radial model matched to the most current field performance data, also found an early $b=0.3$, but $b=0.7$ most of the time. Clearly, no double-depletion stems indicative of a dual-porosity, naturally fractured reservoir can be observed in the rate-time decline data.

Evaluating the Match. We will again illustrate the evaluation of the matching technique and investigate the sensitivity of results to r_e/r_{wa} stems of 20, 50, and 100 for $b=0.6$, now for an oilfield case. For a match point of $b=0.6$, $q(t)=10{,}000$ STB/D [1590 stock-tank m^3/d] oil, $q_{dD}=0.295$, $t=100$ days, and $t_{dD}=0.29$.

With Eq. 5, the field productivity factor is

$$\frac{kh}{\left[\ln\left(\frac{r_e}{r_{wa}}\right)-\frac{1}{2}\right]_F}=\left[\frac{141.2(\overline{\mu_o B_o})}{(p_i-p_{wf})}\right]\left[\frac{q(t)}{q_{dD}}\right] \quad \ldots\ldots\ldots\ldots(5)$$

$$=\left[\frac{141.2(0.416)}{(6{,}300-1{,}500)}\right]\left(\frac{10{,}000}{0.295}\right)$$

$$=414.82 \text{ md-ft [126.43 md·m]}.$$

Because there are seven wells, $q(t)$ is divided by seven and the average well productivity factor is

$$\frac{kh}{\left[\ln\left(\frac{r_e}{r_{wa}}\right)-\frac{1}{2}\right]_W}=59.26 \text{ md-ft [18.1 md·m]}.$$

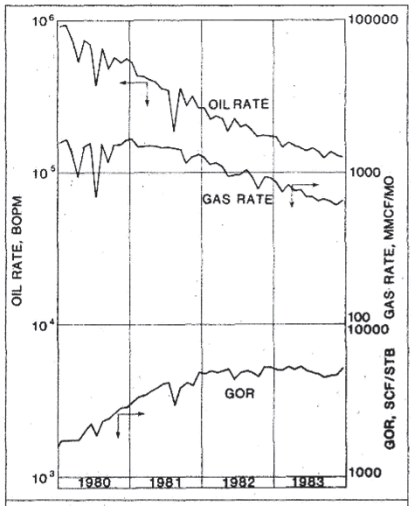

Fig. 32—Edda field production performance.

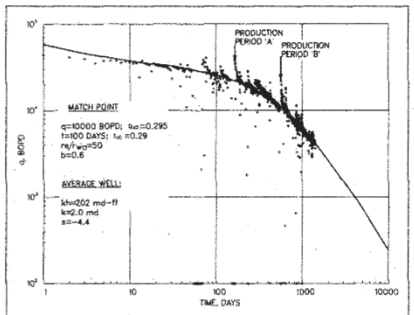

Fig. 33—Edda field type-curve match of daily oil production data on the q_{dD}-t_{dD} type curve.

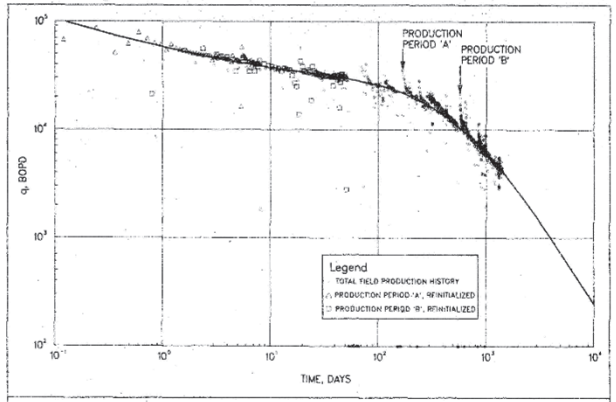

Fig. 34—Edda field—overlay of reinitialized production Periods A and B on the full-field, oil rate-time history.

Eq. 6 will yield the total field PV:

$$V_{pF}=\left[\frac{(\overline{\mu_o B_o})}{(\mu c_t)_i(p_i-p_{wf})}\right]\left(\frac{t}{t_{dD}}\right)\left[\frac{q(t)}{q_{dD}}\right] \quad \ldots\ldots\ldots\ldots(6)$$

$$=\left[\frac{(0.416)}{(0.185\times27\times10^{-6})(6{,}300-1{,}500)}\right]\left(\frac{100}{0.29}\right)\left(\frac{10{,}000}{0.295}\right)$$

$$=202.8\times10^6 \text{ res bbl [}3.22\times10^7 \text{ res m}^3\text{]}.$$

$$r_{eF}=\sqrt{\frac{V_p\times5.615}{\pi h\phi}}$$

$$=\sqrt{\frac{202.8\times10^6(5.615)}{\pi100(0.236)}}=3{,}919 \text{ ft [1195 m]}.$$

Then the oil in place, N_s, at the start of the decline analysis when $p_i=6{,}300$ psia [43 439 kPa] and $B_o=1.92$ is

$$N_s=\frac{V_{pF}(1-S_w)}{B_o}$$

$$=\frac{202.8\times10^6 \text{ bbl}(1-0.365)}{1.92}$$

$$=67.08 \text{ MMSTB [}10.7\times10^6 \text{ stock-tank m}^3\text{]}.$$

Because 1.2×10^6 STB [0.191×10^6 stock-tank m^3] had been produced before the start of the decline analysis, the original oil in place, N_{si}, is indicated to be 68.3 MMSTB [10.9×10^6 stock-tank m^3]. The pressure and GOR history-matched compositional material-balance program obtained an N_{si} of 67.4 MMSTB [10.7×10^6 stock-tank m^3]. The comparison is good.

Using the decline-curve analysis, $N_{si}=68.3$ MMSTB [10.9×10^6 stock-tank m^3], and the cumulative recovery of 16.6 MMSTB [2.64×10^6 stock-tank m^3] to Jan. 1, 1984, results in a 24.3% recovery to date. From the decline-curve projection to an econom-

TABLE 10—EDDA SENSITIVITY TO r_e/r_{wa}

	$r_e/r_{wa}=20$		$r_e/r_{wa}=50$		$r_e/r_{wa}=100$	
	Total Field	Average Well	Total Field	Average Well	Total Field	Average Well
kh, md-ft	1,035.2	147.90	1,415.4	202.2	1,702.9	243.3
k, md	10.35	1.48	14.15	2.02	17.03	2.43
V_p, 10^8 bbl	202.8	29.0	202.8	29.0	202.8	29.0
r_e	3,919	1,481	3,919	1,481	3,919	1,481
r_{wa}	195.95	74.05	78.38	29.62	39.19	14.81
S_F*	−5.34	—	−4.43	—	−3.73	—
s	—	−5.34	—	−4.43	—	−3.73
N_s, MMSTB	67.1	9.6	67.1	9.6	67.1	9.6
N_{si}, MMSTB	68.3	9.8	68.3	9.8	68.3	9.8
Material-Balance N_{si}, MMSTB	67.4	9.6	67.4	9.3	67.4	9.6

*$r_{wa}=\sqrt{\text{number of wells}\times r_w^2}$
$=\sqrt{7(0.354 \text{ ft})^2}$
$=0.9365$ ft.

TABLE 2—MHF GAS WELL A: COMPARISON OF PRODUCTION FORECASTS

Time (months)	Constant-Pressure Solution (Mscf/D)	Infinite-Conductivity Vertical-Fracture Solution (Mscf/D)	Ref. 13 Simulator Results (Mscf/D)
12	182	182	190
18	157	157	165
24	140	136	150
30	130	128	140
36	122	120	135
42	117	112	130
48	110	108	120
54	108	103	110
60	104	100	105
(years)			
6	100	95	
7	96	89	
8	92	86	
9	89	83	
10	86	80	
11	84	78	
12	82	75	
13	80	73	
14	79	71	
15	77	69	
16	76	68	
17	74	67	
18	73	66	
19	72	65	
20	71	64	

will demonstrate this in a full-field rate-time analysis of the total field production.

Fig. 12 illustrates a one-well forecast that was made before any development drilling by extrapolating down an r_e/r_w stem for the premised well spacing. Future rates were read from the real-time scale on which the rate data were plotted. Also shown in Fig. 12 is an extrapolation of the same data fit on an Arps $b=2.5$, which is clearly incorrect. Although one would not attempt an Arps equation fit and extrapolation on only 10 hours of production data, it serves as the only example in which, using transient data, false values of $b>1$ would severely underestimate production.

To summarize, this example illustrated the ability to develop a sound technical decline-curve analysis prediction with basic reservoir engineering principles and only 10 hours of rate-time data.

MHF Well A. Agarwal *et al.*[13] presented 300 days of rate-time data for a massive hydraulically fractured (MHF) well. Fig. 13 illustrates a type-curve match of their data on the radial-flow, constant-wellbore-pressure solution and the infinite-conductivity, single-vertical-fracture, constant-wellbore-pressure solution. Clearly, all the data lie on the transient or infinite-acting period, and there is no evidence of depletion. An evaluation of the match points on the basic radial-flow, constant-wellbore-pressure solution yields $k=0.0081$ md. This value is identical to the Agarwal *et al.* prefracture test result and is the same value obtained from matching on the vertical-fracture, constant-wellbore-pressure solution. Calculated values of skin or L_{x_f} are reasonably close. Table 2 lists the Agarwal *et al.* forecast results obtained when their type-curve analysis and reservoir and fluid properties were entered into their MHF simulator. Listed on the far left is the forecast read directly from the match on the basic radial-flow, constant-wellbore-pressure solution. The middle column is the forecast read directly from the match on the infinite-conductivity, vertical-fracture, constant-wellbore-pressure solution. Note the good agreement between the

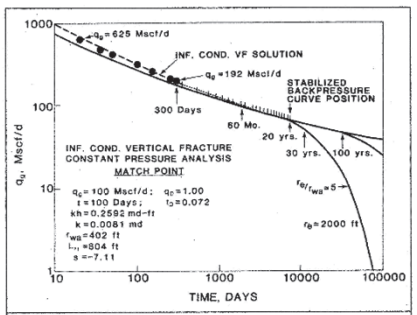

Fig. 14—MHF Well A graphic production forecast.

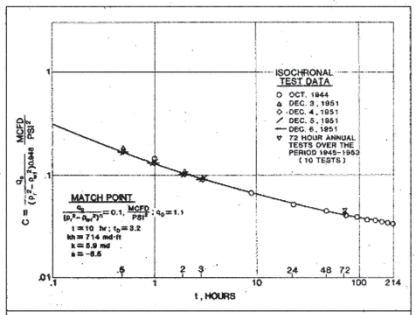

Fig. 15—Type-curve fit of all Cullender's Gas Well 3 data in terms of C, pressure-normalized rate, on the infinite-conductivity, vertical-fracture, constant-wellbore-pressure solution.

TABLE 11—CLYDE COWDEN: RESERVOIR AND WELL DATA

p_i (at discovery), psig	2,250
p_i (match), psig	1,900
p_{wf}, psig	600
c_{ti} at 1,900 psig, 10^{-6} psi^{-1}	75
μ_o at 1,900 psig, cp	0.9
B_o at 1,900 psig, RB/STB	1.43
μB at 1,250 psig, cp-RB/STB	1.2
ϕ	0.15
S_{wi}	0.33
h, ft	48
r_w, ft	0.33
Clyde Cowden: Analysis Results, Average Well From Primary Decline Period Match	
Match Point	
$q(t)$, bbl/month oil	10,000
t, months	10
r_e/r_{wa}	1,000
q_{dD}	0.11
t_{dD}	0.135
b	0.3
Average Well	
kh, md-ft	1,519
k, md	32
V_p, 10^6 res bbl	2.07
r_e, ft	717
r_{wa}	0.717
s	−0.8
N_s (average well), MMSTB	0.97
N_{si} (base), MMSTB	48.5
Produced before decline, MMSTB	1.3
N_{si}, MMSTB	49.8
N_{si} (material-balance calculation), MMSTB	50

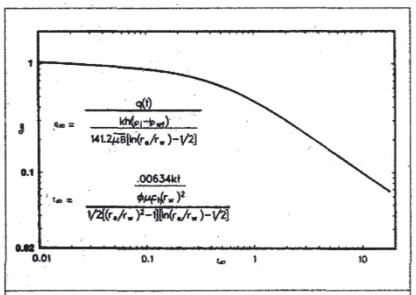

Fig. 41—Monterey constant-wellbore-pressure type curve.

The results of type-curve analysis and relevant reservoir data are summarized in Table 11. The match-calculated average well permeability of 32 md is in good agreement with the permeability range of 20 to 30 md reported for the Upper Clearfork, and the negative skin of −0.8 is consistent with the perhaps only moderately effective acid treatment at completion.

With the method detailed earlier for Edda, the match-derived N_{si} value of 49.8 MMSTB [7.92×10^6 stock-tank m^3] agrees well with the 48 to 52 MMSTB [7.63×10^6 to 8.27×10^6 stock-tank m^3] N_{si} estimates from earlier material-balance calculations.[20]

Production forecasts were made for the primary decline and for Waterflood Period 2 on the basis of the decline match of $b=0.3$ for both. A recovery of 9.8 MMSTB [1.56×10^6 stock-tank m^3] (or 20% of 49.8 MMSTB N_{si} [7.92×10^6 stock-tank m^3]) is forecast for primary recovery; the primary-plus-waterflood forecast is 18.4 MMSTB [2.93×10^6 stock-tank m^3] (or 37% of N_{si}). The

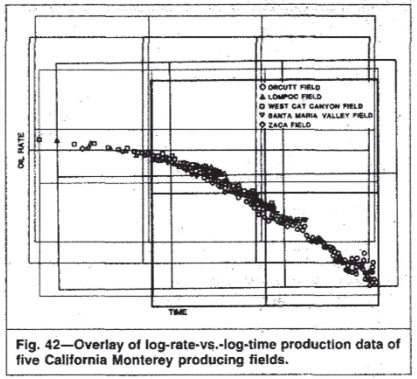

Fig. 42—Overlay of log-rate-vs.-log-time production data of five California Monterey producing fields.

incremental recovery of 8.6 MMSTB [1.37×10^6 stock-tank m^3] resulting from waterflooding represents 88% of primary recovery.

That the primary decline and the waterflood decline appear to *fall on the same decline stem, $b=0.3$, may be coincidental.* While we can think of some possible explanation why this should occur, we can think of none why this must occur. As such, one of the main reasons for presenting this example is to encourage others to examine primary and waterflood histories for their decline exponents. We suppose that if we were asked to produce a waterflood forecast in 1 day given primary production history, we would as a first approximation forecast a waterflood decline on the same value of b as that established during primary recovery.

Monterey Type Curve. In an effort to determine the production performance characteristics of fields producing from the Monterey formation in California, production data from the Lompoc and Orcutt fields were obtained, and an average well rate-time curve was established for each field.[21,22]

A log q-log t tracing-paper plot was made from the data for each of the fields. If these two separate log q-log t plots are overlaid and the vertical and horizontal axes shifted as required, they exactly overlie. This was a surprise at first, yet was consistent with type-curve theory in that the plots should differ only by the coefficients involved in the definition of q_{dD}-t_{dD}—i.e., reservoir and fluid variables. Further, the drive mechanisms, relative permeability relationships, and natural fracturing characteristics also must be similar.

The question of the correctness of the representative average well was immediately raised. Good-quality, unambiguous data available on a single lease within the Orcutt field were also plotted log q-log t, and that plot also exactly overlaid both of the field plots. This appeared to verify the total-field-averaging technique used to obtain our average well plot for each field. Each plot by itself was limited in range; however, all three plots combined virtually doubled the total range of data.

Although suggested by theory, this was the first test of the concept that fields within the same formation having similar drive mechanisms should overlie each other, regardless of the fact that they may have totally different fluid and rock properties, well spacing, stimulation response, and reservoir pressures.

Fluid and rock properties, spacing, and reservoir and flowing pressures were then estimated for the Lompoc and Orcutt fields and a q_{dD}-t_{dD} was calculated for each of the rate-time points to establish a dimensionless type curve for the Monterey formation. Our final dimensionless type curve, which we refer to as the Monterey type curve, is shown in Fig. 41. We further confirmed the type curve with the addition of rate-time data from the West Cat Canyon, the Santa Maria Valley, and the Zaca fields. Fig. 42 shows the complete five-field overlay. This type curve essentially matches the harmonic decline stem $b=1$.

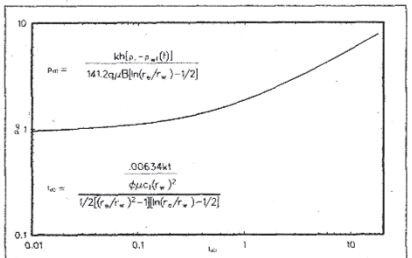

Fig. 43—Monterey constant-rate type curve.

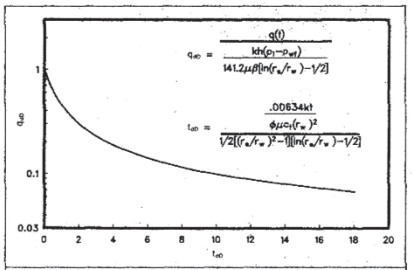

Fig. 44—Semilog plot of the Monterey constant-wellbore-pressure type curve.

The q_{dD}-t_{dD} type curve developed for the Monterey formation was converted to a p_{dD}-t_{dD} type curve to enable us to calculate how long a well or field could produce at a constant rate to a fixed flowing pressure before going on decline (see Fig. 43). The late-time portion of the p_{dD}-t_{dD} type curve appears to be a ½ slope, a $\sqrt{t}$ relationship, which may or may not be significant. It is unlikely that linear flow is from the matrix blocks because the apparent linear flow period is too long and the matrix blocks are considered very small. The Monterey chert is generally overlain with a thick, very-low-permeability mudstone. Therefore, crossflow down from it could be a possible explanation.

The field or formation type curve represents the ultimate use of reservoir or field analogy. The q_{dD}-t_{dD} Monterey type curve is readily applied on an average well basis to develop forecasts for varying reservoir properties and fluid properties, spacing, flowing pressure, and stimulation. Several wells with differing productivities could be used by proportioning total reservoir volume to correspond with each individual well productivity factor to arrive at an average well. Summing each well's forecast developed from the Monterey type curve would result in a more straightforward total field forecast.

Still further flexibility can be added by the use of two conventional one-cell, material-balance forecasts, which when combined match the Monterey type curve. Each material balance allows the inclusion of a drilling schedule, downtime, a relative permeability curve to predict gas rates, and oil and gas production limits. Two forecasts were generated with such a simple model, assuming there exists an intensely fractured area, or volume, and a slightly fractured or nonfractured area or volume with very contrasting deliverabilities. The contrasting deliverability areas can exist areally or vertically. (See Ref. 23 for the effect of hydrocarbon influx of various degrees from a low-permeability outer-boundary region.) The percentage of fractured-area volume to nonfractured-area volume was arrived at by trial and error to get a composite decline rate-time data match of the Monterey type curve. Each separate forecast had the typical solution-gas drive of $b=0.3$.

If one were to develop a sophisticated three-dimensional fracture model, it should first be history-matched to the Monterey type curve before being used to make production forecasts.

Fig. 44 is a semilog plot of the Monterey type curve. Of special note is the precipitous early decline, which later flattens. This behavior can easily be misinterpreted as indicating depletion of the fracture volume followed by flow from only the matrix blocks. The log-log plot of the Monterey type curve does not exhibit in any way the double depletion stems characteristic of the constant-wellbore-pressure solution of the dual-porosity Warren and Root model.

Conclusions

1. For decline-curve analysis, a log q-log t plot should be made to identify transient data and/or depletion data. The plot should be reinitialized in time to eliminate any constant-rate production period.
2. The Arps equation must be applied only to rate-time data that indicate depletion. The limits of the value of b, when the Arps equation applies, are between 0 (exponential) and 1 (harmonic). A forced fit of transient data to the Arps equation results in apparent values of $b>1$; generally, these false values of b fall in the range of 2.2 to 2.5. Further, rapidly declining rate data are characteristic of low-permeability stimulated wells (apparent $b>1$). Often a unique fit of such data can be obtained on the transient portion of a type curve. The misuse of the Arps equation with transient data generally results in overly optimistic forecasts and is technically incorrect.
3. With rate-time data, the double-depletion decline is the only indication of a dual-porosity system. The dual-porosity, constant-wellbore-pressure solution (Warren and Root model) does not anywhere indicate $b>1$, except for the apparent b values from the early transient period; the character of this period is identical to the homogeneous-reservoir solution.
4. The pore volume and reservoir parameters kh and s at the start of decline analysis can be calculated from a type-curve match once depletion is indicated by the data and the decline exponent b is defined or reasonably estimated.
5. In low-permeability gas reservoirs, reserve estimates and production forecasts developed from rate-time data would be more appropriate than conventional curves of p/z vs. cumulative production used with the calculated stabilized backpressure curve approach.
6. Superposition with q_{dD}-t_{dD} with values of $b>0$ can be successfully applied to field problems.
7. Field or formation q_{dD}-t_{dD} type curves can be developed from basic reservoir data and declining rate-time production data.
8. Advanced decline-curve analysis should always be supported by and checked against already existing well and reservoir information.

Recommendations

An effort should be made to obtain accurate rate and surface flowing pressure data to improve the reliability of decline-curve analysis. If these data are taken frequently at early times while producing wide open, if possible, or at a fixed choke setting, then an evaluation of such initial reservoir parameters as kh and s can be made to assist in fixing the r_e/r_w decline-curve stem once depletion sets in. The Edda case history is a classic example of what can be done with good-quality data taken frequently.

Dimensionless type curves to characterize the more important producing formations should be developed from the vast amount of existing field data.

Finally, some analytic work needs to be done with regard to determining what values of b should result from a water displacement process. We need a stronger theoretical basis for waterflood decline-curve analysis.

Nomenclature

b = reciprocal of decline-curve exponent
B_g = gas FVF, surface vol/res vol
B_o = FVF, res vol/surface vol
c_g = gas compressibility, psi^{-1} [kPa^{-1}]
c_t = total compressibility, psi^{-1} [kPa^{-1}]
C = gas-well backpressure-curve coefficient
D_i = initial decline rate, t^{-1}
e = natural logarithm base, 2.71828
G = gas in place at start of decline analysis, surface-measured
G_i = initial gas in place, surface-measured
G_p = cumulative gas production, surface-measured
h = thickness, ft [m]
I_f = fracture index (Eq. 8)
k = effective permeability, md
L_{xe} = reservoir half-length, ft [m]
L_{xf} = fracture half-length, ft [m]
n = exponent of backpressure curve
N_p = cumulative oil production, STB [stock-tank m^3]
N_s = oil in place at start of decline analysis, STB [stock-tank m^3]
N_{si} = original oil in place, STB [stock-tank m^3]
p_i = initial pressure, at start of decline, psia [kPa]
p_p = gas pseudopressure, psi^2/cp [$kPa^2/mPa \cdot s$]
p_{po} = oil pseudopressure, psi/cp [kPa/mPa·s]
p_{wf} = bottomhole flowing pressure, psia [kPa]
q_{dD} = decline-curve dimensionless rate (Eq. 4)
q_D = dimensionless rate
$q(t)$ = surface rate of flow at time t
r_e = external-boundary radius, ft [m]
r_w = wellbore radius, ft [m]
r_{wa} = effective wellbore radius, ft [m]
s = skin
S_w = water saturation
t = time, days for t_D
t_{dD} = decline-curve dimensionless time
t_D = dimensionless time
T = reservoir temperature, °R [K]
V_p = reservoir PV, ft^3 or bbl (consistent units on q and B)
z = gas compressibility factor, dimensionless
Δ = change
λ = type-curve parameter used to characterize gas well drawdown, dimensionless
μ = viscosity, cp [Pa·s]
ϕ = porosity, fraction of bulk volume

Subscripts

BU = buildup
DD = drawdown
F = field
g = gas
i = initial
o = oil
p = production

Superscript

= average

Acknowledgments

We thank Phillips Petroleum Co. for permission to publish this paper. We also wish to thank our Stavanger office and our coventurers in the Greater Ekofisk development for permission to publish the Edda field data.

References

1. Fetkovich, M.J.: "Decline Curve Analysis Using Type Curves," *JPT* (June 1980) 1065-77.
2. Locke, C.D. and Sawyer, W.K.: "Constant Pressure Injection Test in a Fractured Reservoir—History Match Using Numerical Simulation and Type Curve Analysis," paper SPE 5594 presented at the 1975 SPE Annual Technical Conference and Exhibition, Dallas, Sept. 28–Oct. 1.
3. Uraiet, A.A. and Raghavan, R.: "Unsteady Flow to a Well Producing at a Constant Pressure," *JPT* (Oct. 1980) 1803–12.
4. Ehlig-Economides, C.A. and Ramey, H.J. Jr.: "Transient Rate Decline Analysis for Wells Produced at Constant Pressure," *SPEJ* (Feb. 1981) 98–104.
5. Carter, R.D.: "Characteristic Behavior of Finite Radial and Linear Gas Flow Systems—Constant Terminal Pressure Case," paper SPE 9887 presented at the 1981 SPE/DOE Symposium on Low Permeability Gas Reservoirs, Denver, May 27-29.
6. Da Prat, G., Cinco-Ley, H., and Ramey, H.J. Jr.: "Decline Curve Analysis Using Type Curves for Two-Porosity Systems," *SPEJ* (June 1981) 354–62.
7. Carter, R.D.: "Type Curves for Finite Radial and Linear Gas-Flow Systems: Constant-Terminal-Pressure Case," *SPEJ* (Oct. 1985) 719–28.
8. Arps, J.J.: "Analysis of Decline Curves," *Trans.*, AIME (1945) **160**, 228–47.
9. Fetkovich, M.J. and Vienot, M.E.: "Shape Factor, C_A, Expressed as Skin, s_{CA}," *JPT* (Feb. 1985) 321–22.
10. Chatas, A.T. and Malekfam, H.: "The Estimation of Aquifer Properties from Reservoir Performance in Water-Drive Fields," paper SPE 2970 presented at the 1970 SPE Annual Meeting, Houston, Oct. 4–7.
11. van Everdingen, A.F. and Meyer, L.J.: "Analysis of Buildup Curves Obtained After Well Treatment," *JPT* (April 1971) 513–24; *Trans.*, AIME, **251**.
12. Warren, J.E. and Root, P.J.: "The Behavior of Naturally Fractured Reservoirs," *SPEJ* (Sept. 1963) 245–55; *Trans.*, AIME, **228**.
13. Agarwal, R.G., Carter, R.D., and Pollack, C.B.: "Evaluation and Performance Prediction of Low-Permeability Gas Wells Stimulated by Massive Hydraulic Fracturing," *JPT* (March 1979) 362–72; *Trans.*, AIME, **267**.
14. Cullender, M.H.: "The Isochronal Performance Method of Determining the Flow Characteristics of Gas Wells," *Trans.*, AIME (1955) **204**, 137–42.
15. Fetkovich, M.J. and Vienot, M.E.: "Rate Normalization of Buildup Pressure by Using Afterflow Data," *JPT* (Dec. 1984) 2211–24.
16. Gentry, R.W. and McCray, A.W.: "The Effect of Reservoir and Fluid Properties on Production Decline Curves," *JPT* (Sept. 1978) 1327–41.
17. Bailey, W.: "Hyperbolic Decline Curve Analysis of Gas Wells," *Oil & Gas J.* (Feb. 15, 1982) 116–18.
18. Parrott, D.I. and Long, M.G.: "A Case History of Massive Hydraulic Refracturing in the Tight Muddy 'J' Formation," paper SPE 7936 presented at the 1979 SPE/DOE Symposium on Low Permeability Gas Reservoirs, Denver, May 20–22.
19. Al-Kasim, F.: "Decline Type Curve Analysis and Simulation of Edda Production Performance," MS thesis, Norwegian Inst. of Technology, Trondheim (Dec. 30, 1983).
20. Spradlin, B.C.: "Performance of the Goldsmith 5600' Zone, Clyde and Jessie Cowden Leases, Section 13, 14, 23, 24, 25, and 26, Block 44, T1S Ector County, Texas," Phillips Petroleum Co. Report (July 1959).
21. Bradley, M.D. and Craig, D.A.: "A Production History Evaluation of Lompoc Field, Santa Barbara County, California," Phillips Petroleum Co. Report, Denver (Feb. 12, 1981).
22. Bradley, M.D. and Craig, D.A.: "A Production History Evaluation of the Orcutt Field, Santa Barbara County, California," Phillips Petroleum Co. Report, Denver (March 2, 1981).
23. Bixel, H.C. and van Poollen, H.K.: "Pressure Drawdown and Buildup in the Presence of Radial Discontinuities," *SPEJ* (Sept. 1967) 301-09; *Trans.*, AIME, **240**.

SI Metric Conversion Factors

cp	× 1.0*	E+00	= mPa·s
ft	× 3.048*	E−01	= m
ft^3	× 2.831 685	E−02	= m^3
°F	(°F−32)/1.8		= °C
md-ft	× 3.008 142	E−03	= md·m
psi	× 6.894 757	E+00	= kPa
psi^{-1}	× 1.450 377	E−01	= kPa^{-1}

*Conversion factor is exact.

SPEFE

Original SPE manuscript received for review Sept. 16, 1984. Paper accepted for publication Jan. 6, 1986. Revised manuscript received May 21, 1987. Paper (SPE 13169) first presented at the 1984 SPE Annual Technical Conference and Exhibition held in Houston, Sept. 16–19.